AD 295 700

63-2-3

SPACE POWER AND PROPULSION SECTION

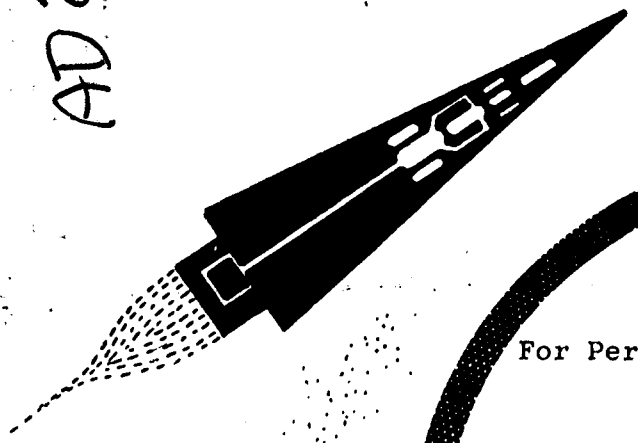

QUARTERLY REPORT NO. 2

For Period Ending October 15, 1962

DYNAMIC SHAFT SEALS IN SPACE

Under Contract #AF33(657)-8459

For

Aeronautical Systems Division

Wright Patterson Air Force Base, Ohio

RE-ENTRY SYSTEMS DEPARTMENT

MISSILE and SPACE DIVISION

GENERAL ELECTRIC

CINCINNATI, OHIO

S P A C E P O W E R A N D P R O P U L S I O N S E C T I O N

Q U A R T E R L Y P R O J E C T S T A T U S R E P O R T

O C T O B E R 1 5 , 1 9 6 2

DYNAMIC SHAFT SEALS IN SPACE

Under Contract #AF33(657)-8459

RE-ENTRY SYSTEMS DEPARTMENT
MISSILE AND SPACE DIVISION
GENERAL ELECTRIC CO.
CINCINNATI 15, Ohio

TABLE OF CONTENTS

LIST OF FIGURES

LIST OF FIGURES (continued)

LIST OF FIGURES (continued)

I. SUMMARY

The Space Power and Propulsion Section of the General Electric Company has been under contract to the Aeronautical Systems Division, Wright Patterson Air Force Base, Ohio, since April 15, 1962 for the development of dynamic shaft seals for space applications. The objective of this program is to acquire the techniques for sealing high speed rotating shafts under the operating conditions of high temperature liquid metals and vapors, the near-vacuum environments of space, and to provide long seal life.

A. The contract specifies the following requirements:

1. The fluid to be sealed shall be potassium.

2. The seals shall be operative at fluid temperatures from the melting point of the fluid selected to 1400°F.

3. The pressure on the fluid side of the seal shall be 15 psi and the external pressure shall be 10^{-6} mm Hg.

4. The speed of the rotating shaft shall be a maximum of 36,000 rpm.

5. The seal, or seal combinations, shall be designed for 10,000 hours of maintenance-free life.

6. The working fluid, potassium, shall be used as the seal lubricant.

7. The seal, or seal combinations, shall be capable of maintaining zero leakage - in the technical sense - under all conditions of operation.

8. The seals shall be designed for a 1.0 inch diameter shaft.

9. The seals shall be capable of operating in a zero "g" environment.

B. The seal evaluation shall consist of:

1. Preliminary experiments with water.

2. 100-hour operational screening test with liquid metal.

3. Thermal-cycling test with liquid metal.

4. 3000-hour life test with liquid metal.

This report covers progress during the quarter ending October 15, 1962. The main events of this reporting period are:

1. Completion of water testing with the rotating housing-stationary disk seal configuration to 20,000 rpm.

2. Analytical review of the rotating disk-squeeze seal configuration for use in the water test rig to 20,000 rpm.

3. Design and placement of manufacturing order for the rotating disk-squeeze seal configuration for 20,000 rpm water tests.

4. Analytical review of the screw seal configurations with attempts to optimize the seal for 20,000 rpm water tests.

5. Design, manufacture and preliminary checkout of 20,000 rpm screw seal test rig.

6. Initiation of 36,000 rpm liquid metal seal test rig design. Final selection of the test rig material and shaft sizing was made with the aid of computer programs for analyzing the vibration characteristics and internal temperature distributions.

7. Preliminary design was completed for the liquid metal seal test facility and orders were placed for the long lead time facility components.

A schedule of forthcoming milestones is shown in Figure 1.

II. FLUID DYNAMIC TESTING

Preliminary fluid dynamic testing in the laboratory has continued throughout this reporting quarter. Analytical investigation of the forecoming tests, as well as evaluation of the completed testing is in process.

A. Rotating Housing-Stationary Disk

The preliminary fluid dynamic testing to 20,000 rpm with the rotating housing-stationary disk has been completed. The high speed dynamic seal test rig on which the test configuration was installed is shown in Figure 2. The three rotating housing stationary disk configurations which were tested are shown in Figures 3a, b, and c. A discussion of the seal test data and analytical data is presented in the following.

1. Power Requirements

Curves characterizing the slinger seal power requirements are enclosed in Figures 7a through 7i. The curves show the slinger seal power requirement plotted versus the rotating housing angular velocity for various radius ratios.

The general equation for the power requirement in a slinger seal may be derived from the fundamental laws of physics. The equation will be:

$$HP = \text{constant} \times \Delta C_m \; p \; N^3 \; a^5$$

The constant term is a known and will be equal to 1.044×10^{-6} when using the English system of units. Therefore,

$$HP = 1.044 \times 10^{-6} \times \Delta C_{mp} N^3 a^5$$

The frictional torque coefficient, ΔC_m will vary with seal immersion on wetted surface. This coefficient is discussed later in this report. All the other terms in the equation are strictly determinable from seal geometry and type of working fluid.

A comparison of various S_L/a ratios for a given configuration in Figure 7 indicates no significant change in the power requirement. Analysis of the data agrees with the derived equation with respect to the power requirement increase as angular speed increased. Both revealed a third power increase. It can be seen from the data that greater disk immersion results in increased power requirements. This is caused by an increase in ΔC_m, the frictional torque coefficient.

Injection of the cooling water flow also affects the power requirement. Since the flow is injected at nearly zero velocity, there is necessarily a momentum exchange. This results in increasing the power requirement as cooling flow is increased, however, the increase is very much smaller than the frictional effect.

2. Pressure Capacity

Curves characterizing the slinger seal pressure capability are enclosed in Figures 8a through 8i. The curves show the sealing pressure plotted versus the rotating housing angular velocity for various radius ratios. The limiting case of maximum sealing has been calculated and is plotted on the curves. However, this case is strictly an ideal situation since it

assumes no water on the high pressure side of the seal. The case of $\frac{a - r_H}{a} \rightarrow 0$ was the closest the calculated limit could be reached in actual experiments without leaking past the seal. In addition to determining the maximum sealing pressure for each seal configuration, testing was performed with various water immersions on the high pressure side of the stationary disk. The experimental test points when plotted on curves of sealing pressure versus rpm form families of $\frac{a - r_H}{a}$ lines. It should be noted that the points plotted did not necessarily coincide with the lines drawn. This condition exists because the test points were run and plotted and then the family of lines representing various ratios of $\frac{a - r_H}{a}$ were drawn to match the data.

A comparison of Figure 8 indicate that the S_L/a ratios which were obtainable in the test rig did not have a significant effect on sealing pressures. However, it should be understood that the stationary disk and rotating housing boundary layers were not submerged in any of the completed experiments.

Analysis of the plotted data revealed that the sealing pressure increase was proportional to the square of the rpm increase. This experimental result agrees with analytical results obtained prior to the initiation of the tests. Analytical investigation has shown that sealing pressure is a function of seal dimensions and the working fluid. Operation of the seal is dependent upon the velocity of the water ring velocity. These characteristics are represented in the following equation which is derived from the

fundamental laws of physics.

$$\Delta P_{max} = 1/2\ \rho\ (k\omega)^2\ (a^2 - r_L^2)$$

Values of "k" were obtained throughout the test and will be discussed later in this report.

3. Frictional Torque Coefficient

Curves characterizing the slinger seal frictional torque coefficient are enclosed in Figures 9a through 9i. The curves show the frictional torque coefficient plotted versus the Reynolds number at the disk tip for various radius ratios. The symbol ΔC_m was used in place of the accepted C_m for the frictional torque coefficient because the disk and housing were only partially submerged in the working fluid instead of being completely submerged. The experimental test points when plotted on curves representing frictional torque coefficient versus disk tip Reynolds number formed families of $\frac{a - r_H}{a}$ lines.

The frictional torque coefficient was obtained from calculations of experimental data. The equation used to calculate it was of the following form.

$$\Delta C_m = \frac{2M}{\rho\ \omega^2\ a^5}$$

As may be seen in the equation, the frictional torque coefficient was dependent on seal geometry, working fluid and measured torque.

A comparison of Figures 9 indicate that the S_L/a ratio had a minor effect on the frictional torque coefficient. The effect was

characterized by a decrease in torque as the spacing between the stationary disk and rotating housing was decreased on the low pressure side. This slight change in the frictional torque coefficient did not significantly affect the power requirements.

The line on each curve labeled $C_m = 0.0622\ R^{-1/5}$ represents an empirical equation derived by Dr. Hermann Schlichting in his book, "Boundary Layer Theory". The equation was derived for a fully submerged disk in the turbulent flow region. However, it is significant to note that the data taken in these tests followed the same slope on the curve as Dr. Schlichting's equation. The frictional torque coefficient decrease is inversely proportional to the one-fifth power of the Reynolds number.

4. Seal Efficiency

Curves characterizing the slinger seal efficiency are enclosed in Figures 10a through 10i. The curves show the slinger seal efficiency plotted versus the dimensionless radius ratio, $\frac{a - r_H}{a}$. The seal efficiency has been defined as the ratio of the maximum sealing pressure experimentally obtained to the theoretical maximum sealing pressure. When considering the theoretical maximum sealing pressure, the ratio of the water ring velocity was taken as unity. The sealing efficiency is represented by the following equiation.

$$\eta = \frac{P_H}{\frac{\rho}{2}(k\omega)^2 (a^2 - r_L^2)} \qquad \text{where } k = 1.$$

Analysis of various S_L/a ratios for a given configuration in Figures 10 insicates no significant difference in efficiency as the disk spacing is changed.

5. Seal Water Ring Velocity Ratio

Curves characterizing the slinger seal water ring velocity ratio are enclosed in Figures 11a through 11i. The curves show "k", the dimensionless ratio of the water ring angular velocity to the rotating housing angular velocity plotted versus the rotating housing angular velocity.

The local value of "k" as well as an average value of "k" may be cauculated from static pressure data taken at various radii on the stationary disk. The general equation used to make this calculation may be derived and will become.

$$k_{xy} = \frac{1}{\omega} \quad \frac{2\,(P_a - P_y)}{\rho\,(r_a^2 - r_y^2)}$$

Comparison of Figures 11 for a given configuration revealed no significant effect on the water ring angular velocity when the axial spacing, S_L/a or the dimensionless radius ratios, $\frac{a - r_H}{a}$ was varied over a wide range. However, the water ring angular velocity varied significantly from one configuration to another. The water ring angular velocity was about 15% lower when changing from $\frac{r_L}{a} = 0.52$ to $\frac{r_L}{a} = 0.87$.

B. Rotating Disk-Squeeze Seal

The rotating disk-squeeze seal water test configuration was designed during this reporting period. The manufacture of the configuration has been released and parts are now being assembled. Casting and machining of the detail parts was completed without any serious problems. This configuration should be available for water testing by November 1, 1962.

The rotating disk-squeeze seal configuration was designed to be mounted on the 20,000 rpm spindle. This spindle was previously used for the rotating housing-stationary disk seal configuration. The test rig configuration was designed to permit interchanging of the various components which will vary significant seal parameters. This interchangeability allows investigation of seventy-two (72) separate configurations with the manufactured hardware. The number of configurations can be doubled and tripled by installing plastic inserts on the low pressure side of the seal to vary the water level. The outside seal diameter will remain constant throughout the testing of this basic seal principle.

Testing of the rotating disk-squeeze seal configuration with water as a working fluid is directed toward determination of the following:

a. What is the maximum sealing pressure possible for a given diameter seal?

b. What is the power requirement for a given diameter seal?

c. What is the pressure profile within the seal?

d. What is the required clearance between the rotating disk and the stationary wall to minimize heating problems?

e. What cooling flow is required to remove the heat generated by fluid friction?

Research into the above questions was done prior to the test configuration design. The answers to several of them have been determined analytically and test data is required to verify some basic assumptions of the physical characteristics. Discussion of the above questions follow.

a. The maximum sealing pressure is a function of the seal dimensions and the working fluid. The operation of the seal is dependent upon the velocity of the water ring velocity. These characteristics are represented by the following equation which may be derived from the fundamental laws of physics.

$$\Delta P_{max} = 1/2\ \rho\ (k\omega)^2\ (a^2 - r_L^2)$$

Engineering judgement indicates that values of "k" may vary from 0.3 to 0.5. Experimentation will define this value much closer and thereby help predict seal performance.

b. The power requirement for the rotating disk seal is also a function of the seal dimensions and the working fluid. However, the power requirements is also related to the frictional torque coefficient. This coefficient is strictly a function of Reynolds Number when applied to fully submerged disks. It is discussed by Schlichting in "Boundary Layer Theory". The power requirement is represented by the following equation which may also be derived from the fundamental laws of physics.

$$HP = \text{constant} \times \Delta C_m\ \rho\ N^3\ a^5$$

The constant term is known and is equal to 1.044×10^{-6} when using the English system of units.

$$HP = 1.044 \times 10^{-6} \times \Delta C_m \rho N^3 a^5$$

It can be seen that ΔC_m is the only variable in the equation which is not strictly determined. Although previous work provides values for ΔC_m, this value was based on completely submerged disks. The hydrodynamic seal in reality is only a partially submerged disk. Therefore, it is not uncommon for the value of ΔC_m to vary as much as 500%. This experimental work will accurately determine the value of ΔC_m as applied to partially submerged disks.

In addition to the frictional resistance caused by the rotating disk, the rotating disk-squeeze seal has an additional drag. Namely, the drag on the shaft or sleeve by the working fluid. This drag results in additional power requirement which may be calculated by assuming the sleeve is a plain cylindrical bearing.

c. The pressure profile will be determined by recording the static pressures at various significant locations within the seal. Data obtained from this pressure profile will be used to determine the water ring velocity.

d. The optimum spacing between the rotating disk and stationary housing will be determined experimentally. The extreme limits of operation can be defined experimentally also. The limits can be recognized readily since the case of having the disk to close to the housing would result in submerging of the boundary layers and the case of having the axial clearance excessive would result in low water ring velocity and low sealing capability. The case

of submerged boundary layers presents the potential problem of cavitation and excessive frictional heating.

e. The cooling flow will be determined by direct experimentation and by power requirement calculations.

C. Screw Seal

1. Summary

Because of a three week delay in the receipt of the test quills, the manufacture of the test rig will not be completed until October 19, 1962. Preliminary check-out of the test rig started on October 1, however, since all of the component parts except the test quills had been received by that date.

2. Test Rig Check-Out

The necessary piping and wiring work have been completed. The high speed spindle without the quill inserted has been run to 35,000 rpm. A very slight resonance in the system was found to exist at 28,000 rpm.

3. Selection of Test Parameters

The many investigators who have studied the operation of screw seals and pumps have used a wide variety of nomenclature and dimensionless parameters. The determination of which of the many possible parameters to use to present the test data is a difficult choice. A wise selection can ease the comparison of present test data with the results of previous investigators and aid in the determination of the number of tests required to completely define the problem.

In Reference 1 it is shown that the solution for the sealing capacity of a screw seal takes the form:

$$\frac{\Delta P h^2}{\mu V L} = K_1 + K_2 \, Re^n \qquad (1)$$

For laminar flow, as pointed out in Reference 2, K_1' has been optimized by solving simultaneously the system of equations obtained by setting the partial derivatives of K_1' with respect to γ, β, γ, and φ or similar parameters equal to zero. Several investigators have done this. The values of K_1' found were:

	Investigator	(K_1') opt.
1.	Zotov (Referene 4)	.69
2.	Asanuma (Reference 5)	.45
3.	Boon and Tal (Reference 3)	.55
4.	Whipple et al (References 8 - 12)	.55

The values of γ, β, γ, and φ found by these various investigators to give an optimum K_1' are presented in Reference 2.

The test data will be presented in the following manner. Dimensionless pressure coefficients will be plotted versus Reynolds number. It is expected that the curve will take the form shown below.

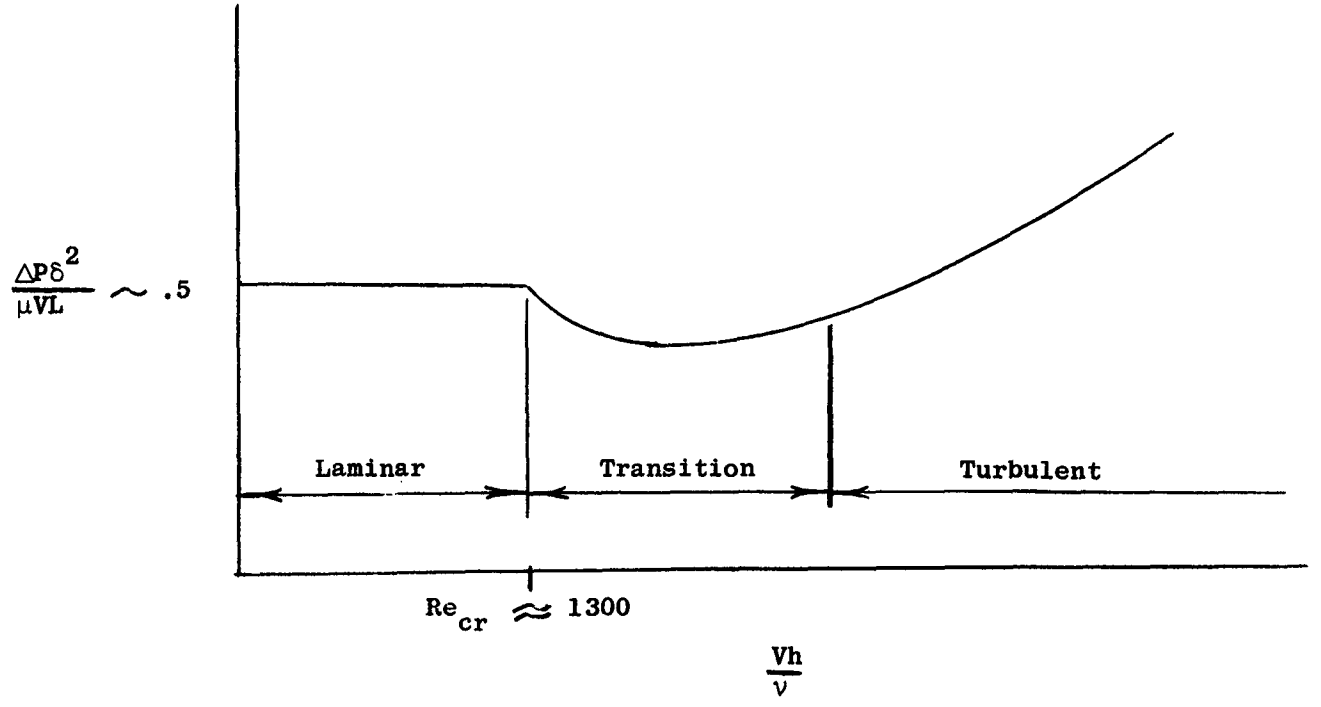

which reduces to

$$\frac{\Delta P h^2}{\mu V L} = K_1 \tag{1a}$$

for the laminar solution. The constants K_1 and K_2 are a function of geometry alone.

By multiplying the sealing equation by $\left(\frac{\delta}{h}\right)^2$ we can write it as:

$$\frac{\Delta P \delta^2}{\mu V L} = K_1' + K_2' Re^n \tag{2}$$

where:

$$K_1' = K_1 \left(\frac{\delta}{h}\right)^2$$
$$K_2' = K_2 \left(\frac{\delta}{h}\right)^2 \tag{2a}$$

The primed constants still remain a function of geometry alone. There still remains the problem of selecting the number and form of parameters to define the constants K_1' and K_2'. Most of the investigators agree that four parameters are sufficient, but none of them agree on which four parameters it will be. In fact, there are about as many geometrical parameters used to describe screw seals as there are investigators studying them. The only parameter they all agree on is the helix angle. The four parameters we have found most convenient to use are:

α = aspect ratio = $\frac{h}{w}$

β = ratio of clearance to groove depth = $\frac{\delta}{h}$

γ = $\frac{\text{groove width}}{\text{thread width + groove width}} = \frac{w}{w + w'} = \frac{t^* - e}{t^*}$

φ = helix angle

Most of the experimental work done to date has been in the laminar regime and a laminar sealing coefficient of about .5 has been found by most researchers. Zotov experienced a dropoff in sealing coefficient at a Reynolds number of about 1300. He did not proceed to a much higher Reynolds number than 1300, however, and it is felt that he never got out of the transition range. Because of this, he did not experience the rise in sealing coefficient predicted in Reference 1.

4. Test Quills

If we allow each geometrical parameter to assume just four values and test all of the possible combinations, we would need 256 test quills. Within the present budget, it is estimated that there are funds enough to test just three quills. The first quill to be tested is designed after the laminar optimization of Zotov. It is described in Reference 2. Variations in only one geometrical parameter, γ will be studied. It had previously been planned to test a triangular groove thread. However, it was decided to be of more value to systematically study the variation of one parameter in one thread geometry rather than haphazardly jump from one type of thread to another. A summary of the geometrical parameters for the three test quills are listed below.

TEST QUILL GEOMETRY

Quill Number	α	β	γ	φ	Type
1*	.08	.32	.63	14.5	rect.
2	.08	.32	.5	14.5	rect.
3	.08	.32	.4	14.5	rect.

*Optimization of Zotov

III. MECHANICAL DESIGN

A. Rotating Disk-Squeeze Seal

Final design of the water test rig for the rotating disk-squeeze seal configuration has been completed and is shown in Figure 4. The test configuration will be mounted on the 20,000 rpm test spindle. This rotating disk-squeeze seal configuration will be capable of generating sealing pressures of 50 psig at 20,000 rpm.

B. High Speed Spindle

Design of the 36,000 rpm high speed test rig for use with liquid metal has been progressing throughout the reporting period. The seal drive spindle consists of an air turbine mounted on a ball bearing spindle similar to the present 20,000 rpm rig. The seal support spindle consists of a 3" diameter hollow shaft supported in two argon bearings. The spindle mounts the liquid metal seal configuration in an overhung position with vacuum connections at the end of the seal.

The design of the spindles for 36,000 rpm operation is very dependant upon the vibrational characteristics of the rotating shaft. Therefore, various configurations of shaft diameters, length and bearings were investigated prior to making a selection of the seal support spindle. These configurations are summarized as follows:

Config.	Shaft Dia. in. O.D.	I.D.	No. of Brgs.	Length of Shaft	Calculated Brg. Stiffness lb/in	Shaft Weight lb.	Polar Moment of Shaft lb - in^2
1	2.5	Solid	2	22.3	200,000	19.21	13.13
2	3.0	1.5	2	22.8	520,000	23.18	25.53
3	3.0	1.5	2	26.6	520,000	26.64	32.19
4	2.5	1.2	2	24.0	250,000	16.39	13.37
5.	2.5	1.2	3	24.0	(2) 250,000 (1) 190,000	13.54	13.37
6.	2.13	1.0	2	19.3	178,000		
7.	2.25	1.1	2	19.2	200,000	16.88	9.63

The vibrational investigation consisted of determining the first and second critical speeds, the potential energy of the shaft at the critical speeds and the normalized deflection of the shaft. For all work the bearing housing was considered rigid since its mass was many times that of the shaft. The vibration analysis was done with the help of General Electric Company's "VAST" computer program on the 7090 computer.

Following is a tabulation of the results of the computations:

Config.	Critical Speeds rpm		Potential Energy (in-lb) System	Springs	Normalized Deflections Cold End	Hot End
1	1st	17,494	1886	6,209	.5	7.0
	2nd	29,280	2066	33,242	1.25	6.95
2	1st	21,992	5560	15,092	.2	7.08
	2nd	43,413	6875	27,750	7.0	1.9
3	1st	23,899	8195	16,119	.08	7.0
	2nd	39,819	8259	56,375	1.0	7.0

Config.	Critical Speeds rpm		Potential Energy (in-lb) System	Springs	Normalized Deflections Cold End	Hot End
4	1st	Below 15,000				
	2nd	35,733	4007	21,518	7.0	2.0
5	1st	Below 15,000				
	2nd	39,790	6611	16,265	10.0	.7
6	1st	Below 15,000				
	2nd	37,526	2931	61,907	7.0	1.0
7	1st	12,265	925	6,035	2.0	9.0
	2nd	34,959	1169	48,462	7.0	1.2

The computations were made based on the shaft material being M-252. The temperature distribution along the shaft affected the modulus of elasticity and had to be accounted for to make the calculations realistic. The temperature distribution also affected the running clearance between the shaft and bearing housing.

The temperature distribution throughout the seal and the spindle was determined with the aid of General Electric Company's "THTB" computer program on the 7090 computer. The distribution varied from 1400°F in the hot potassium seal to about 200°F at the cold end.

After careful analysis of the vibrational data and the temperature distribution, a selection of Configuration #2 was made. The materials selected were M-252 for the shaft and SS316 for the bearing housing. It should be noted from the foregoing data that the test rig will operate above the first critical speed, but about 24% below the second critical under the worst condition.

A vibration analysis of the ball bearing drive spindle revealed a first critical speed at about 30,000 rpm and a second critical speed above 50,000 rpm. The air turbine which will drive the spindle is capable of continuous operation above 40,000 rpm.

Detail drafting of the high speed test rig is in process. Competitive bids for the test hardware will be solicited when the drawing is completed.

IV. TEST FACILITY

Preliminary design of the seal test facility has been completed. Detailed design of all components and loop layout is about 75% complete. The majority of the remaining design work is electrical and instrumentation.

Figure 15 is a schematic of the test facility which shows the major mechanical components and their relative location. Both the alkali metal loop and the argon gas loop are shown in this schematic. Argon gas is primarily used as a cover gas over the alkali metal and as a lubricant for the gas bearings in the test rig. Due to the relatively large rate of argon consumption (36 to 50 scfm), it is necessary to reclaim the argon for reuse. Reclamation is accomplished by a system independent to the seal test facility. The reclamation system is not shown.

Liquid alkali metal will be circulated by a General Electric E.M. Pump which is capable of pumping 4 gpm at 80 psig. Liquid metal is pumped through a heat exchanger where the temperature is increased to within 200°F of that in the return line. After the heat exchanger the alkali metal passes through a 15 micron filter. From the filter the alkali metal flows through two parallel, electrically heated tubes and flow control valves to the test bearing or test seal. From the test rig the alkali metal (possibly containing a small amount of argon) is returned through the heat exchanger where it is cooled to within 200°F of the incoming liquid metal. Out of the heat exchanger the liquid metal passes through a cooler (cold trap) where the

metal is cooled by air to 200 - 300°F. The cooler is packed with wire mesh for trapping oxides at the lower temperature. From the cooler, the liquid metal enters a head tank where the entrapped argon is released from the alkali metal. The argon, containing some alkali metal vapor, is removed from the top of the head tank and is cooled to near room temperature before it enters a liquid nitrogen cooled vapor trap. Essentially all traces of alkali metal are to be removed from the argon gas by the vapor trap and subsequent filter system. Argon from the vapor trap goes to the reclamation system where is is further cleaned and repressurized.

Temperature throughout the test facility will be measured with Cr-Al thermocouples. Alkali metal pressure will be measured with "Taylor Company" volumetric type pressure transducers. Argon pressure will be measured with stainless steel bourdon tube type pressure gauges. Liquid level in the dump tank will be measured with "Ohmart Company" nuclear radiation liquid level gauges. Liquid metal flowrate will be measured with a "MSA" E.M. Flowmeter.

For seal testing a vacuum of 10^{-6} mm Hg is required on one side of the seal. This vacuum will be obtained by a 5-1/4" I.D. diffusion pump in series with a 15 cfm mechanical pump. A liquid nitrogen cooled vapor trap and a liquid nitrogen cooled chevron baffle separate the test seal from the diffusion pump. These traps are to prevent mixing of alkali metal vapor with the diffusion pump oil vapor.

SYMBOLS

1. Slinger Seal

R	Reynolds number, taken at the disk tip, dimensionless, $\frac{\omega a^2}{\nu}$.
ΔC_m	Torque coefficient for disk partially wetted on two sides, dimensionless, $\frac{2M}{\rho \omega^2 a^5}$.
P_H	Static pressure being sealed by the water, psig.
$P_{\text{Dynamic L}}$	Dynamic pressure of sealing fluid, water, on the low pressure side of the disk, psig.
a	Radius of stationary disk, ft.
r_L	Radius of fluid from the center of the disk on the low pressure side, ft.
r_H	Radius of fluid from the center of the disk on the high pressure side, ft.
ν	Kinematic viscosity, ft^2 per second.
ρ	Sealing fluid mass density, lb sec^2/ft^4.
k	Ratio of angular velocities, dimensionless, $\frac{\beta}{\omega}$.
ω	Angular velocity of rotating housing, radians per second.
N	Rotating housing velocity, rpm.
β	Angular velocity of sealing fluid, water, radians per second.

SYMBOLS (continued)

M	Frictional torque (moment), ft. lb.
$\frac{a - r}{a}$	Radius Ratio, dimensionless.
HP	Horsepower.
W	Cooling flow, gpm water.
S_L	Spacing between disk and rotating housing on the low pressure side of the disk, ft.
η	Seal Efficiency.
F_N	Thrust.

2. Screw Seal

D	Shaft diameter.
e	Flight width.
h	Depth of groove in shaft.
K_1 , K_2	Constants in sealing equation.
L	Threaded length of shaft.
n	Number of threads.
N	Shaft angular velocity, rpm.
ΔP	Pressure drop across seal.

SYMBOLS (continued)

Re	Reynolds number
t	Thread pitch = $\pi D \tan \varphi$
t*	$t^* = t/n$
V	Shaft Speed.
w	Width of thread channel.
w'	Width of thread land.
α	h/w
β	δ/h
γ	$w/(w + w')$
δ	Radial clearance.
μ	Absolute viscosity.
ν	Kinematic viscosity.
φ	Thread helix angle

Subscripts

cr	Critical
opt	Optimum value.

Figure 1. Dynamic Seal

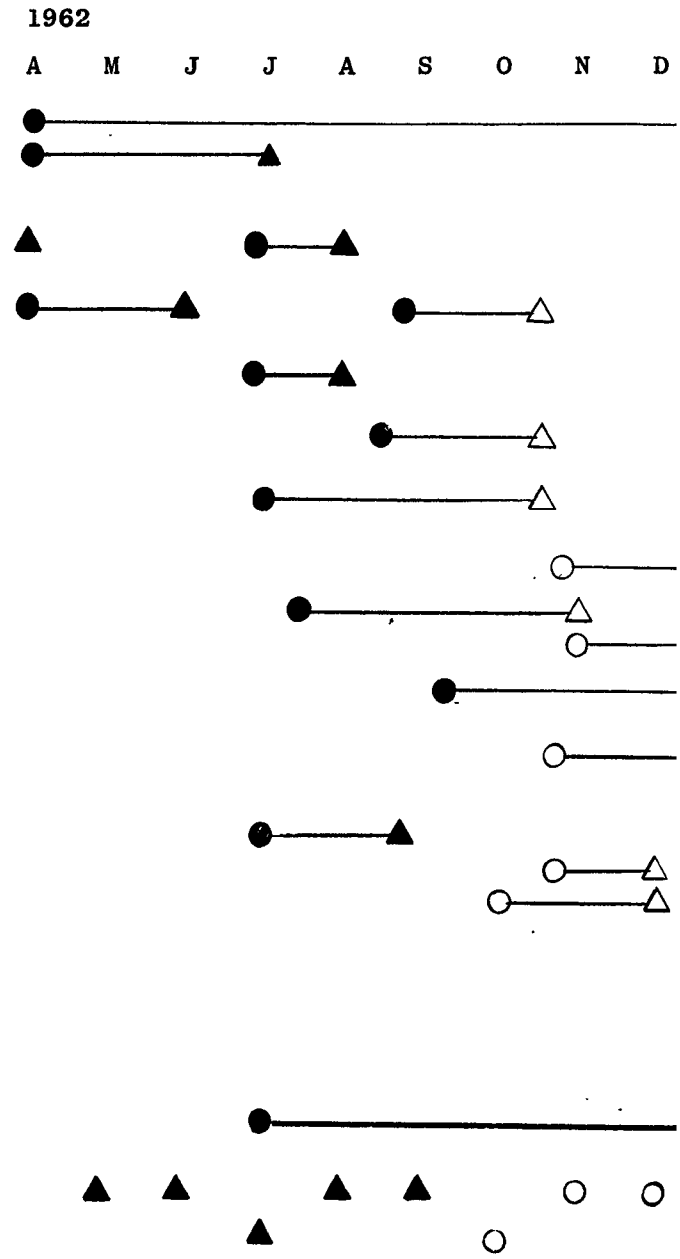

c Seal Work Schedule

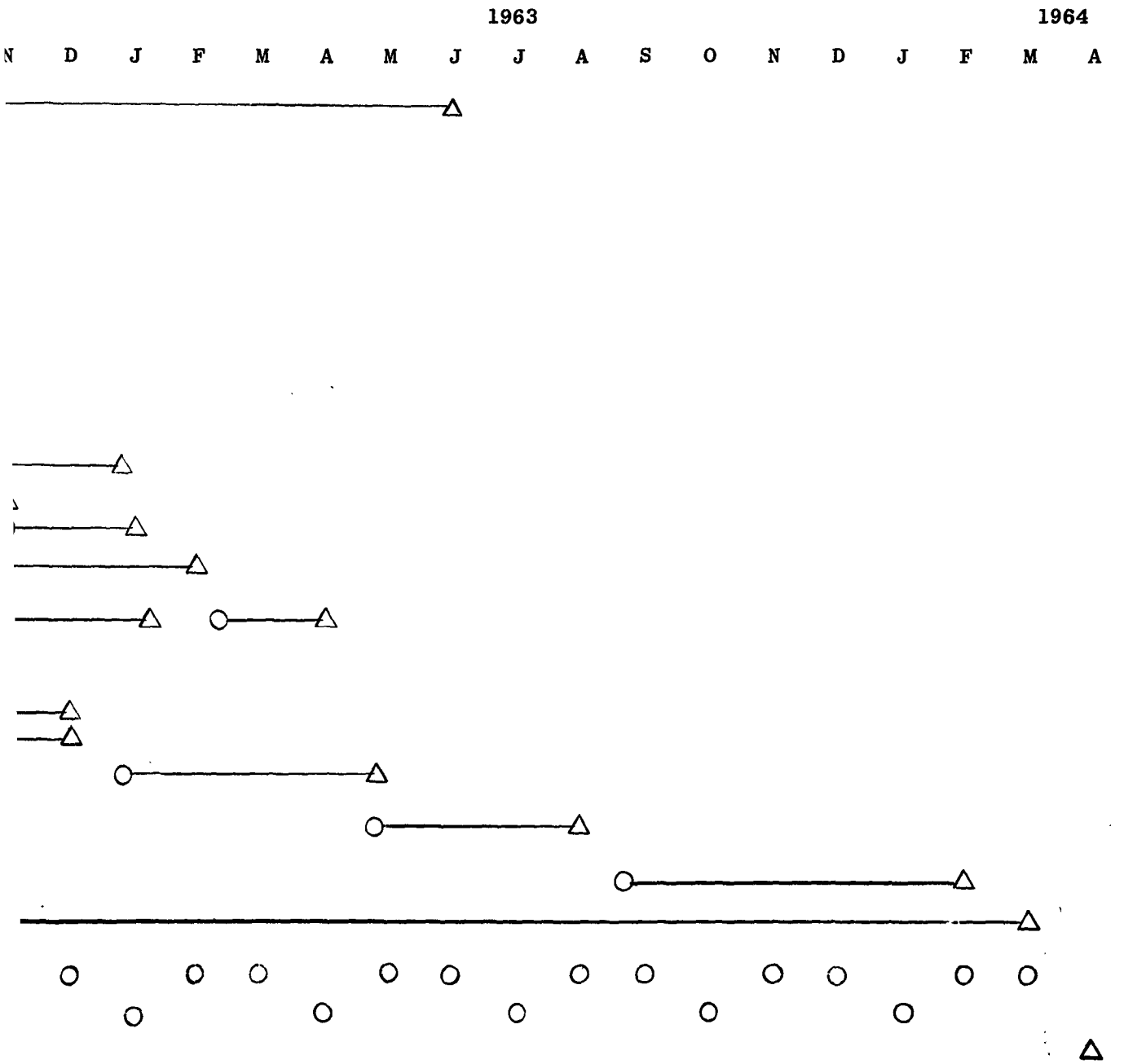

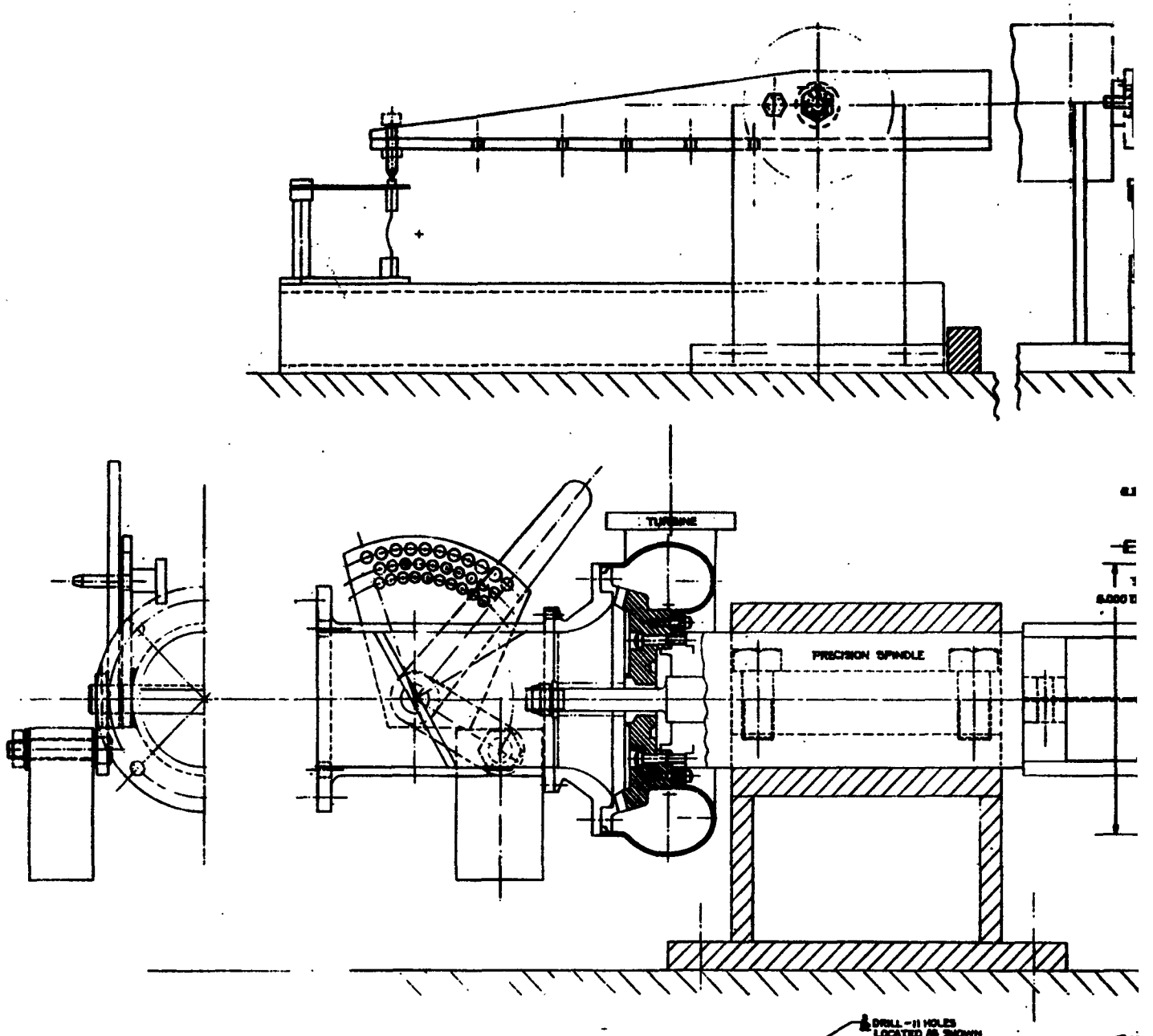

Figure 2. High Speed Dynamic Seal Test Rig
(Working Fluid Water)

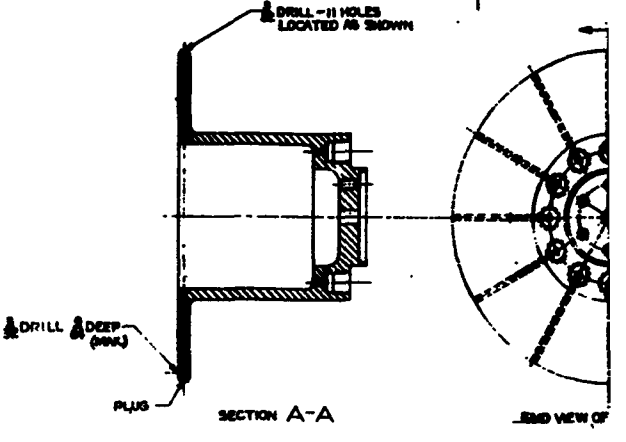

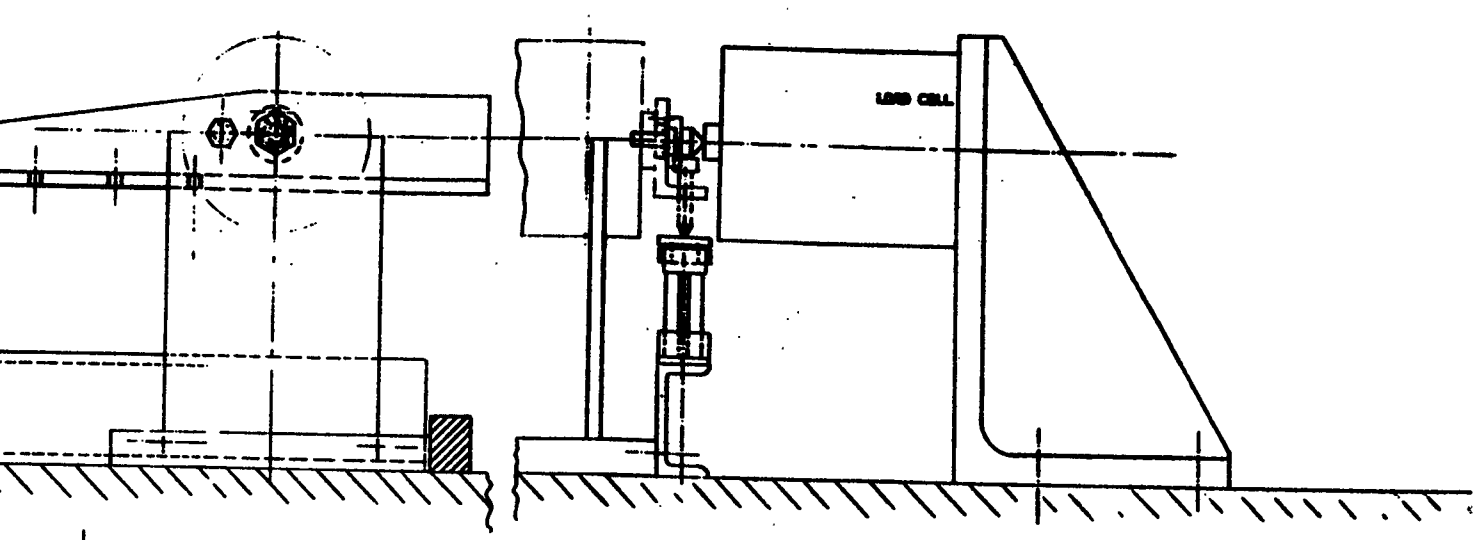
LOAD CELL

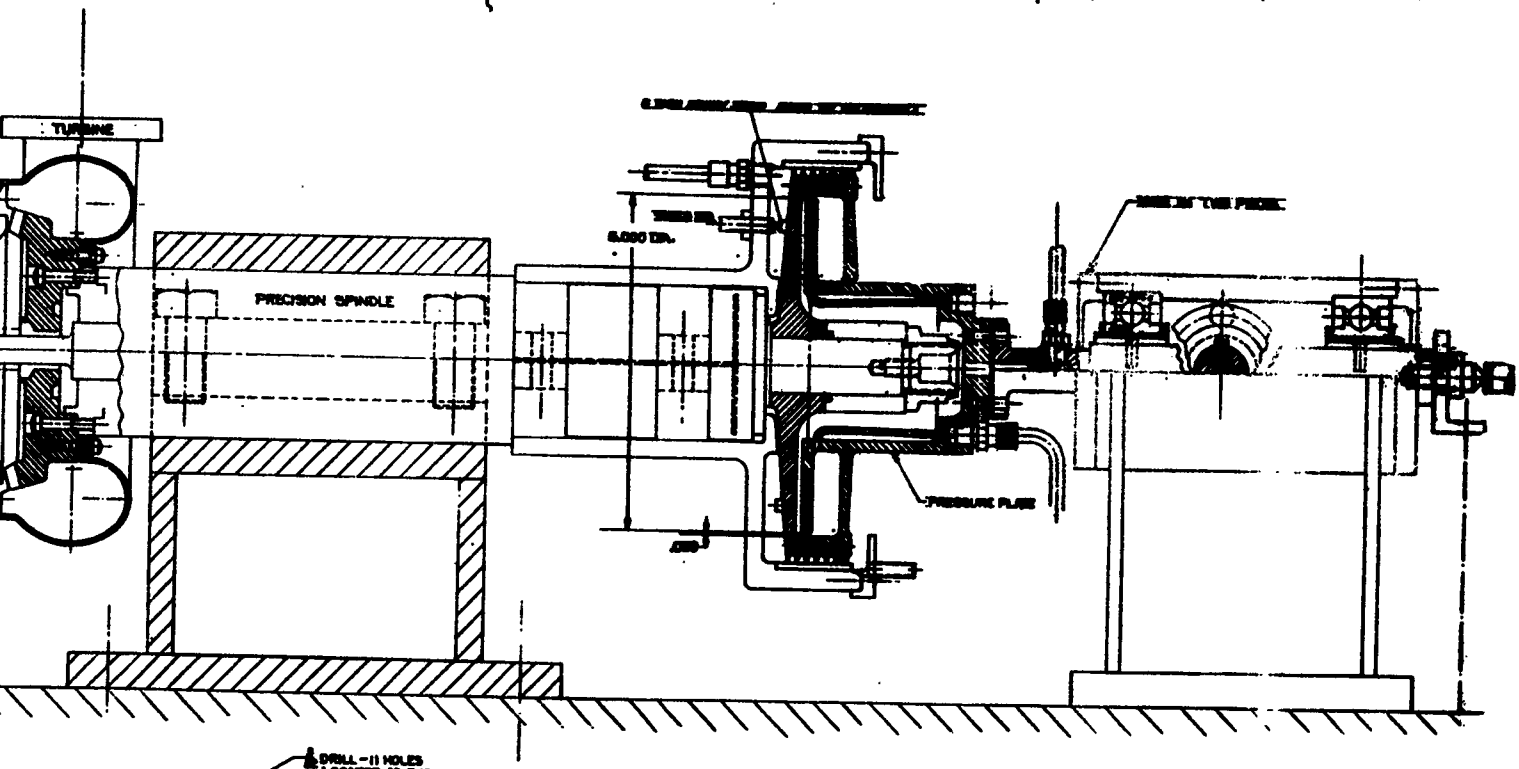
TURBINE
PRECISION SPINDLE
PRESSURE PLATE

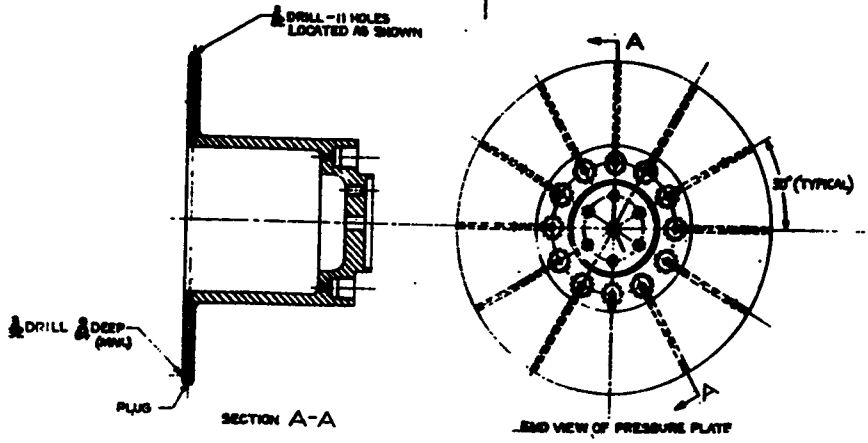
DRILL - 11 HOLES LOCATED AS SHOWN
A
30° (TYPICAL)
DRILL DEEP (MIN.)
PLUG
SECTION A-A
END VIEW OF PRESSURE PLATE

2

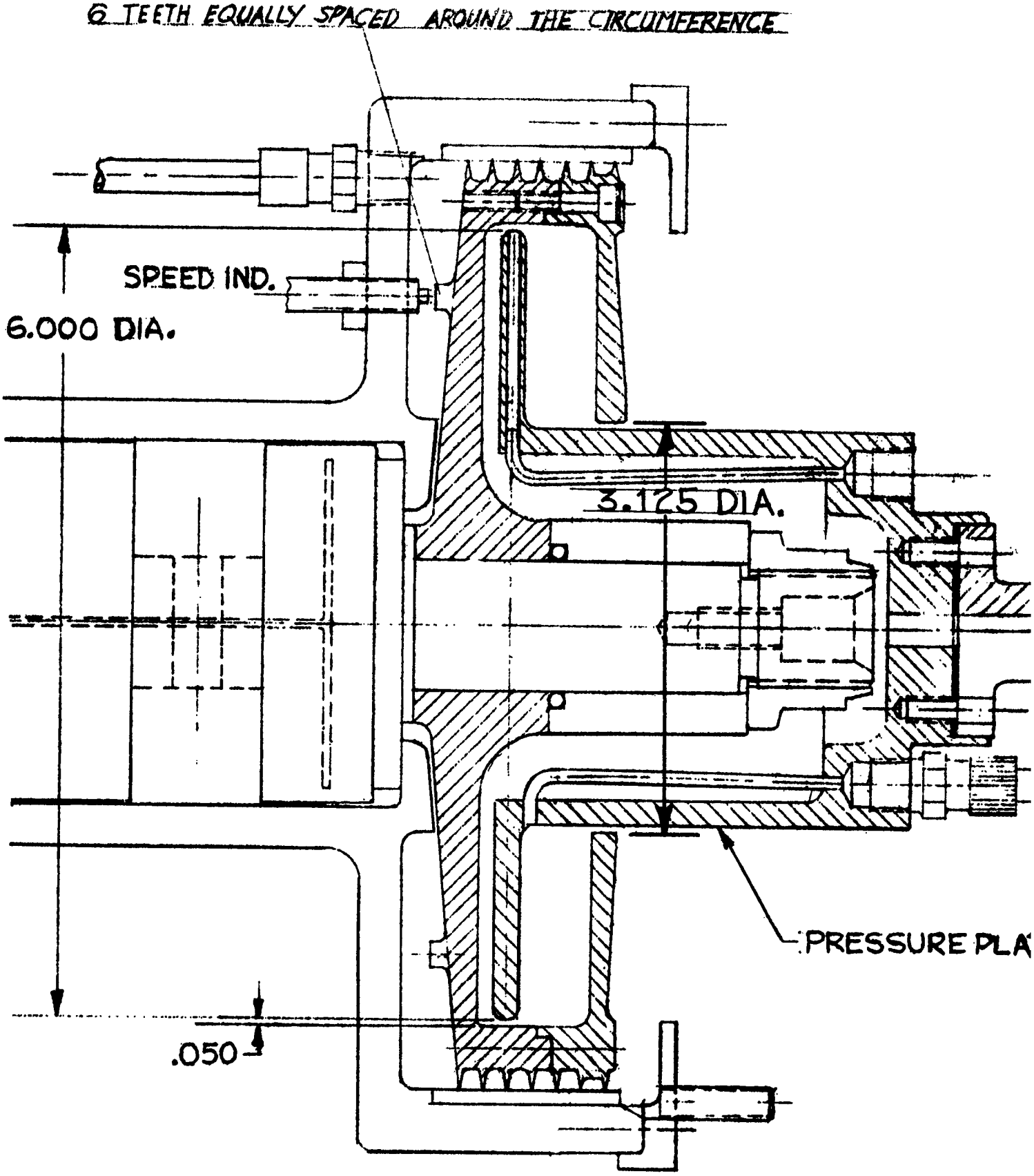

Figure 3a. **Housing-Disk Configuration I, Actual Size,** $\frac{r_L}{a} = 0.52$.

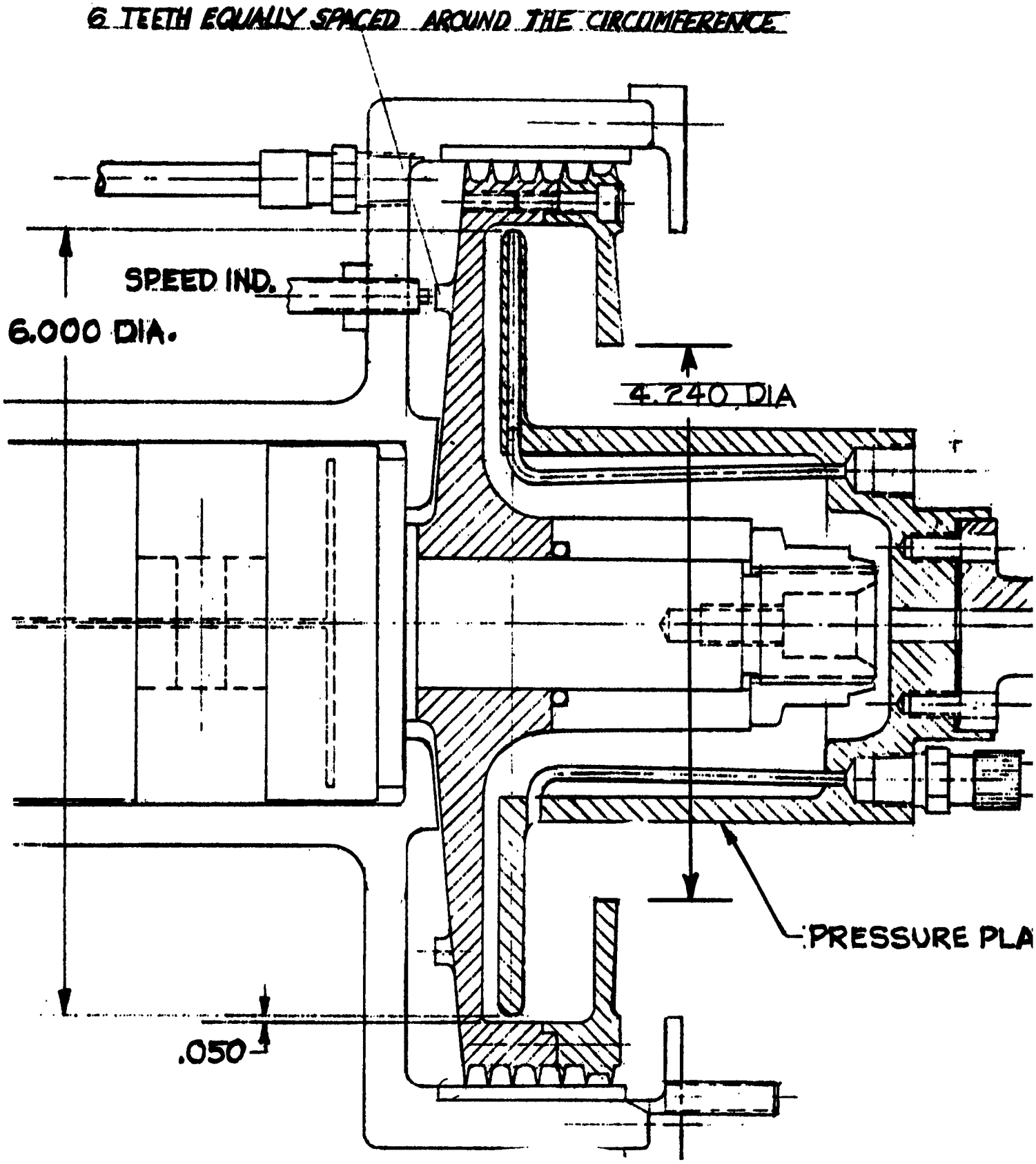

Figure 3b. **Housing-Disk Configuration II, Actual Size,** $\frac{r_L}{a} = 0.71$.

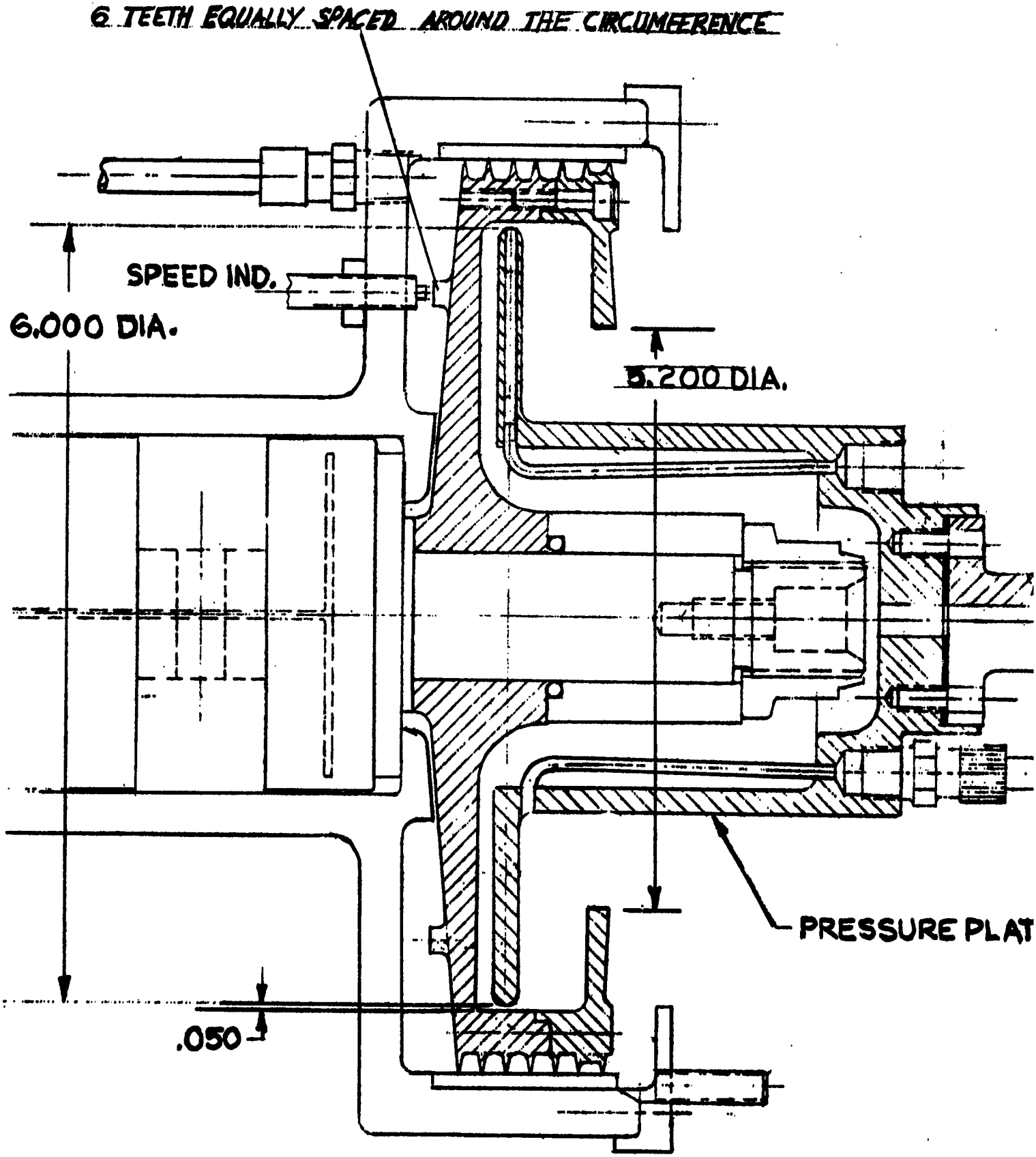

Figure 3c. **Housing-Disk Configuration III, Actual,** $\frac{r_L}{a} = 0.87$.

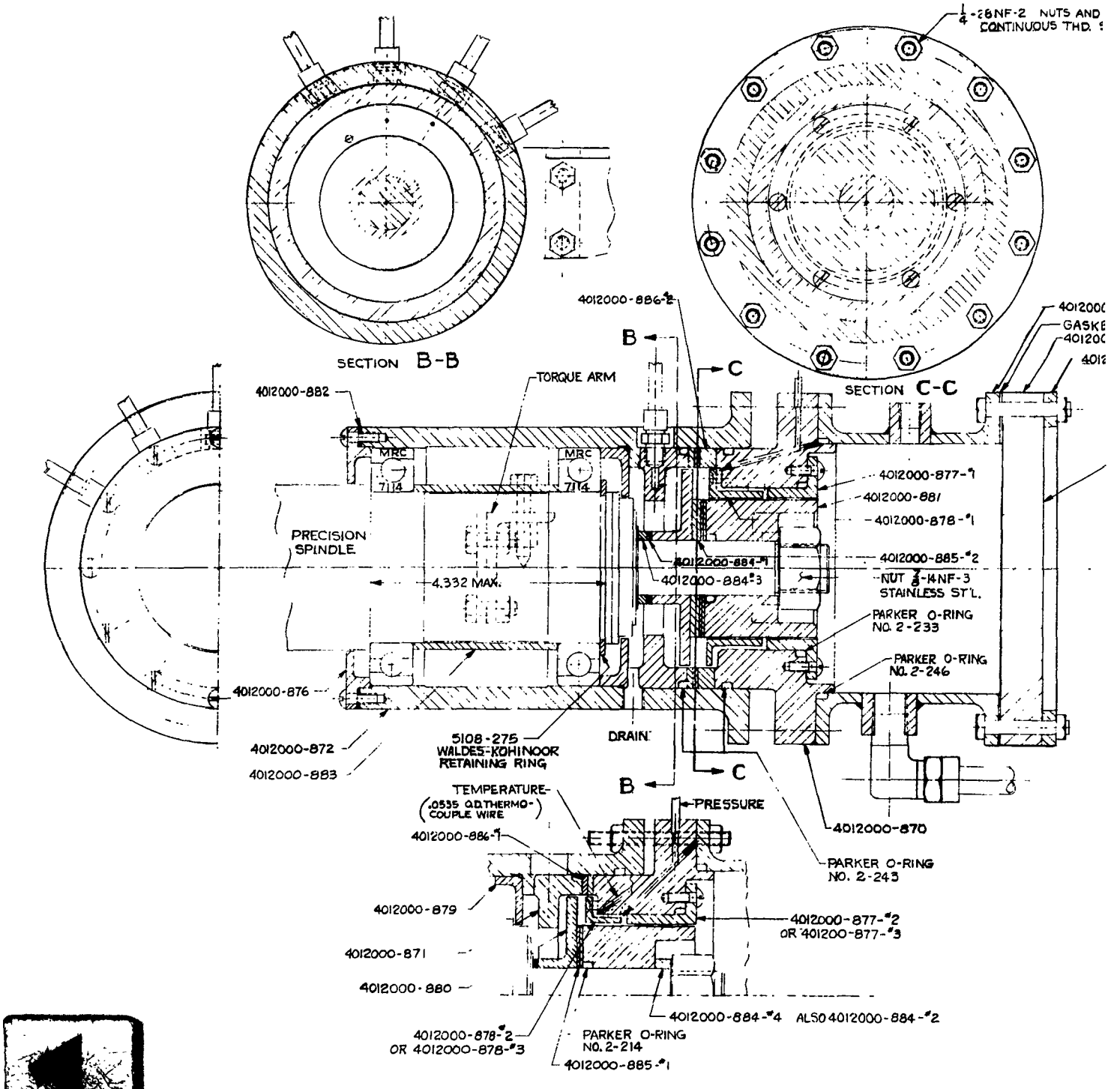

Figure 4. Seal Test Machine - Design No. 2

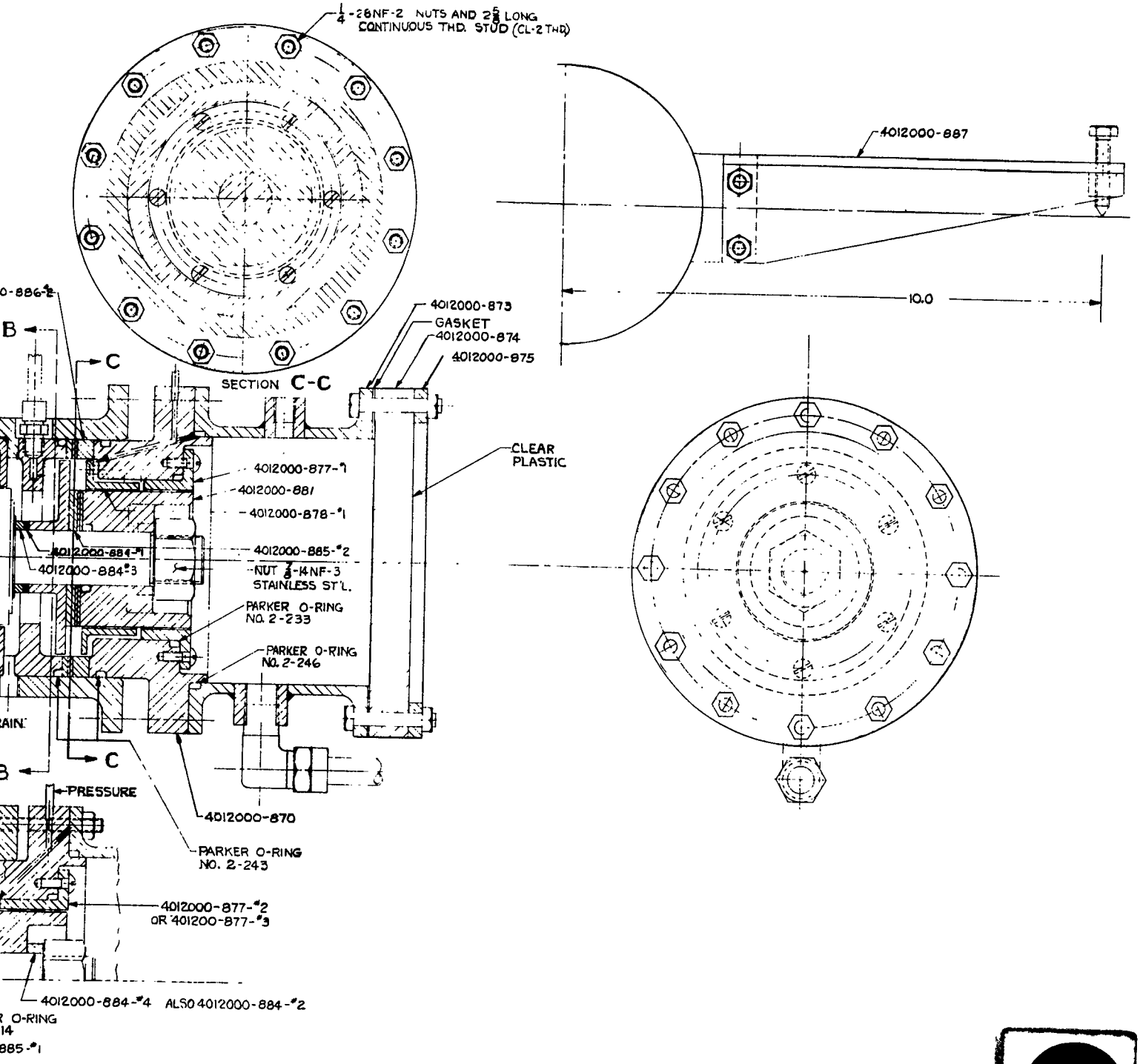

gure 4. Seal Test Machine - Design No. 2

2

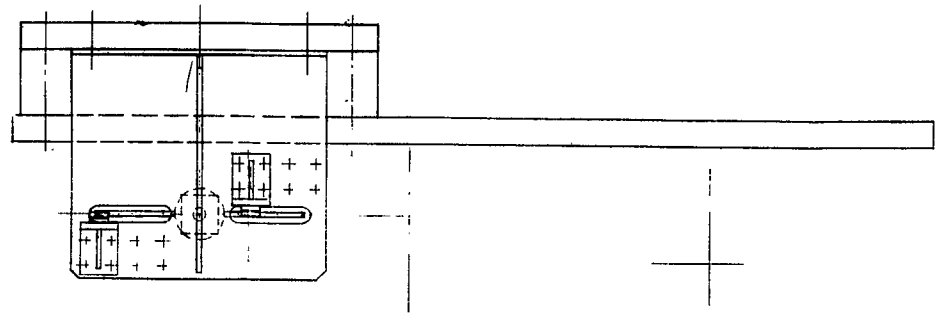

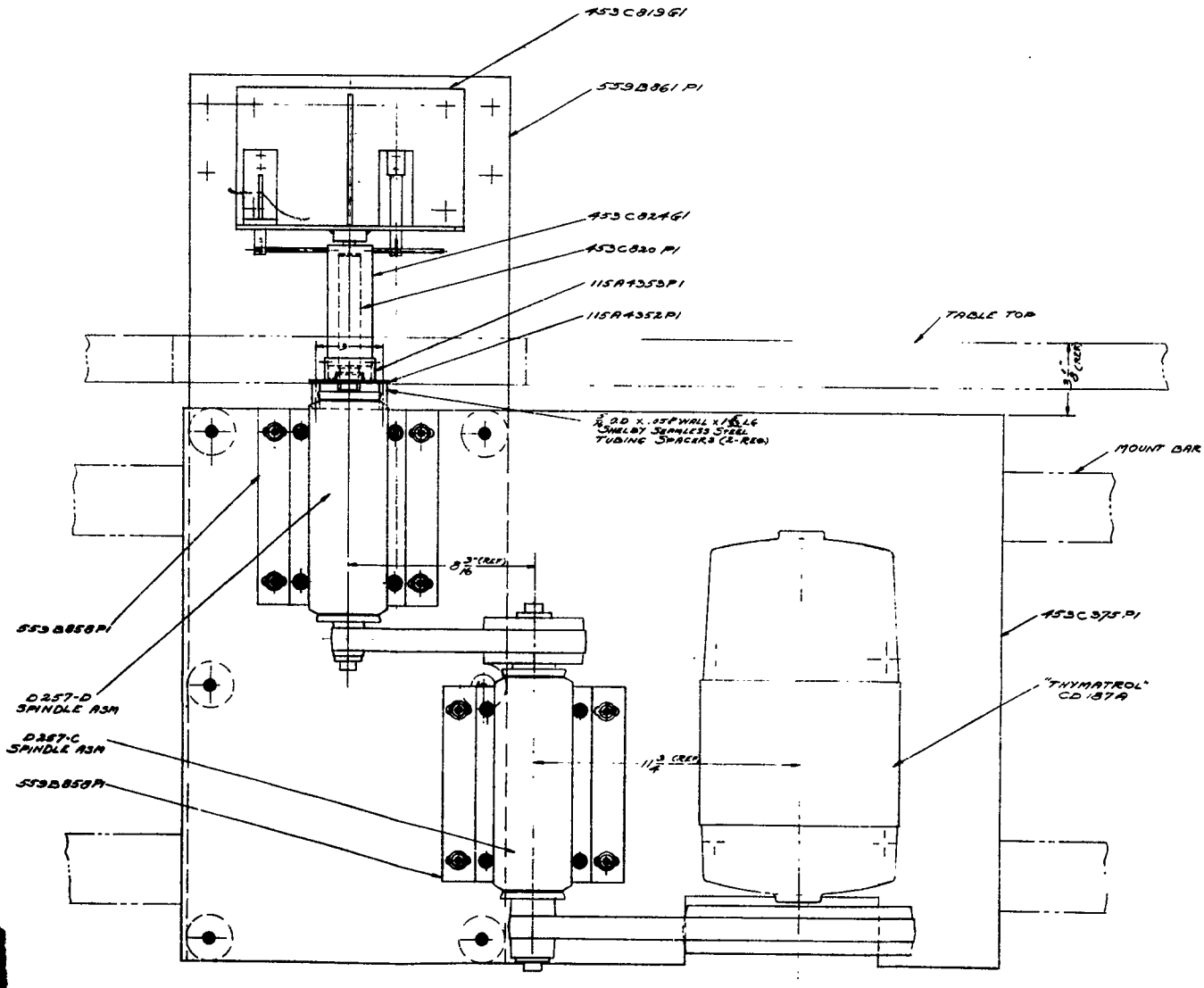
453C819G1
539B861P1
453C824G1
453C820P1
115A4353P1
115A4352P1
TABLE TOP
MOUNT BAR
539B858P1
D257-D SPINDLE ASM
D257-C SPINDLE ASM
539B859P1
453C375P1
"THYMATROL" CD 187A

Figure 5.

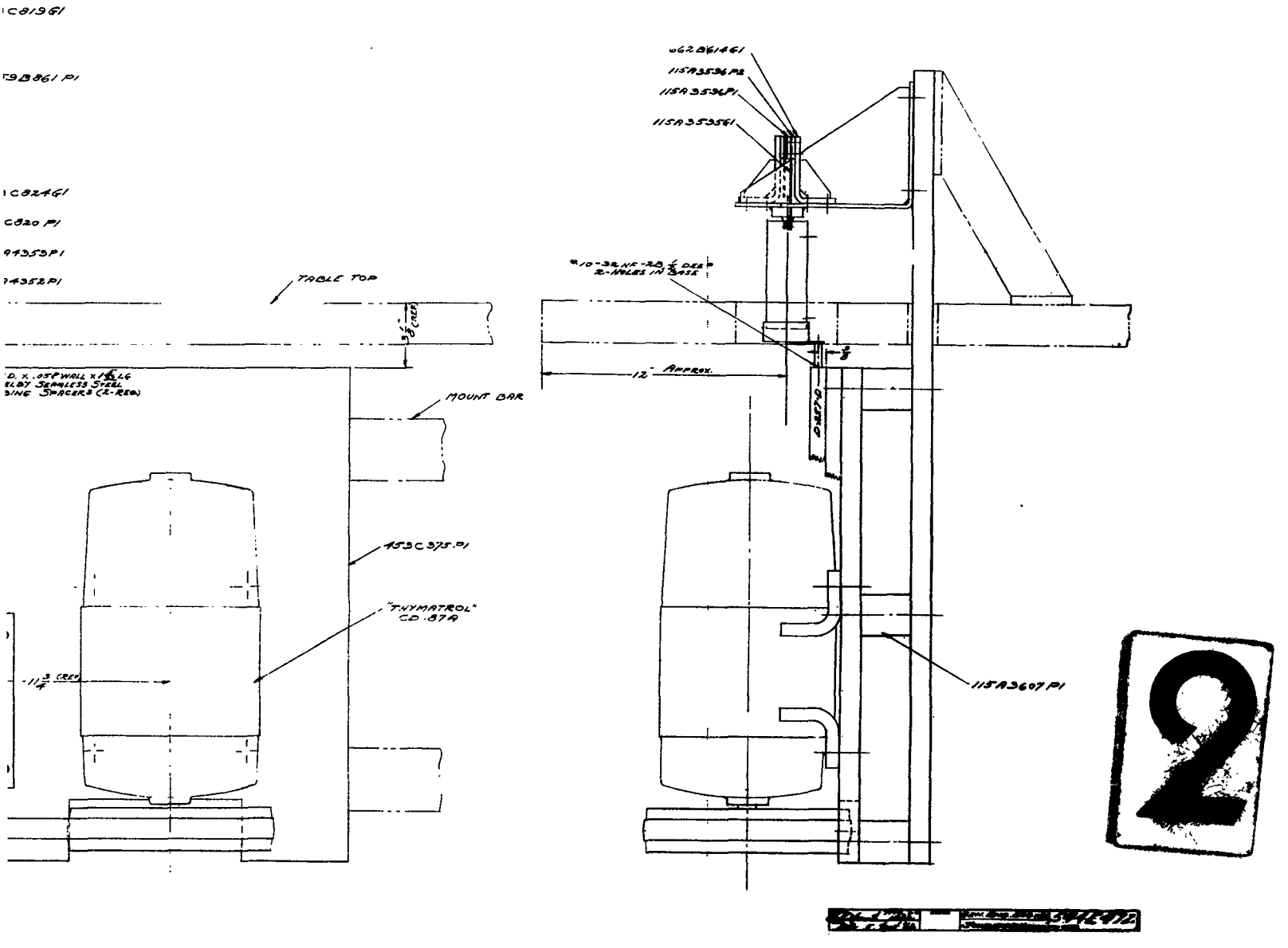
C81961
T9B861 P1
C82461
C820 P1
94353P1
94352P1
TABLE TOP
MOUNT BAR
453C375 P1
"THYMATROL" CD-87A
11SA3607 P1
APPROX.
12

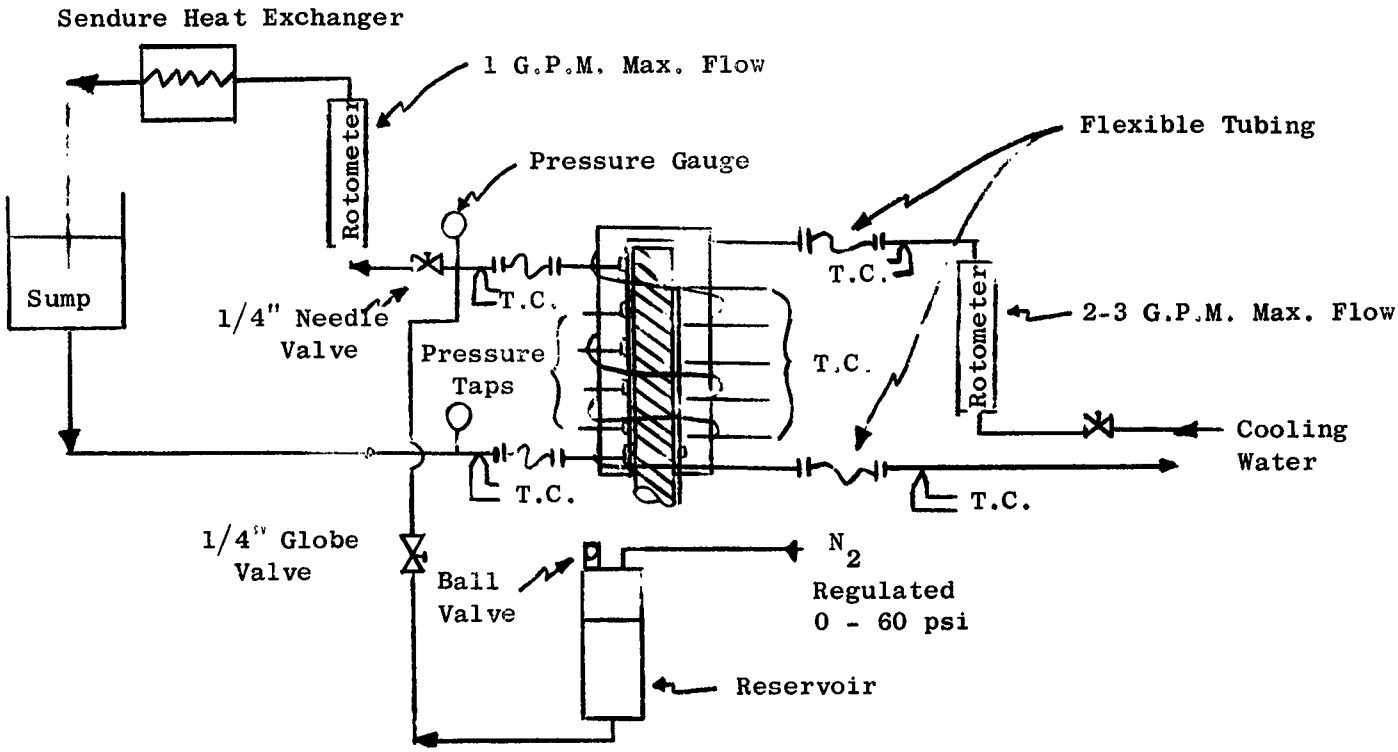

Figure 6. Test Loop and Instrumentation for Screw Seal Test.

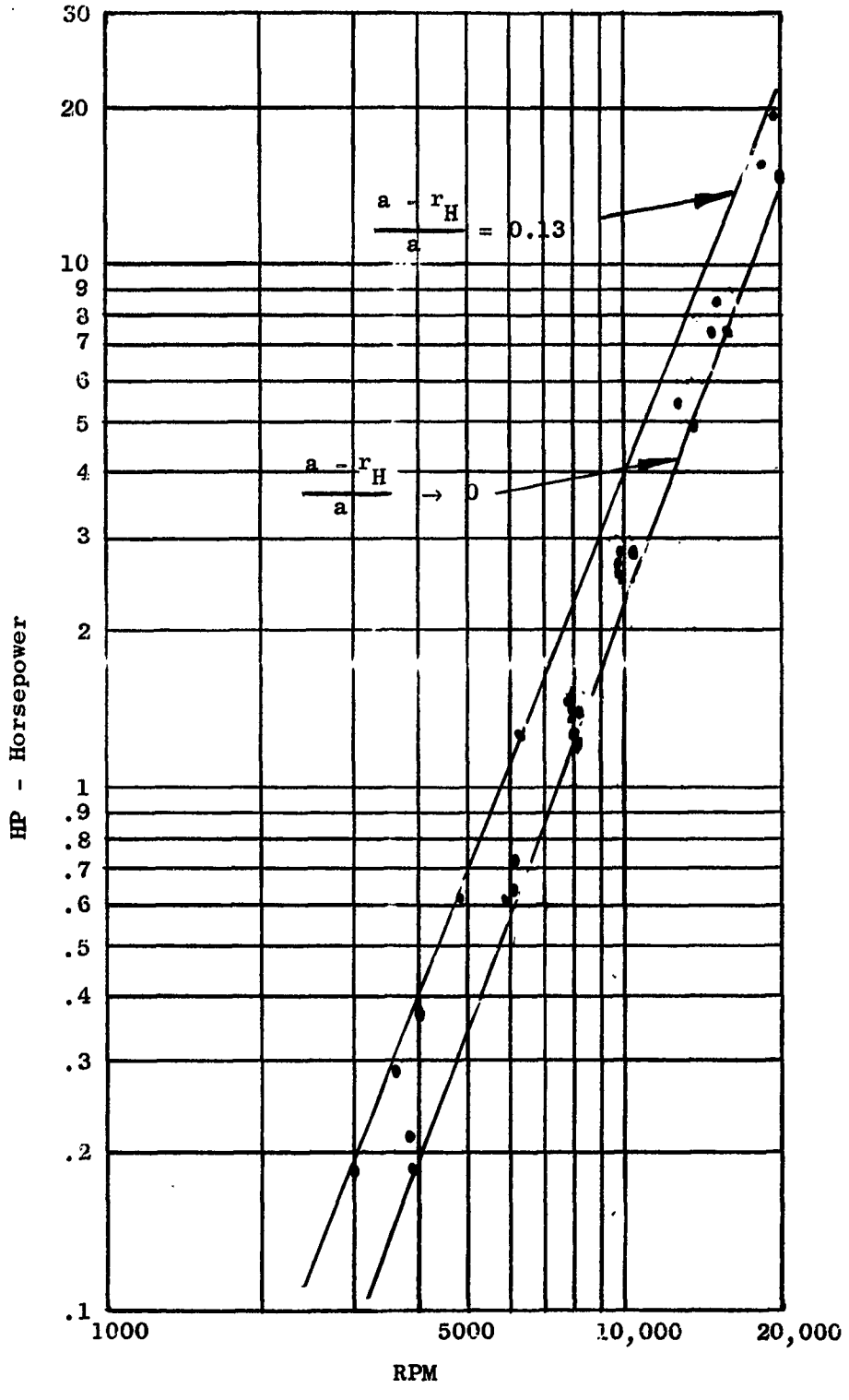

Figure 7a. Slinger Seal Power Requirement, $\frac{r_L}{a} = 0.87$, $\frac{S_L}{a} = 0.167$.

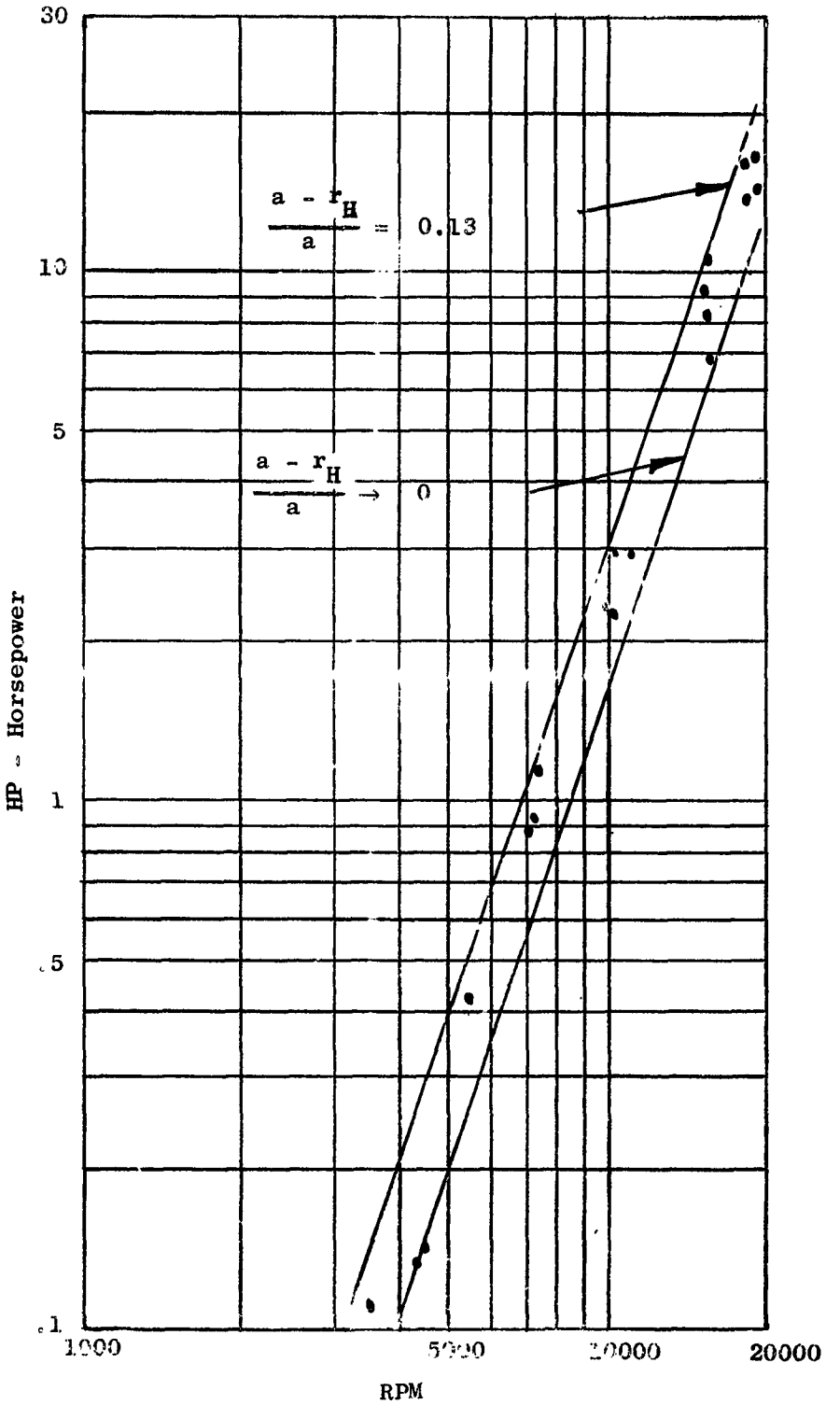

Figure 7b. Slinger Seal Power Requirement, $\frac{r_L}{a} = 0.87$, $\frac{S_L}{a} = 0.092$.

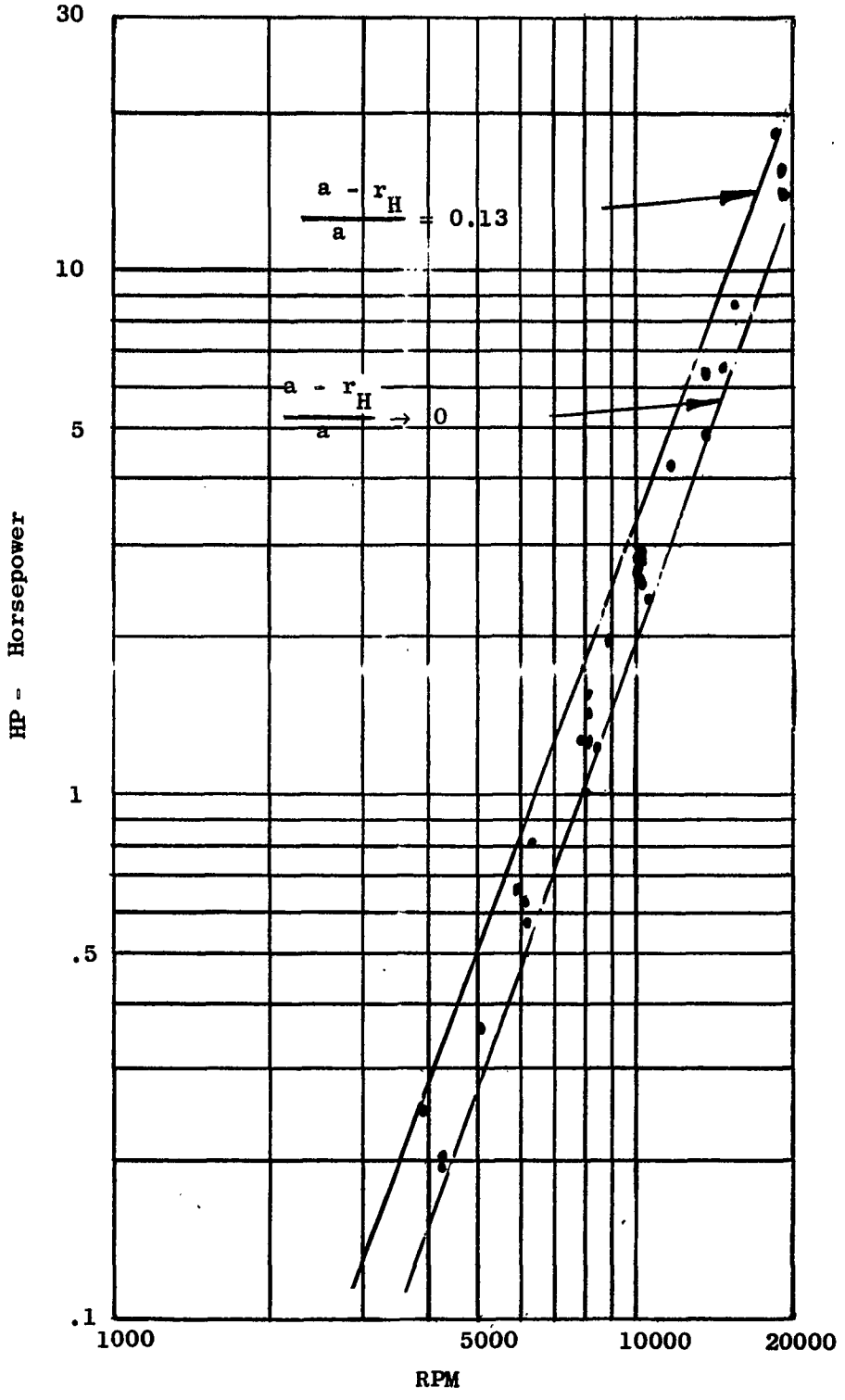

Figure 7c. Slinger Seal Power Requirement, $\frac{r_L}{a} = 0.87$, $\frac{S_L}{a} = 0.019$.

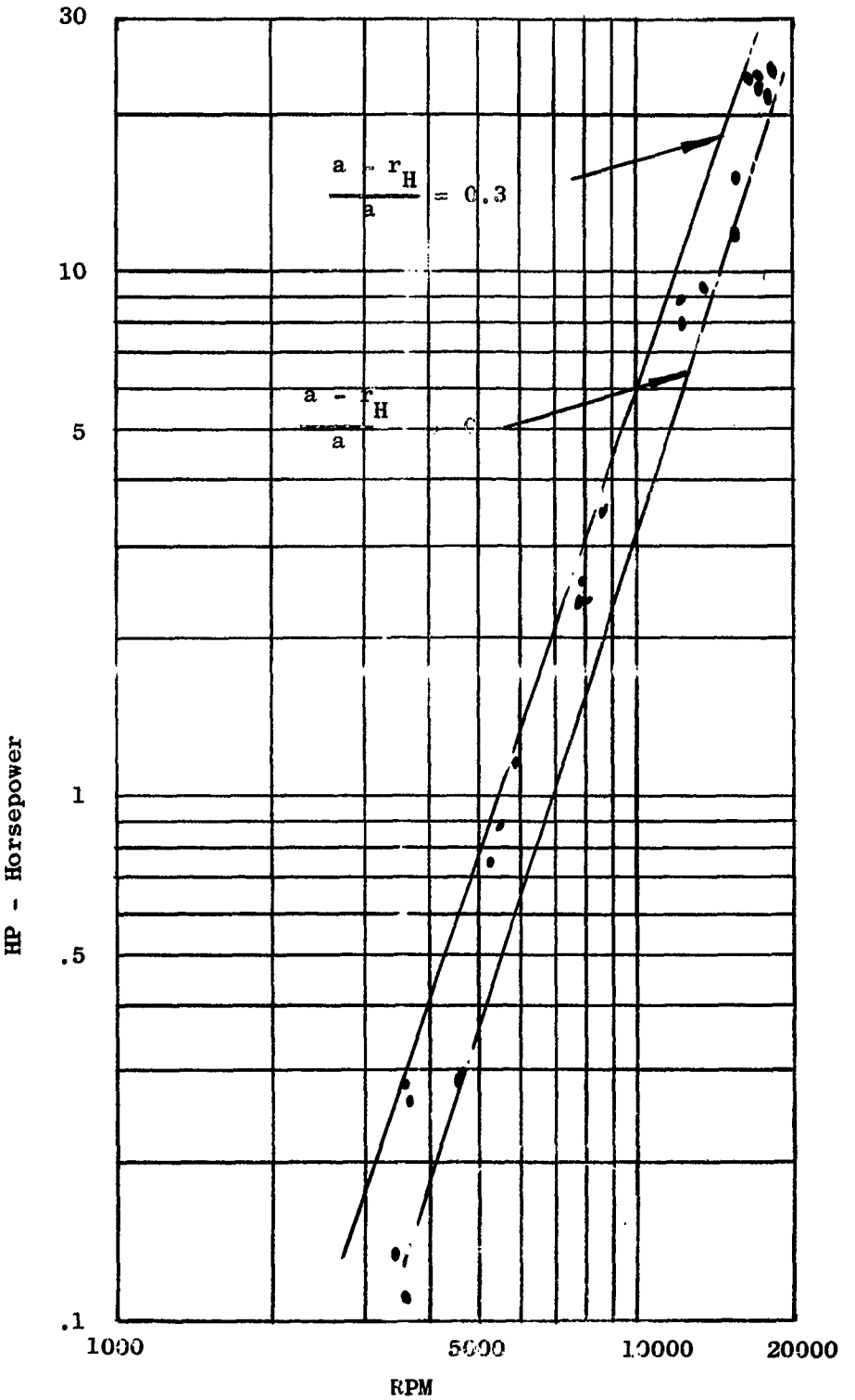

Figure 7d. Slinger Seal Power Requirement, $\frac{r_L}{a} = 0.71$, $\frac{S_L}{a} = 0.167$.

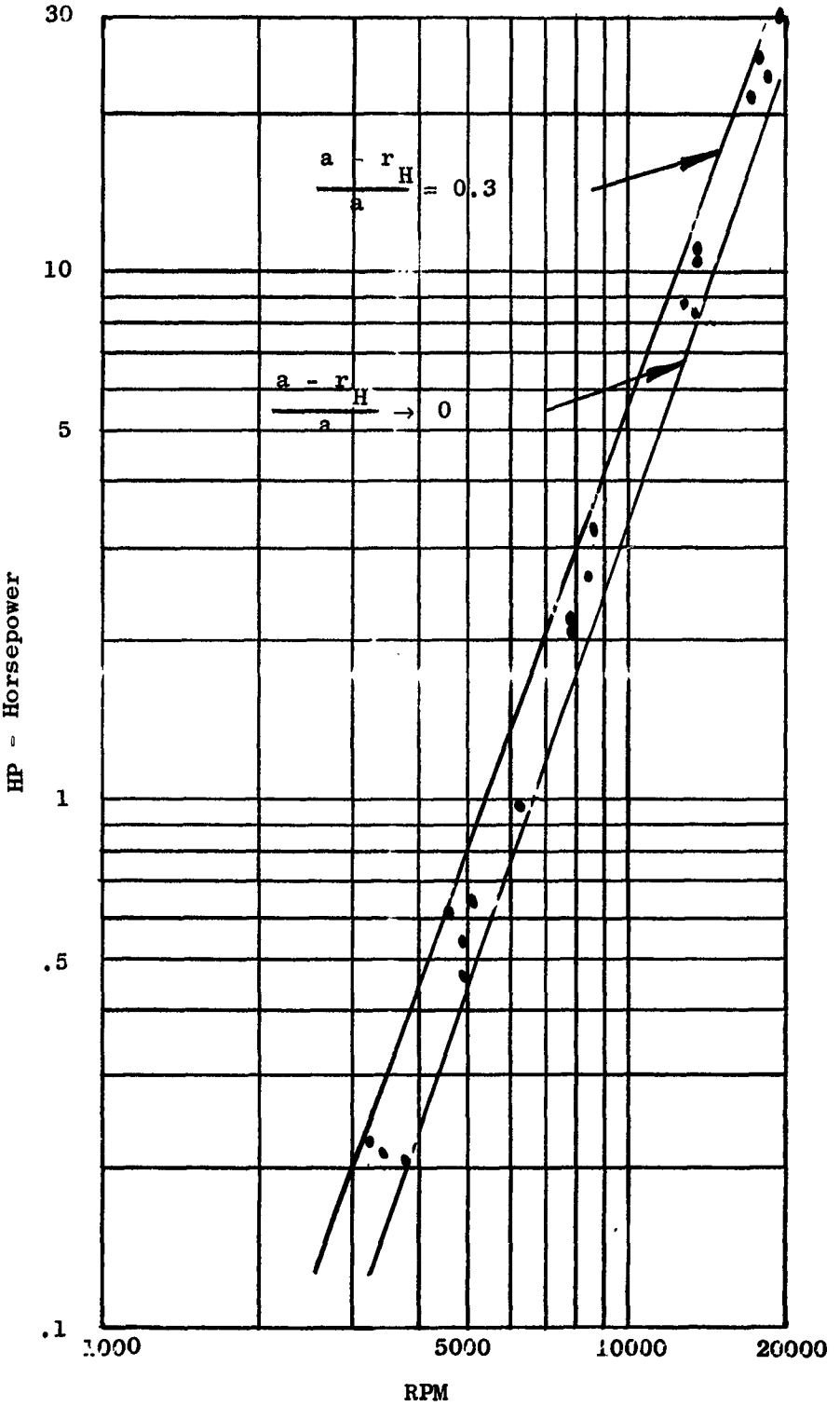

Figure 7e. Slinger Seal Power Requirement, $\frac{r_L}{a} = 0.71$, $\frac{S_L}{a} = 0.092$.

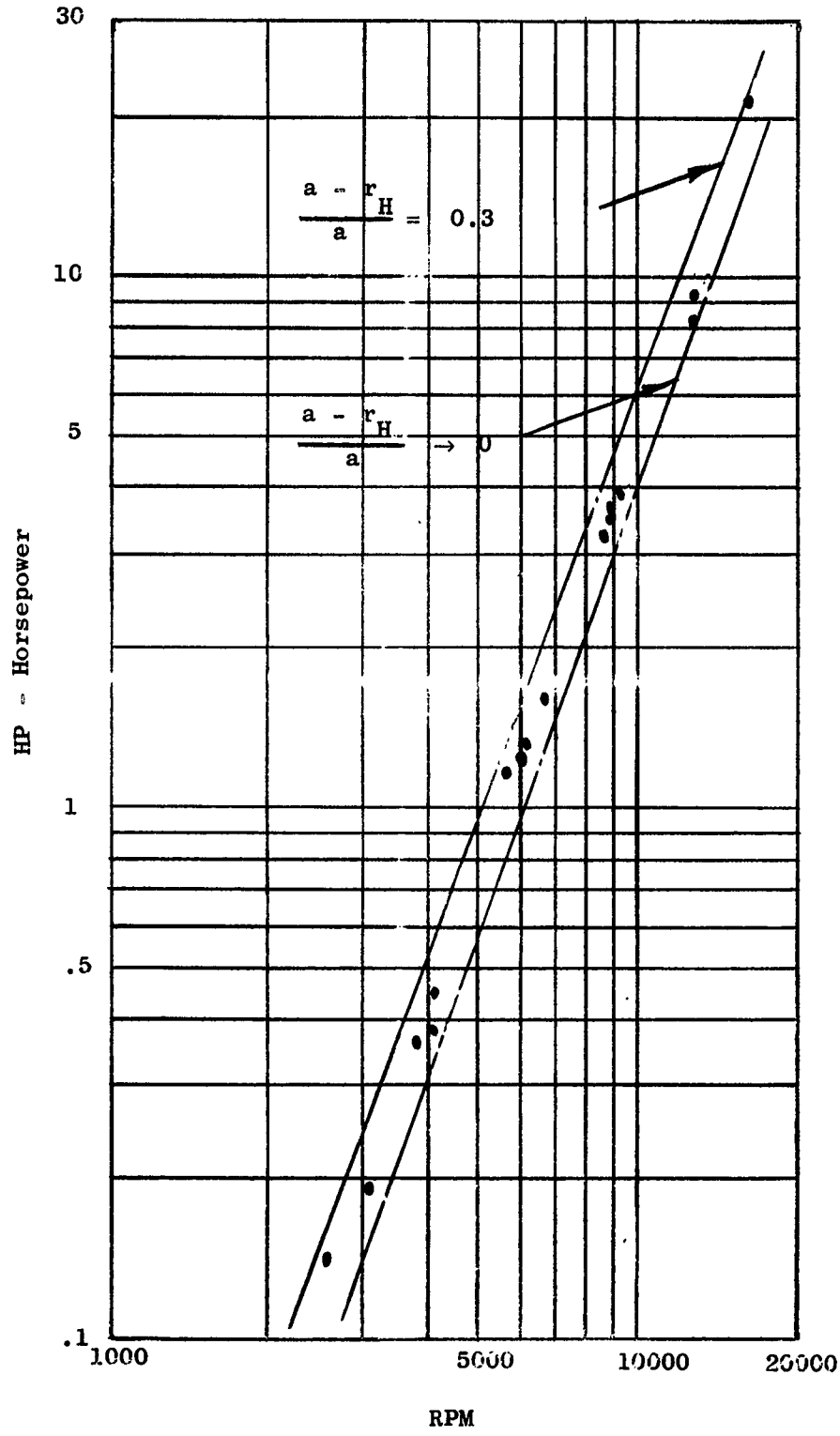

Figure 7f. Slinger Seal Power Requirement, $\frac{r_L}{a} = 0.71$, $\frac{S_L}{a} = 0.019$.

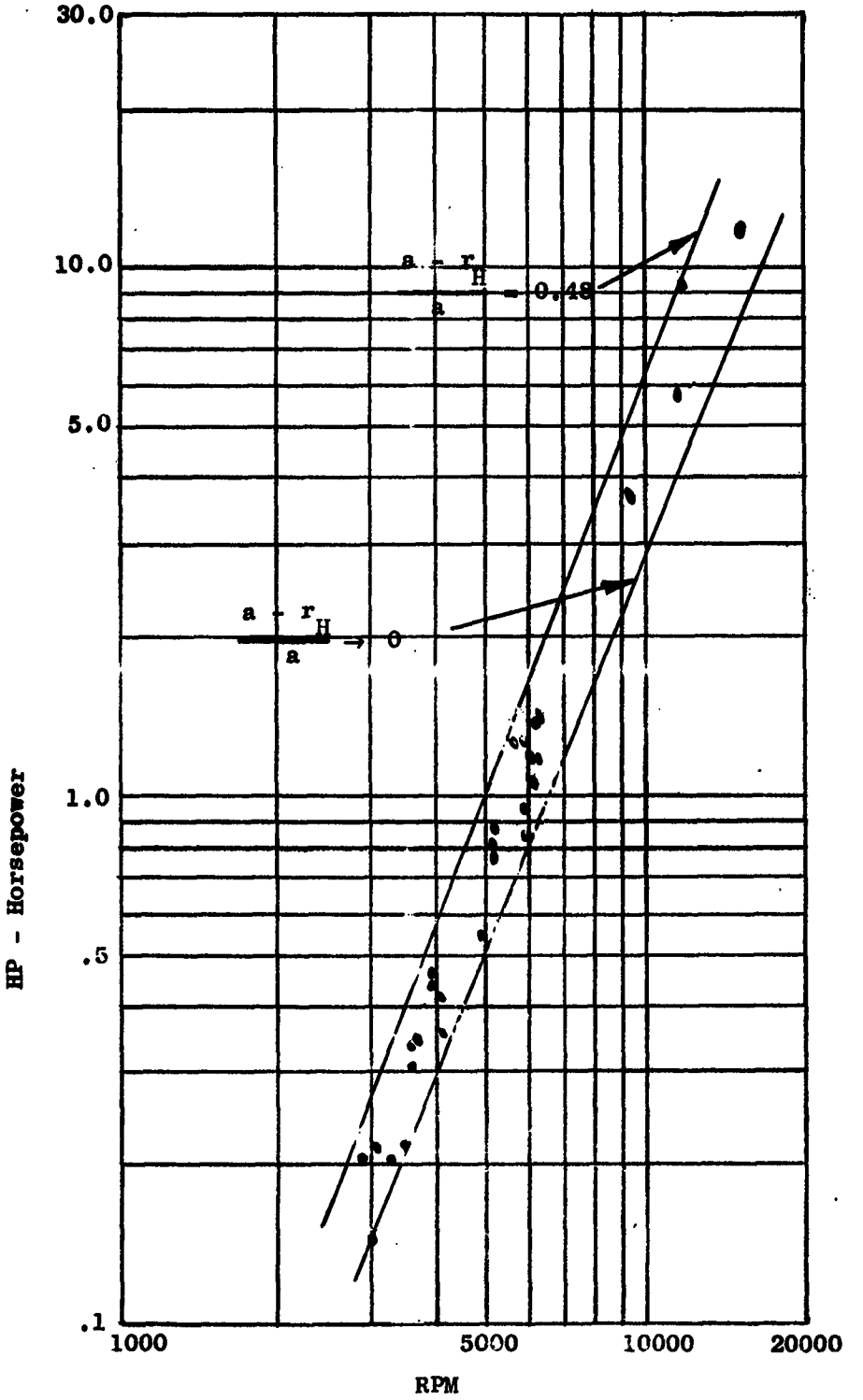

Figure 7g. Slinger Seal Power Requirement, $\frac{r_L}{a} = 0.52$, $\frac{S_L}{a} = 0.167$.

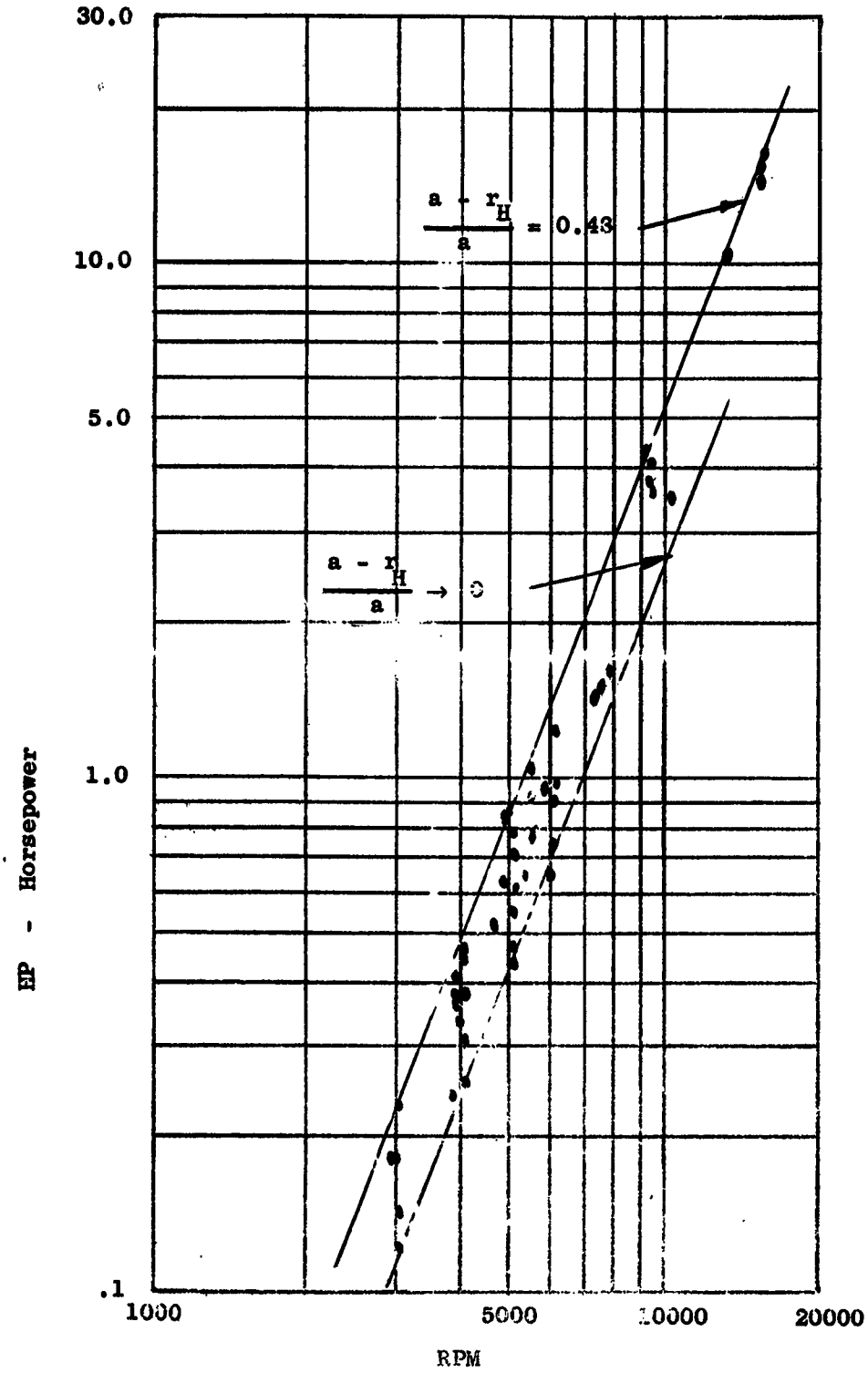

Figure 7h. Slinger Seal Power Requirement, $\frac{r_L}{a} = 0.52$, $\frac{S_L}{a} = 0.092$.

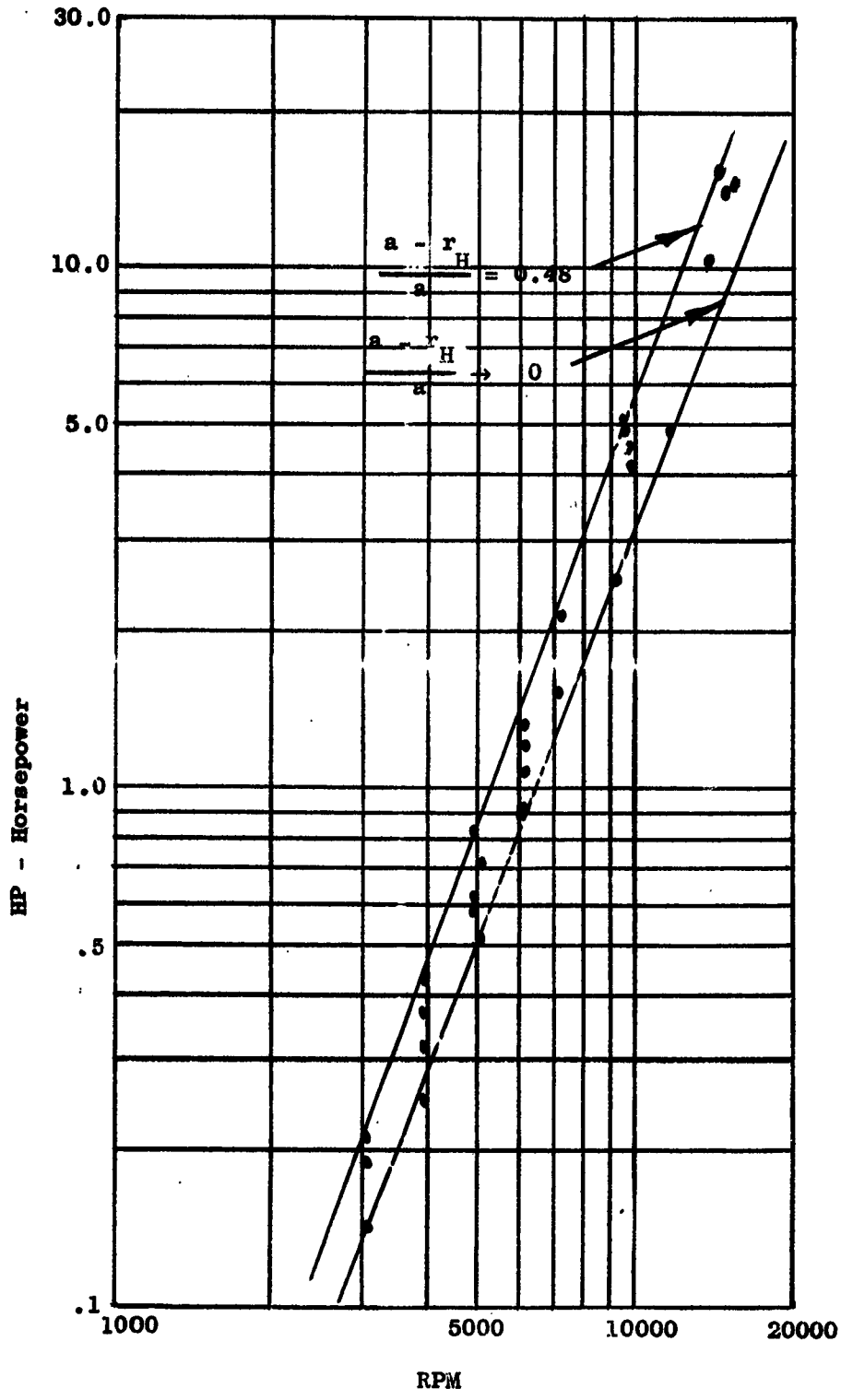

Figure 7i. **Slinger Seal Power Requirement,** $\frac{r_L}{a} = 0.52$, $\frac{S_L}{a} = 0.019$.

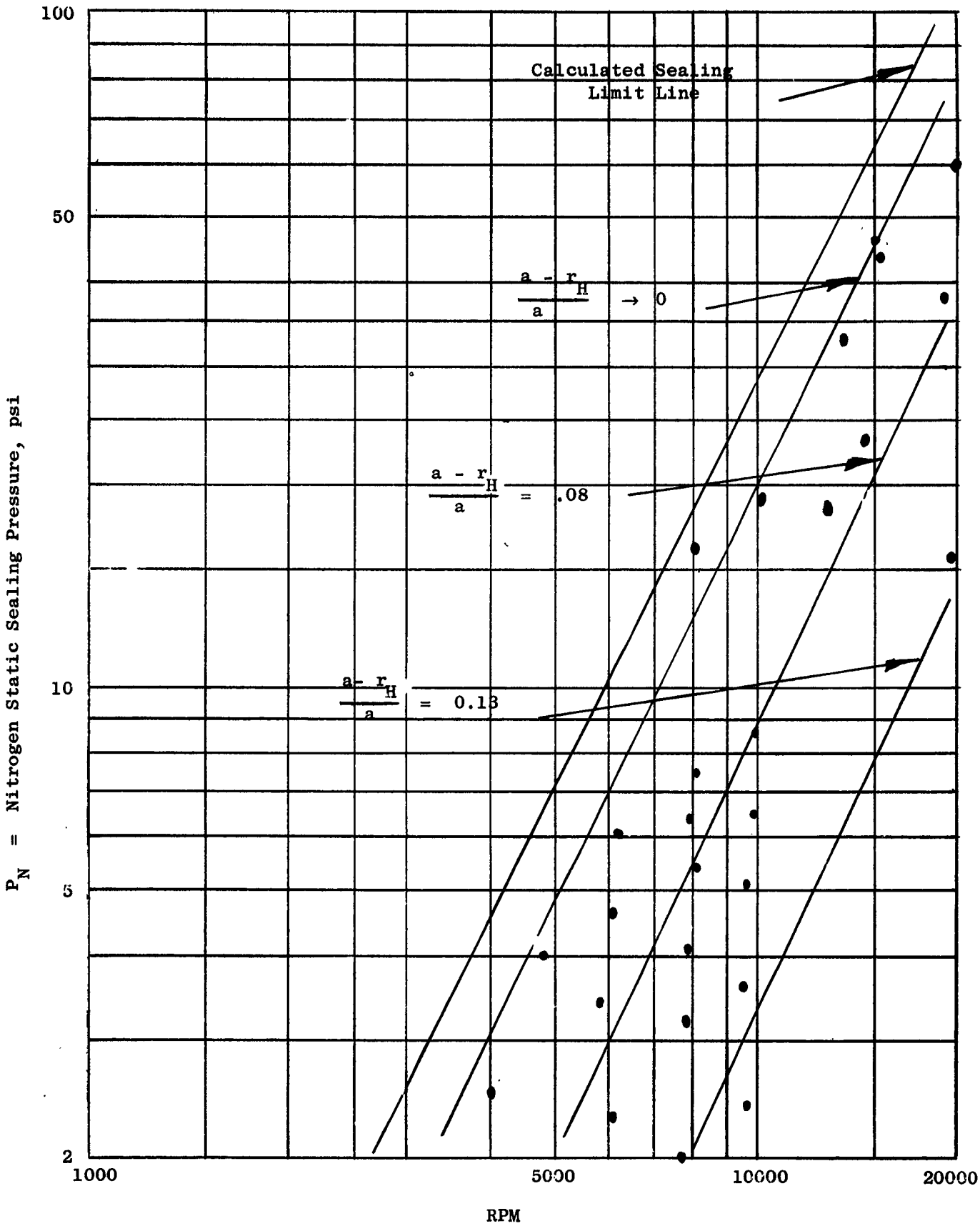

Figure 8a. Slinger Seal Pressure Capacity, $\frac{r_L}{a} = 0.87$, $\frac{S_L}{a} = 0.167$.

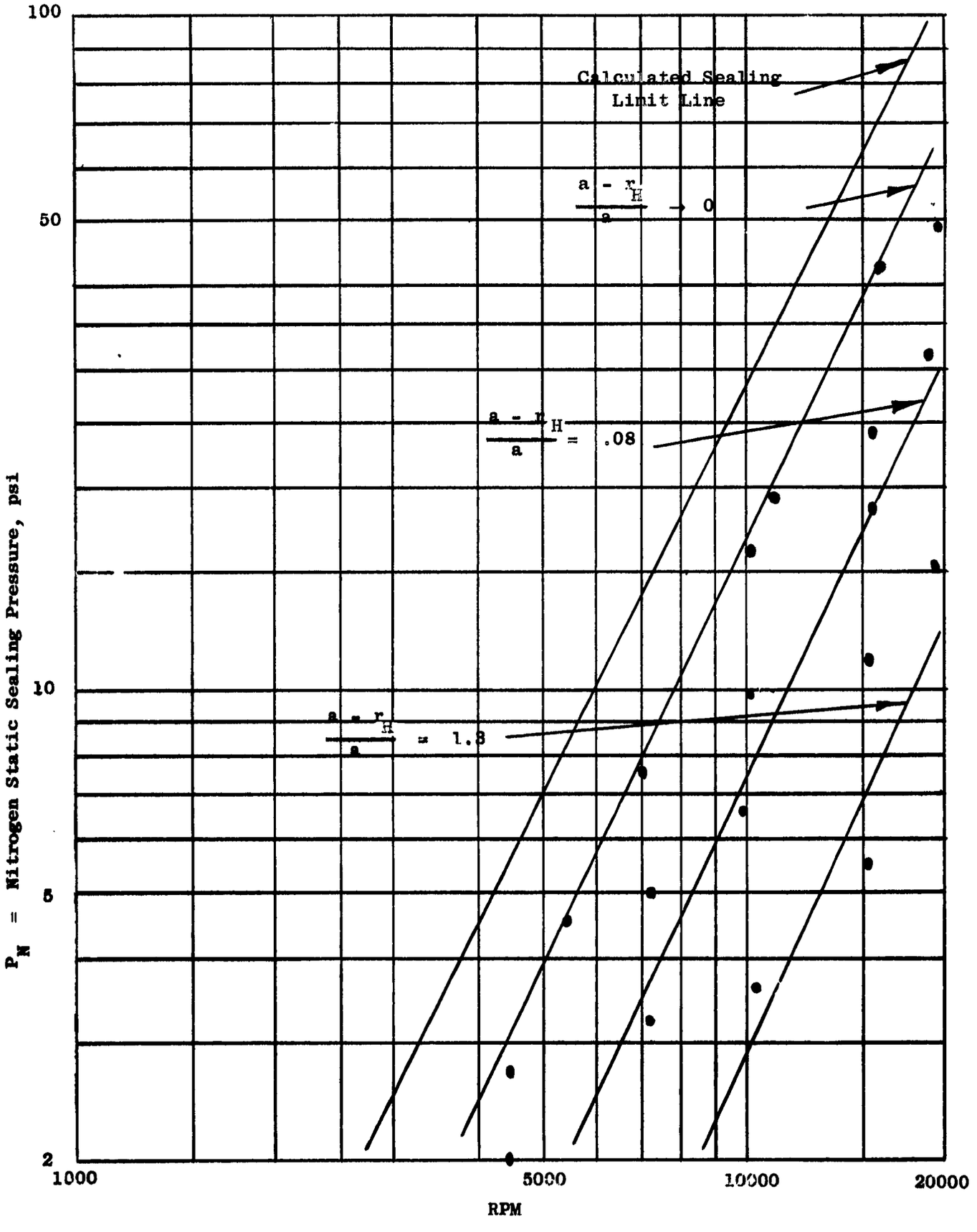

Figure 8b. Slinger Seal Pressure Capacity, $\frac{r_L}{a} = 0.87$, $\frac{S_L}{a} = 0.092$.

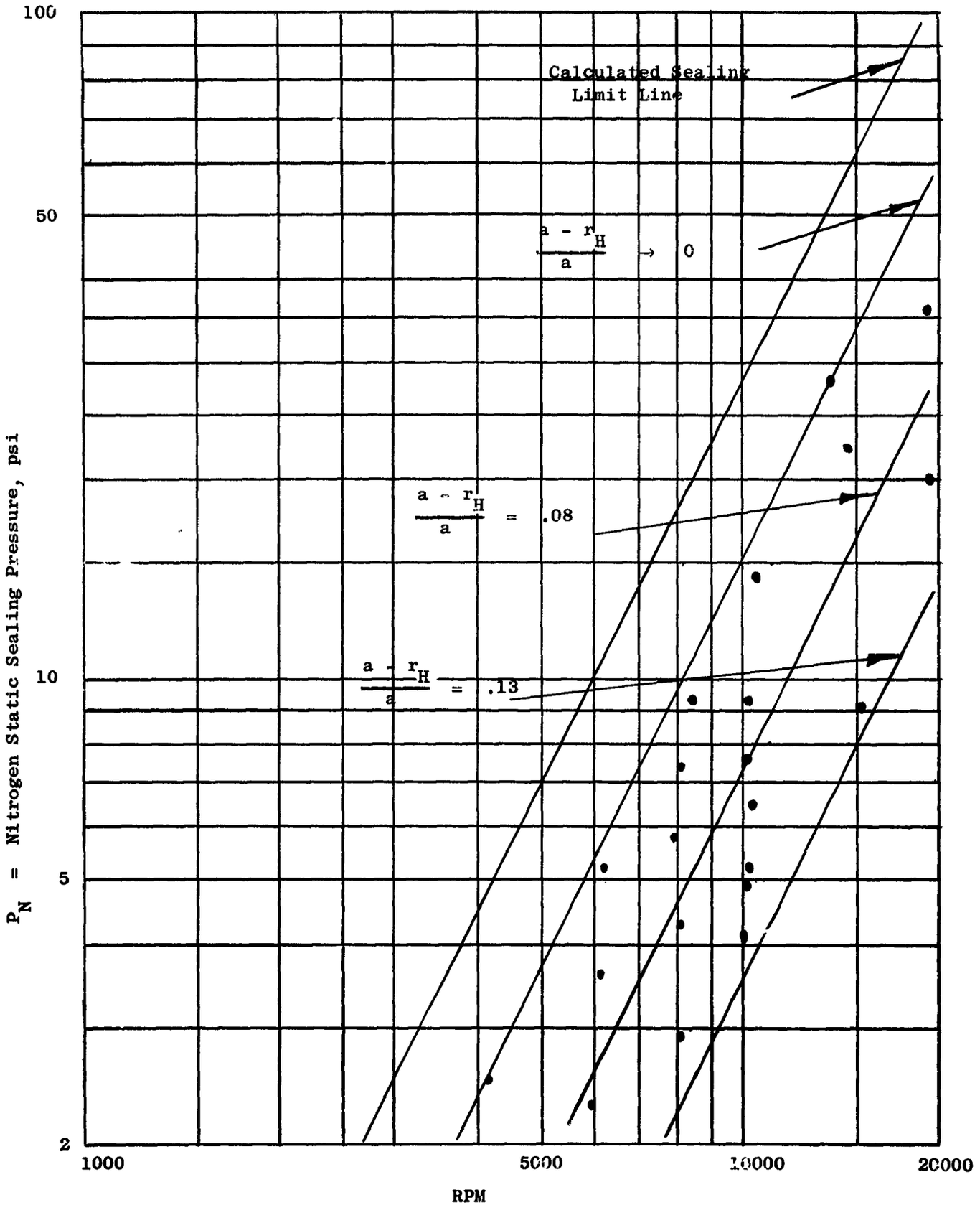

Figure 8c. Slinger Seal Pressure Capacity, $\frac{r_L}{a} = 0.87$, $\frac{S_L}{a} = 0.019$.

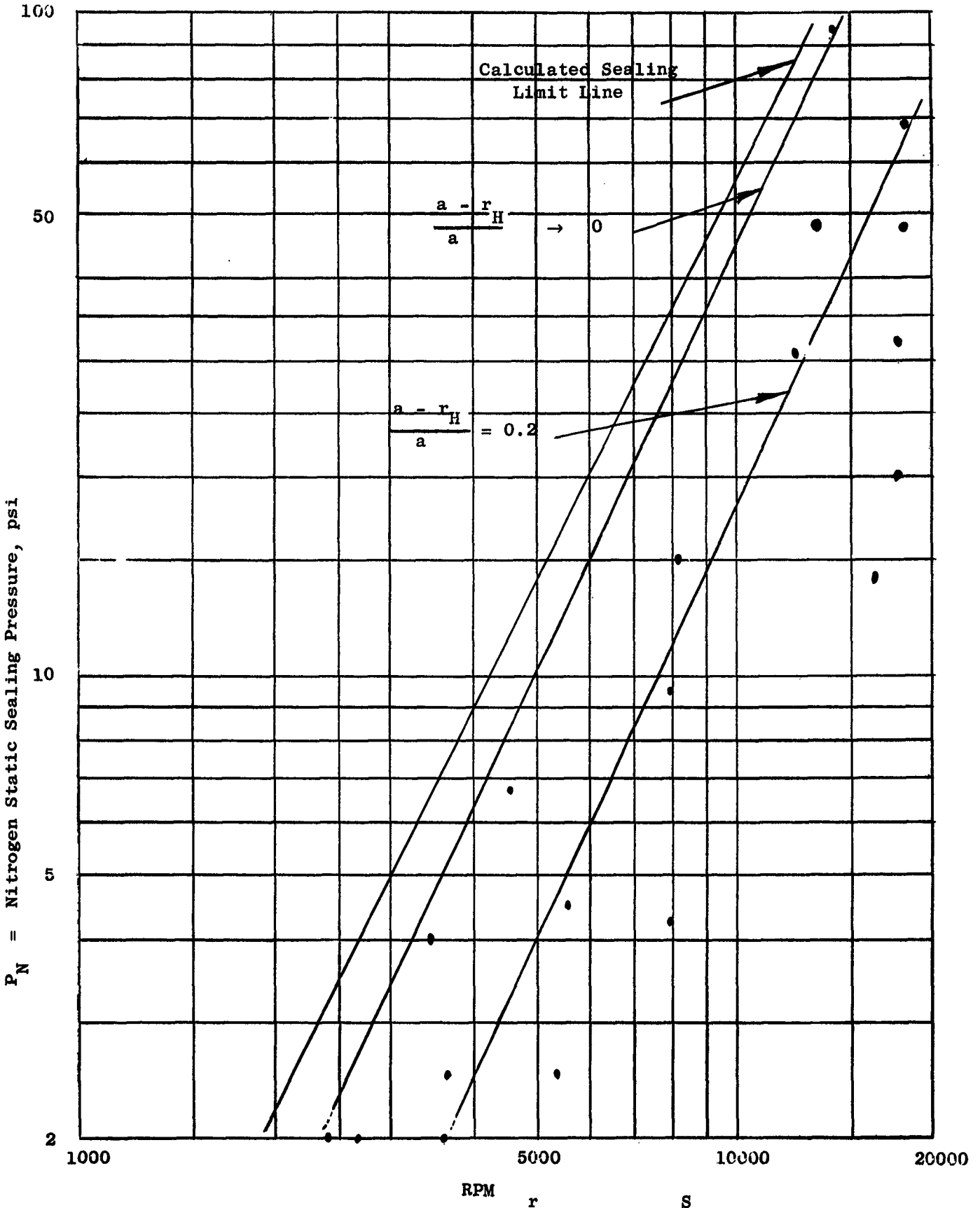

Figure 8d. Slinger Seal Pressure Capacity, $\frac{r_L}{a} = 0.71$, $\frac{S_L}{a} = 0.167$.

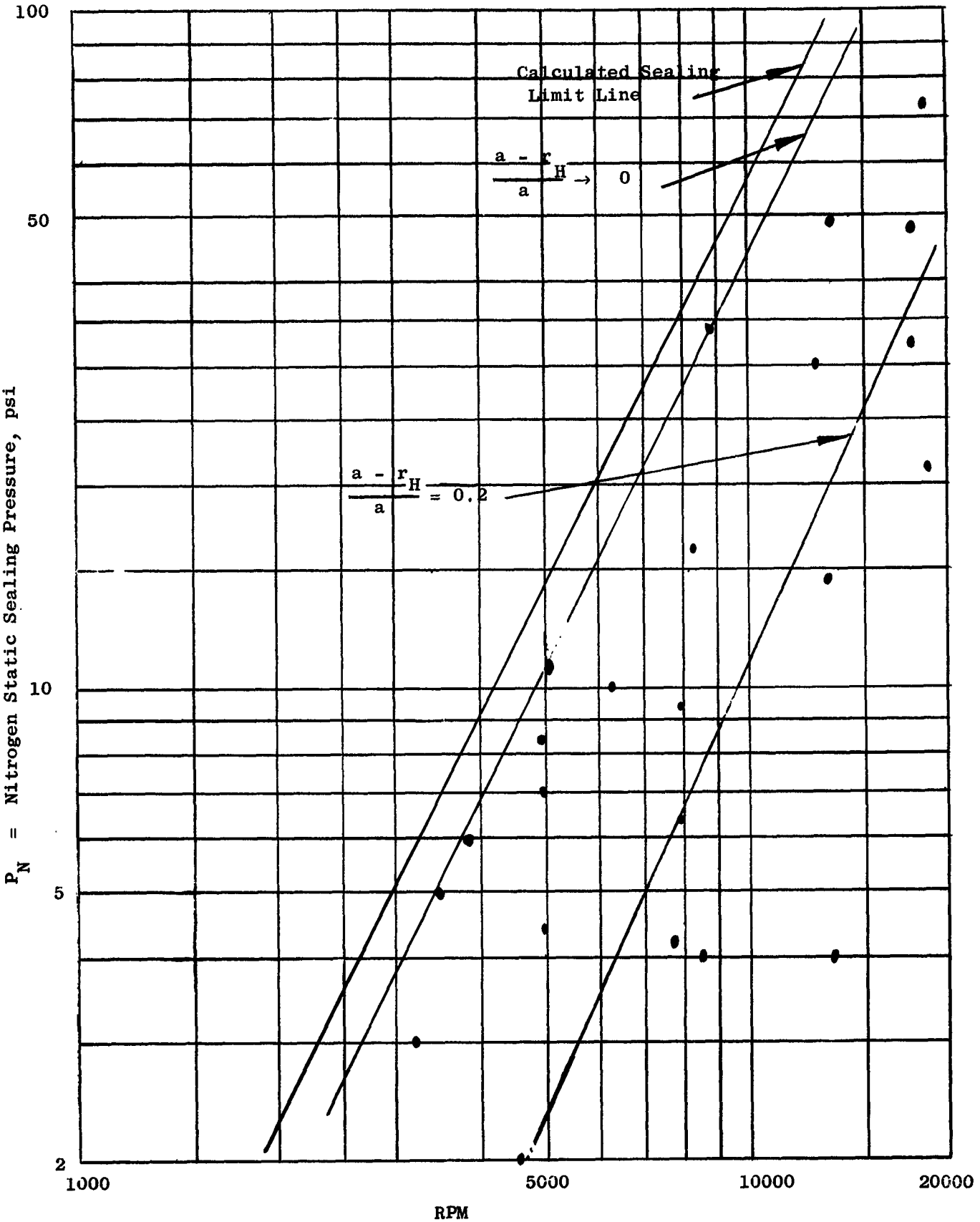

Figure 8e. Slinger Seal Pressure Capacity, $\frac{r_L}{a} = 0.71$, $\frac{S_L}{a} = 0.092$.

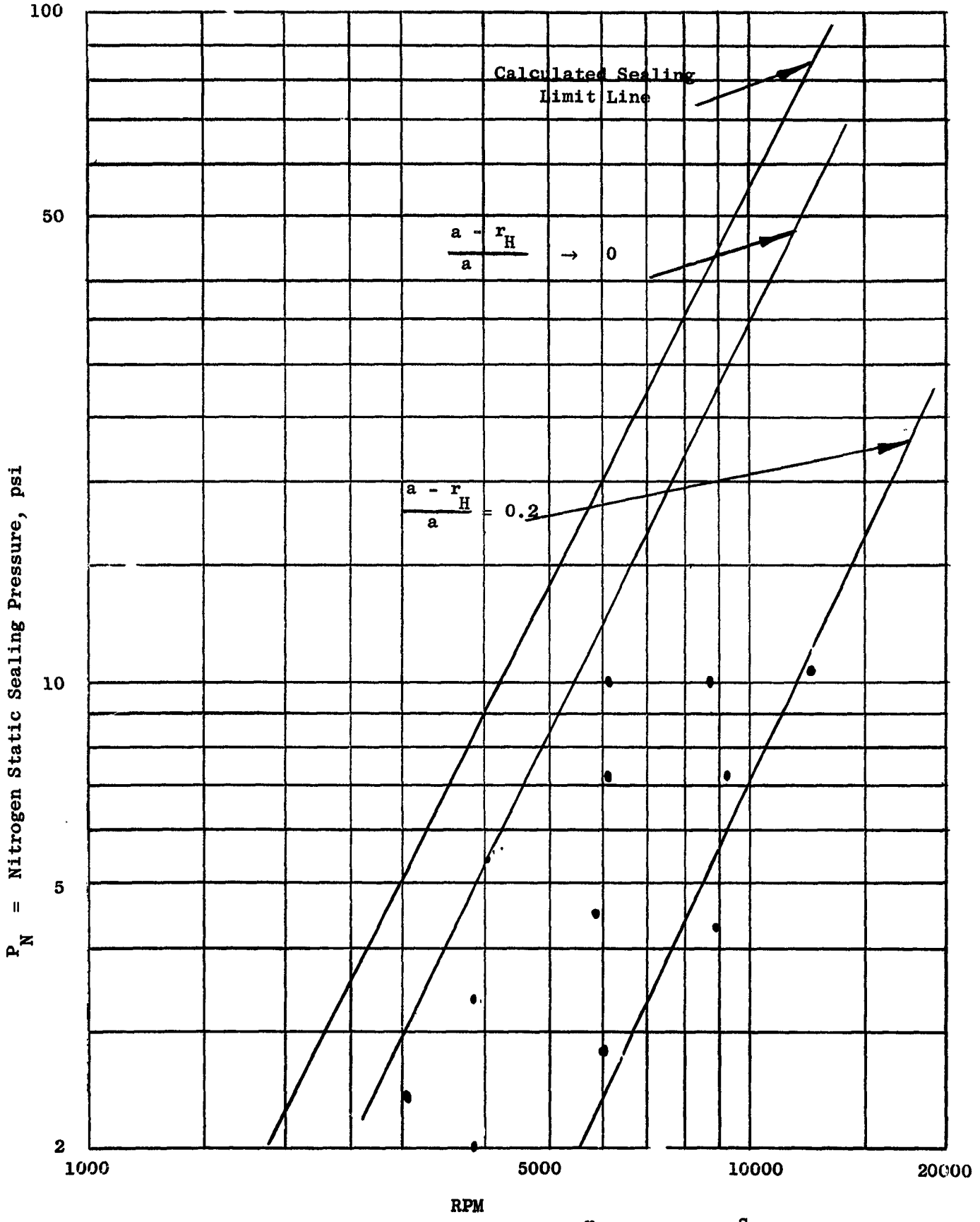

Figure 8f. Slinger Seal Pressure Capacity, $\frac{r_{\cdot}}{a} = 0.71$, $\frac{S_L}{a} = 0.019$.

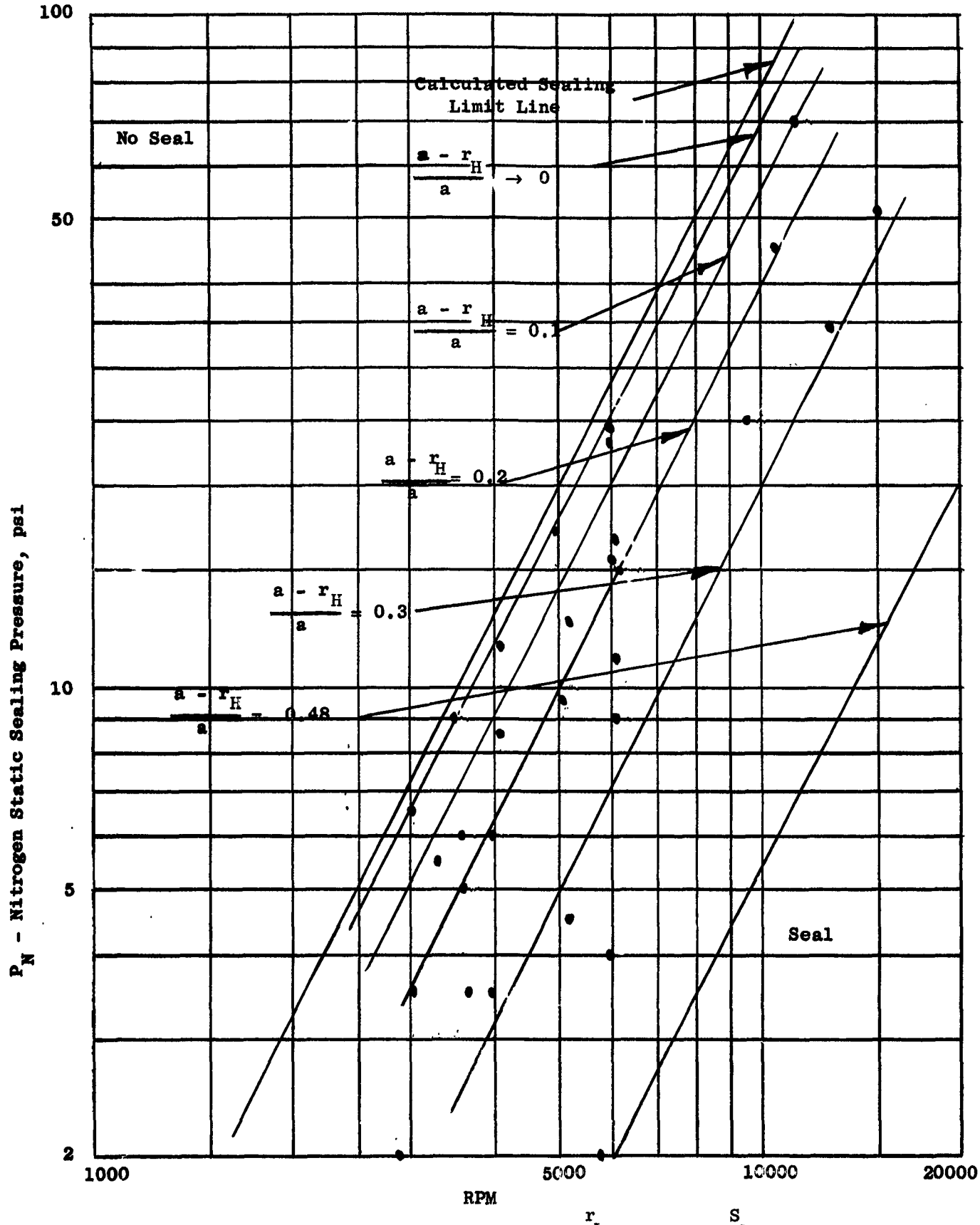

Figure 8g. Slinger Seal Pressure Capacity, $\frac{r_L}{a} = 0.52$, $\frac{S_L}{a} = 0.167$.

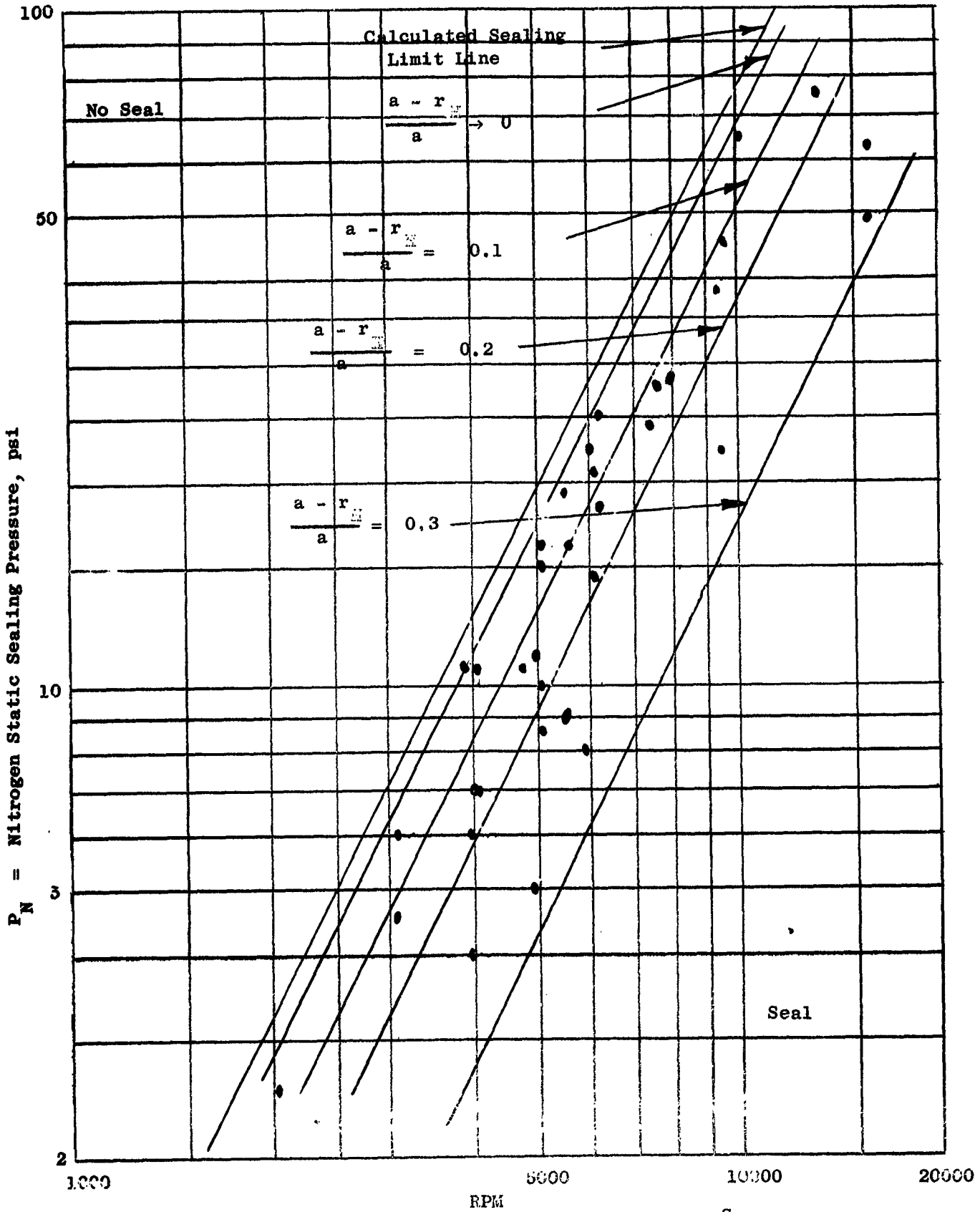

Figure 8h. Slinger Seal Pressure Capacity, $\frac{r_L}{a} = 0.52$, $\frac{S_L}{a} = 0.092$.

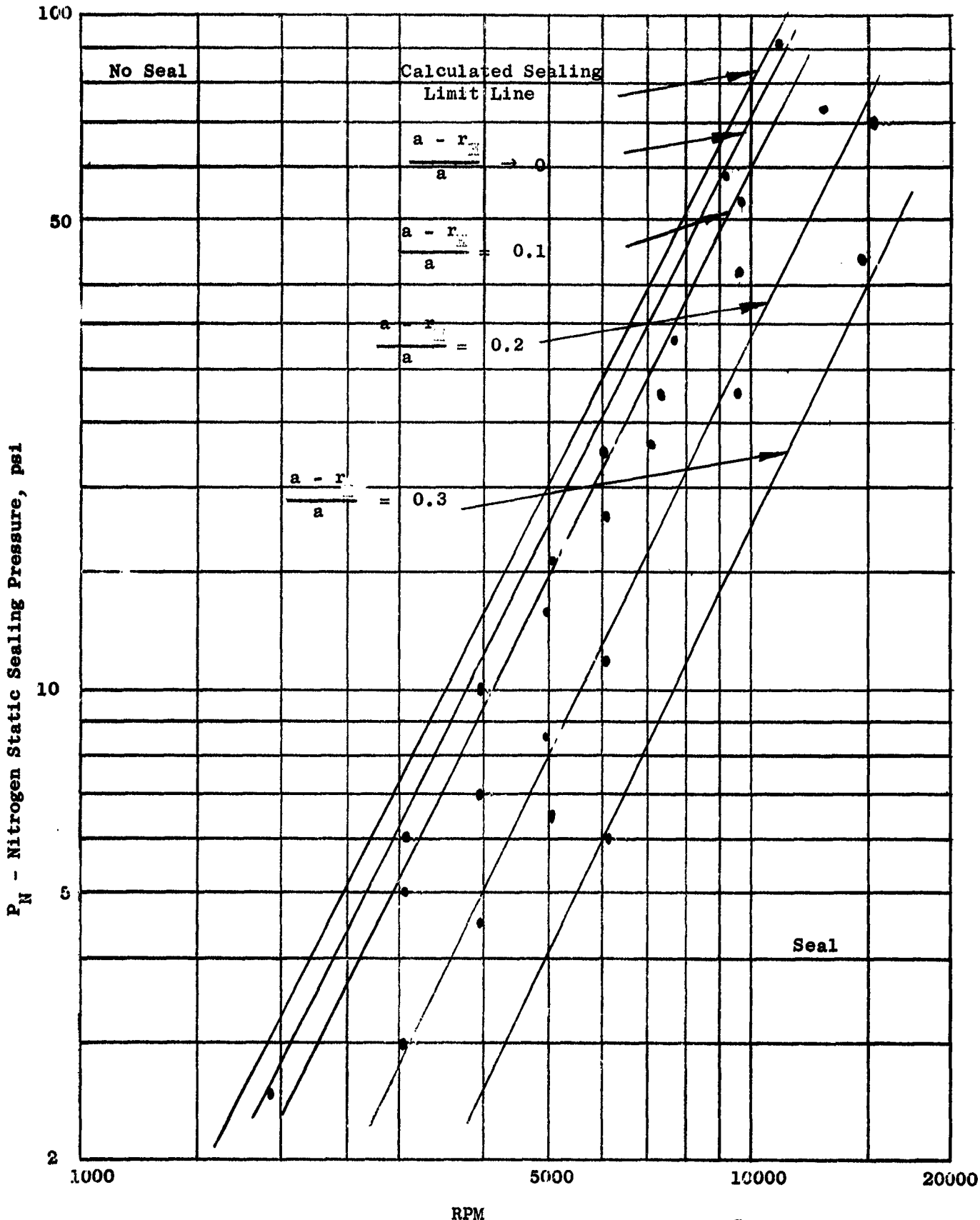

Figure 8i. Slinger Seal Pressure Capacity, $\frac{r_1}{a} = 0.52$, $\frac{S}{a} = 0.019$.

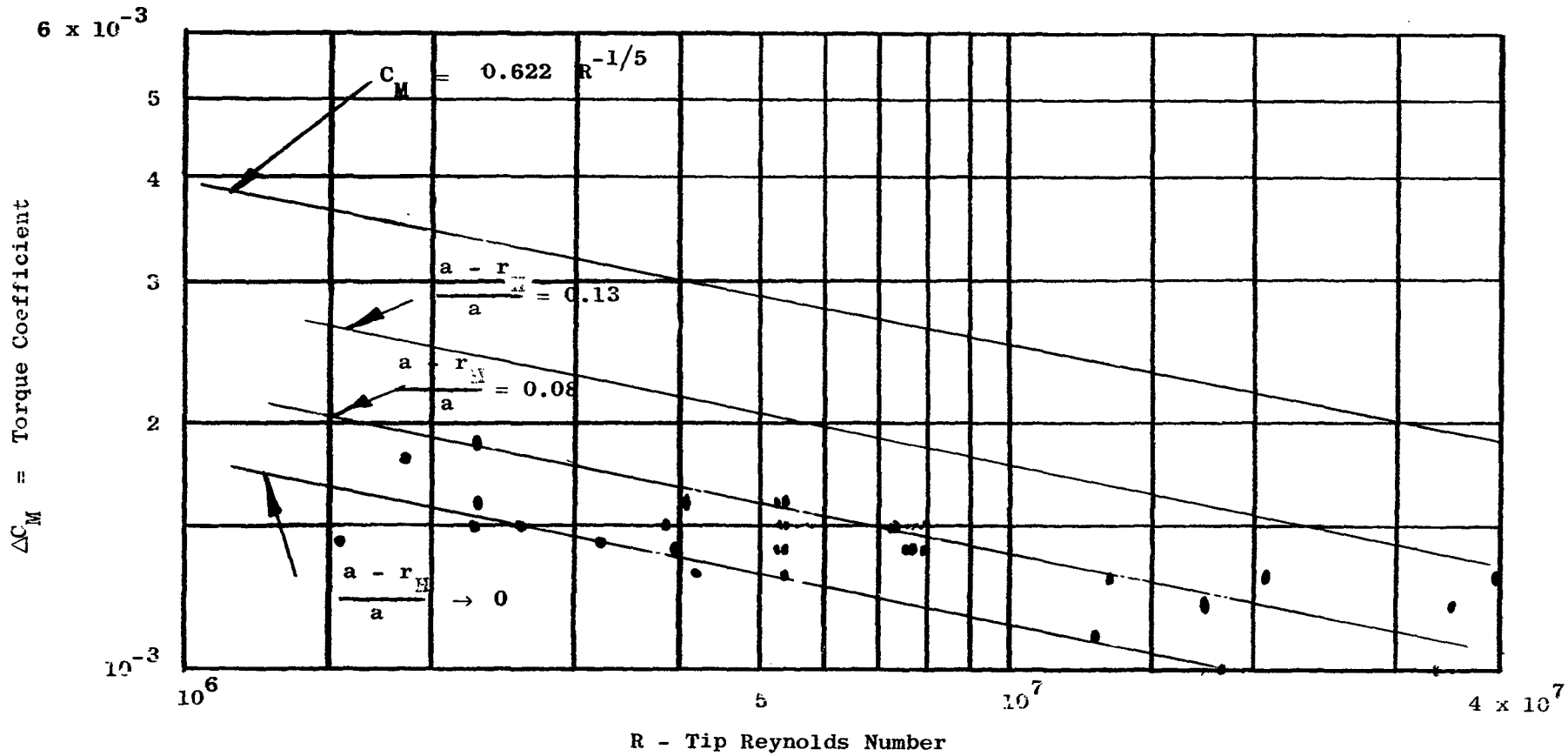

Figure 9a. Slinger Seal Torque Coefficient, $\frac{r_L}{a} = 0.87$, $\frac{S_L}{a} = 0.167$.

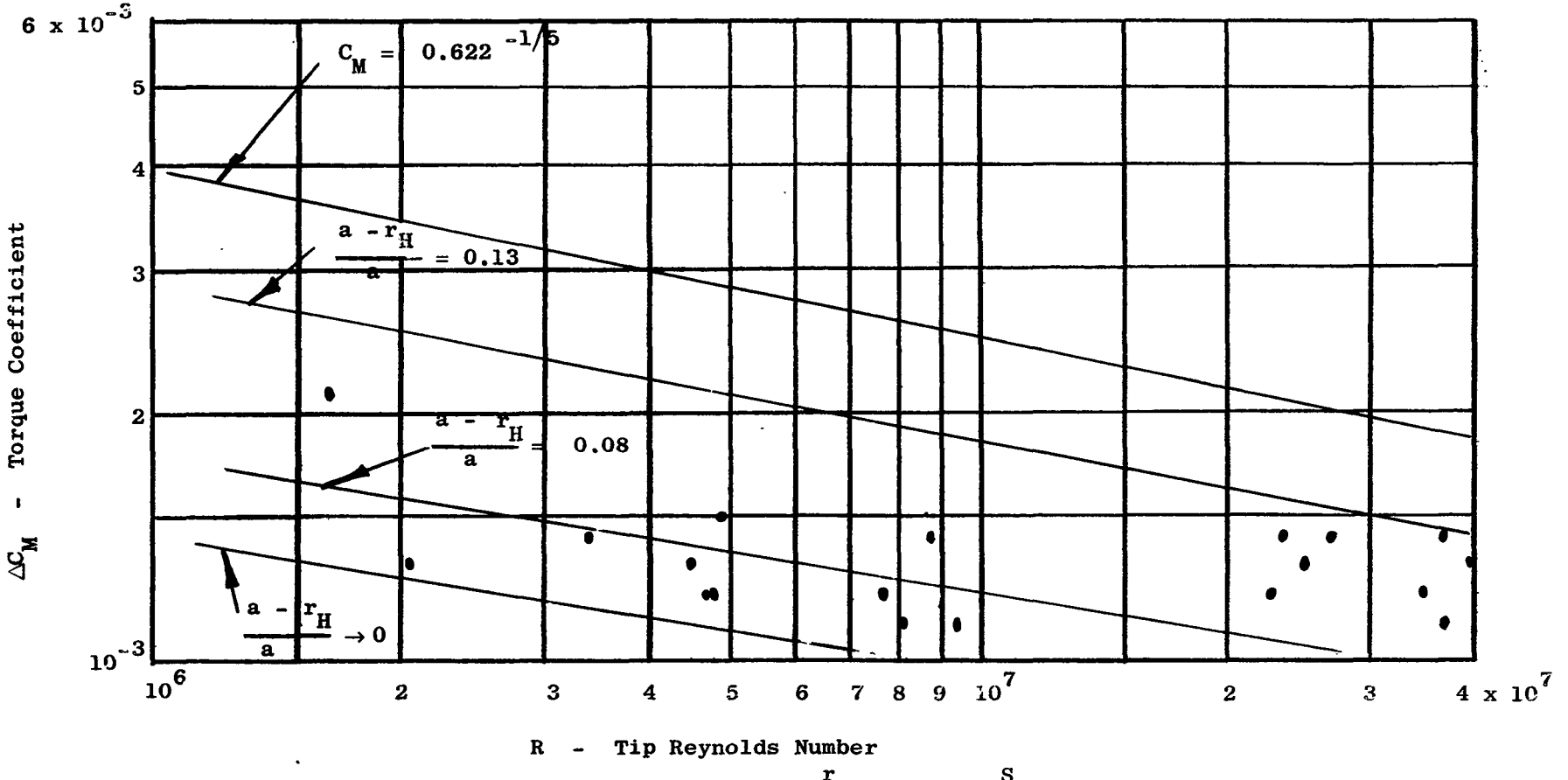

Figure 9b. Slinger Seal Torque Coefficient, $\frac{r_L}{a} = 0.87$, $\frac{S_L}{a} = 0.092$.

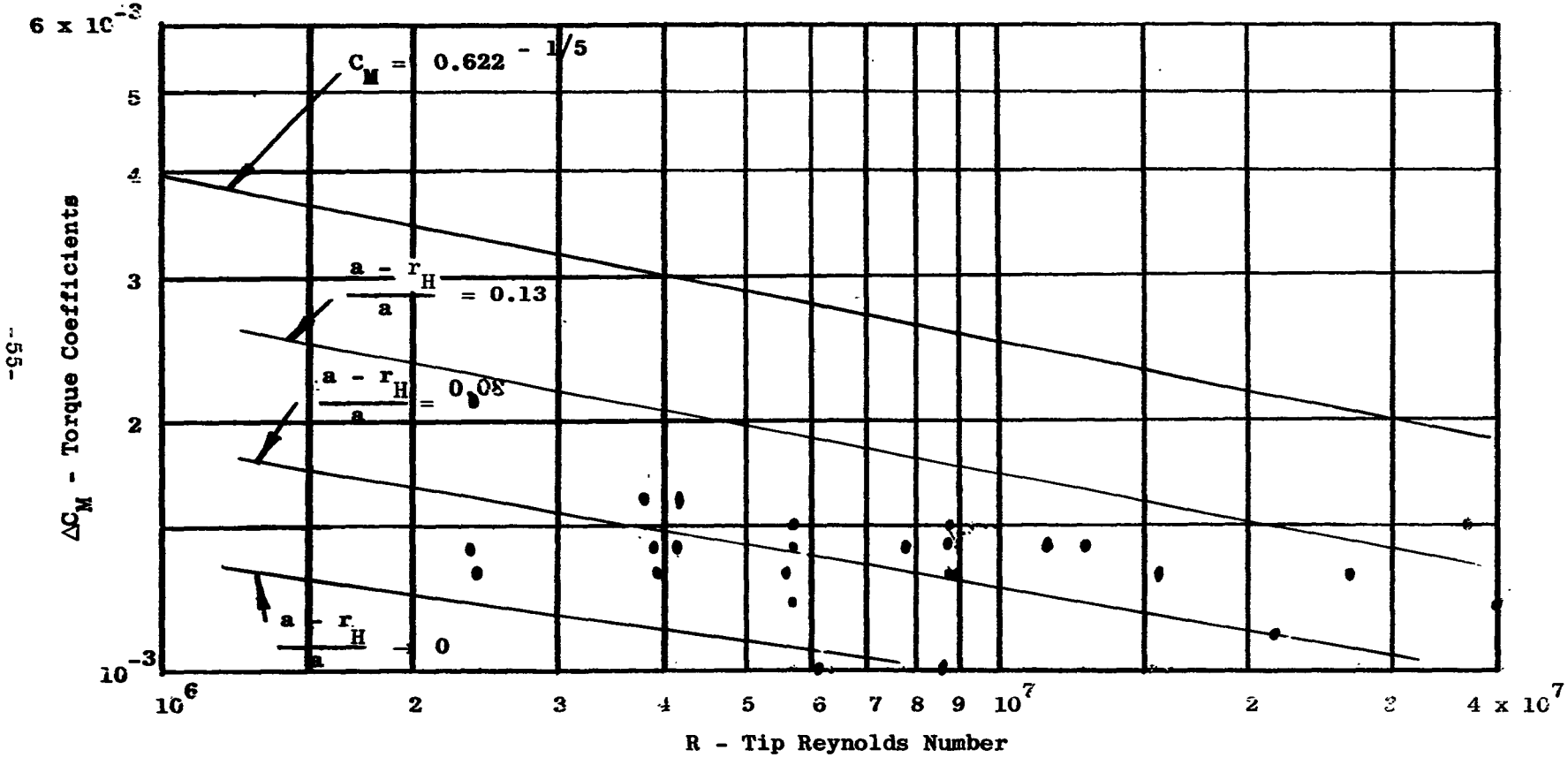

Figure 9c. Slinger Seal Torque Coefficient, $\frac{r_L}{a}$ = 0.87, $\frac{S_L}{a}$ = 0.019.

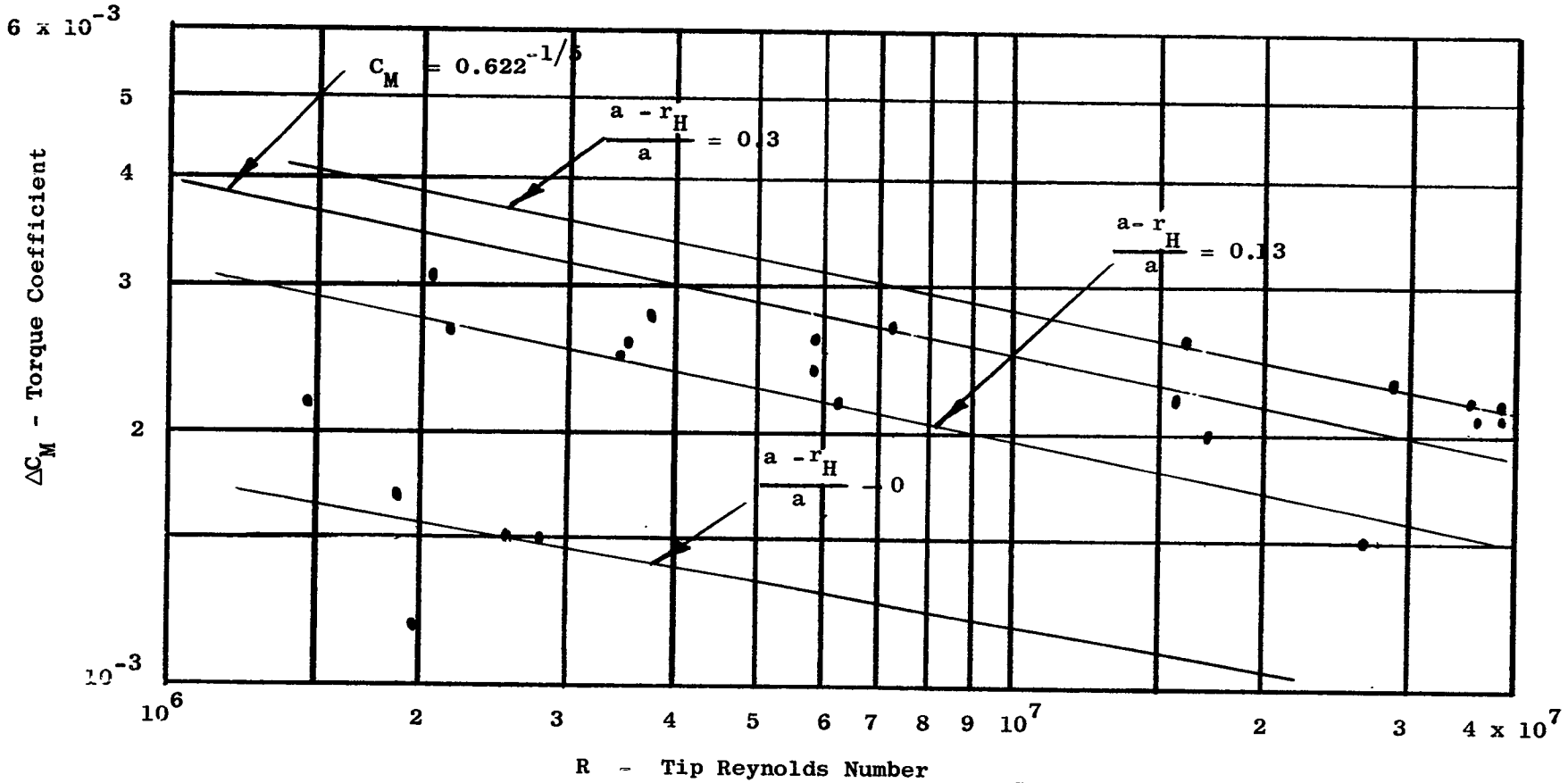

Figure 9d. Slinger Seal Torque Coefficient, $\frac{r_L}{a} = 0.71$, $\frac{S_L}{a} = 0.167$.

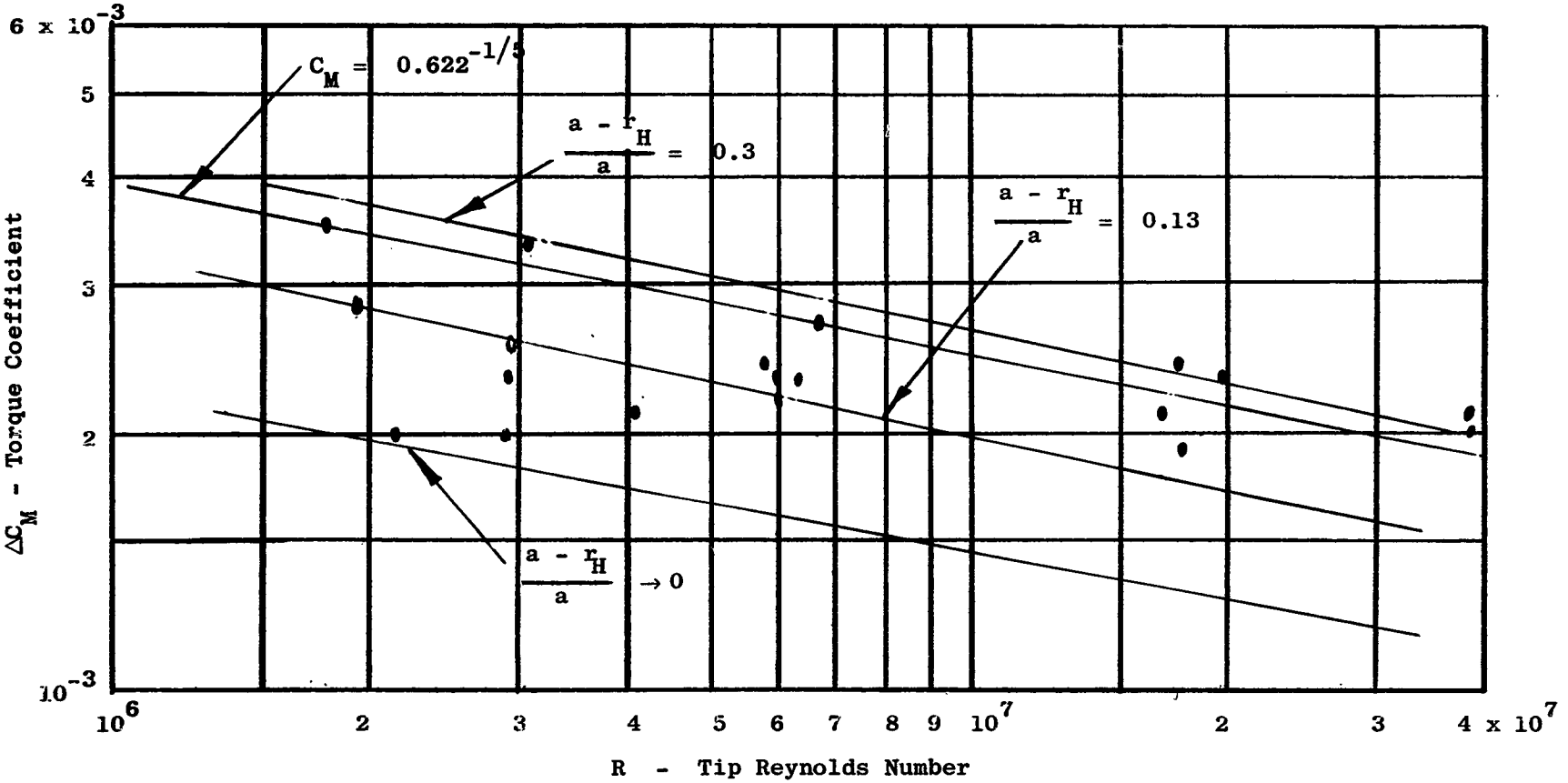

Figure 9e. Slinger Seal Torque Coefficient, $\frac{r_L}{a} = 0.71$, $\frac{S_L}{a} = 0.092$.

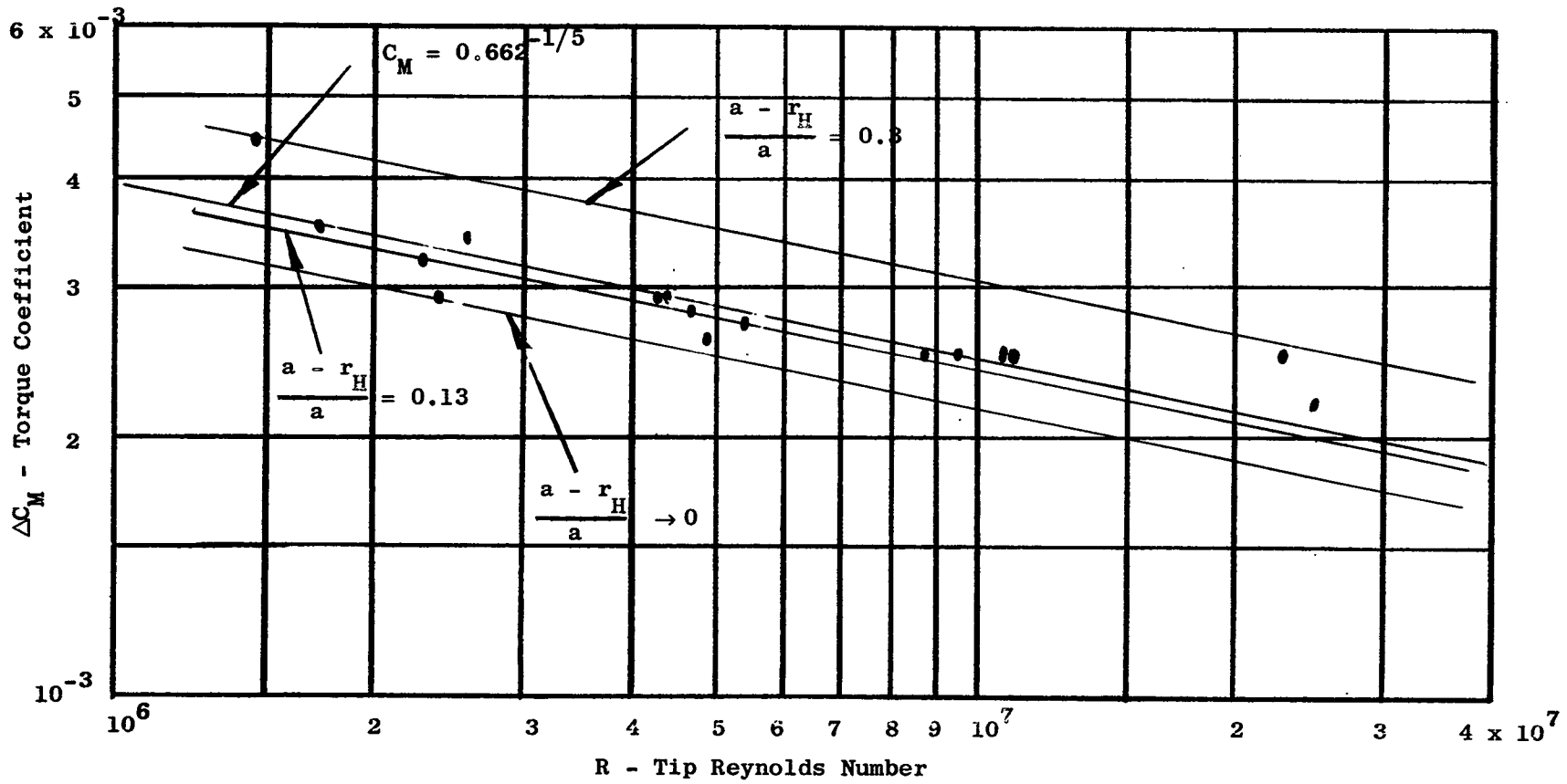

Figure 9f. Slinger Seal Torque Coefficient, $\frac{r_L}{a} = 0.71$, $\frac{S_L}{a} = 0.019$.

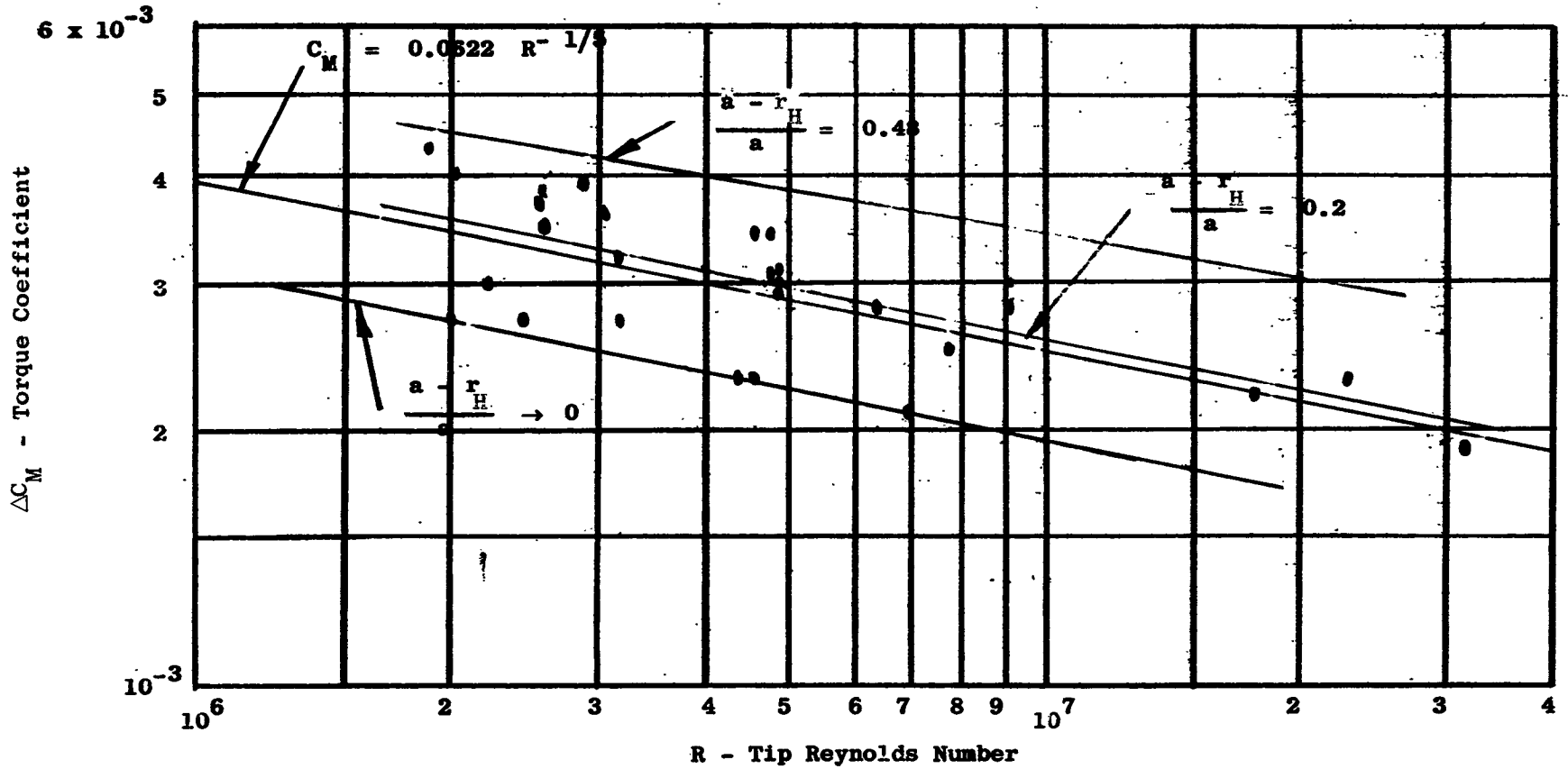

Figure 9g. Slinger Seal Torque Coefficient, $\frac{r_L}{a} = 0.52$, $\frac{S_L}{a} = 0.167$.

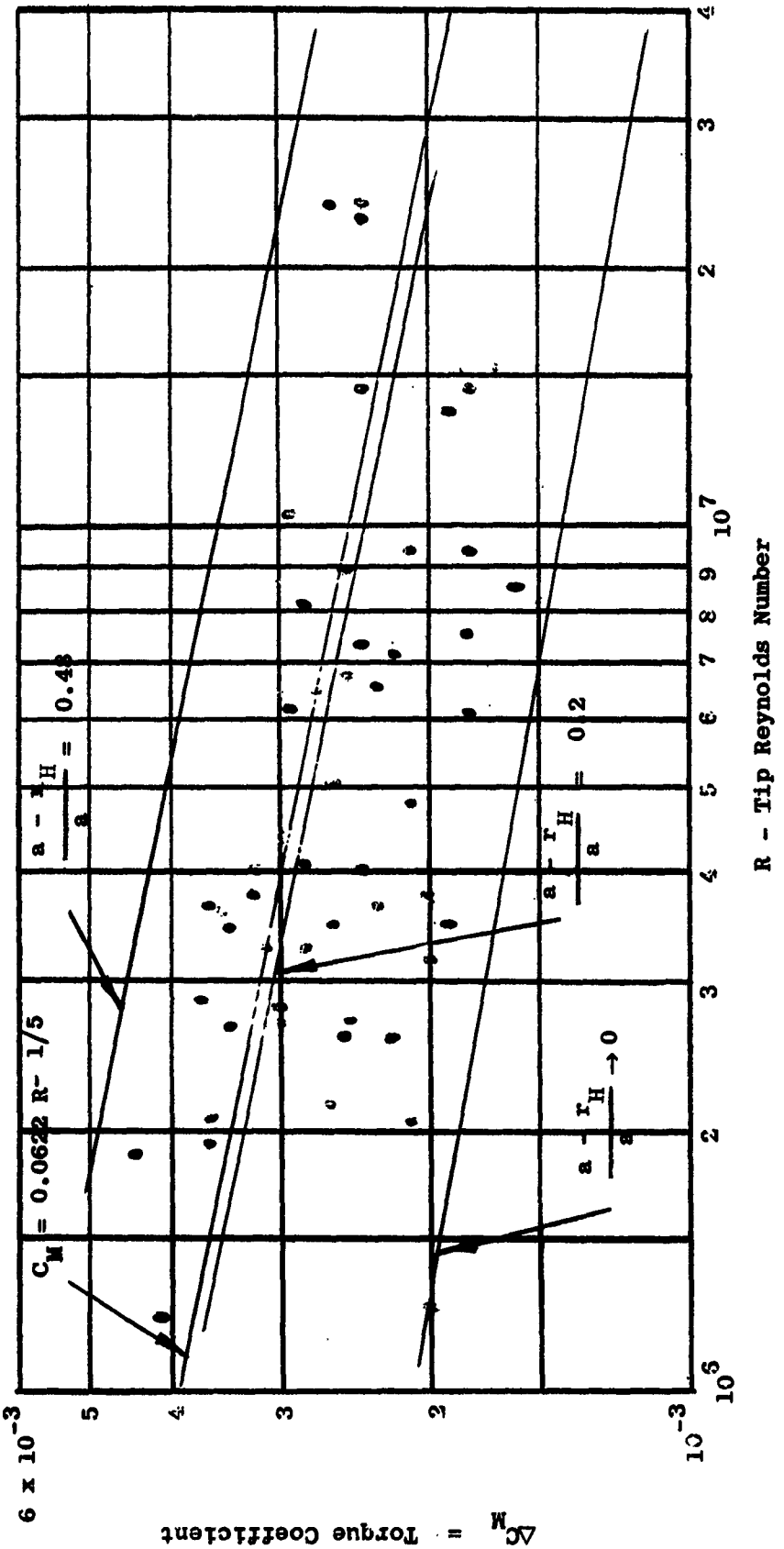

Figure 9h. Slinger Seal Torque Coefficient, $\frac{r_L}{a} = 0.52$, $\frac{S_L}{a} = 0.092$.

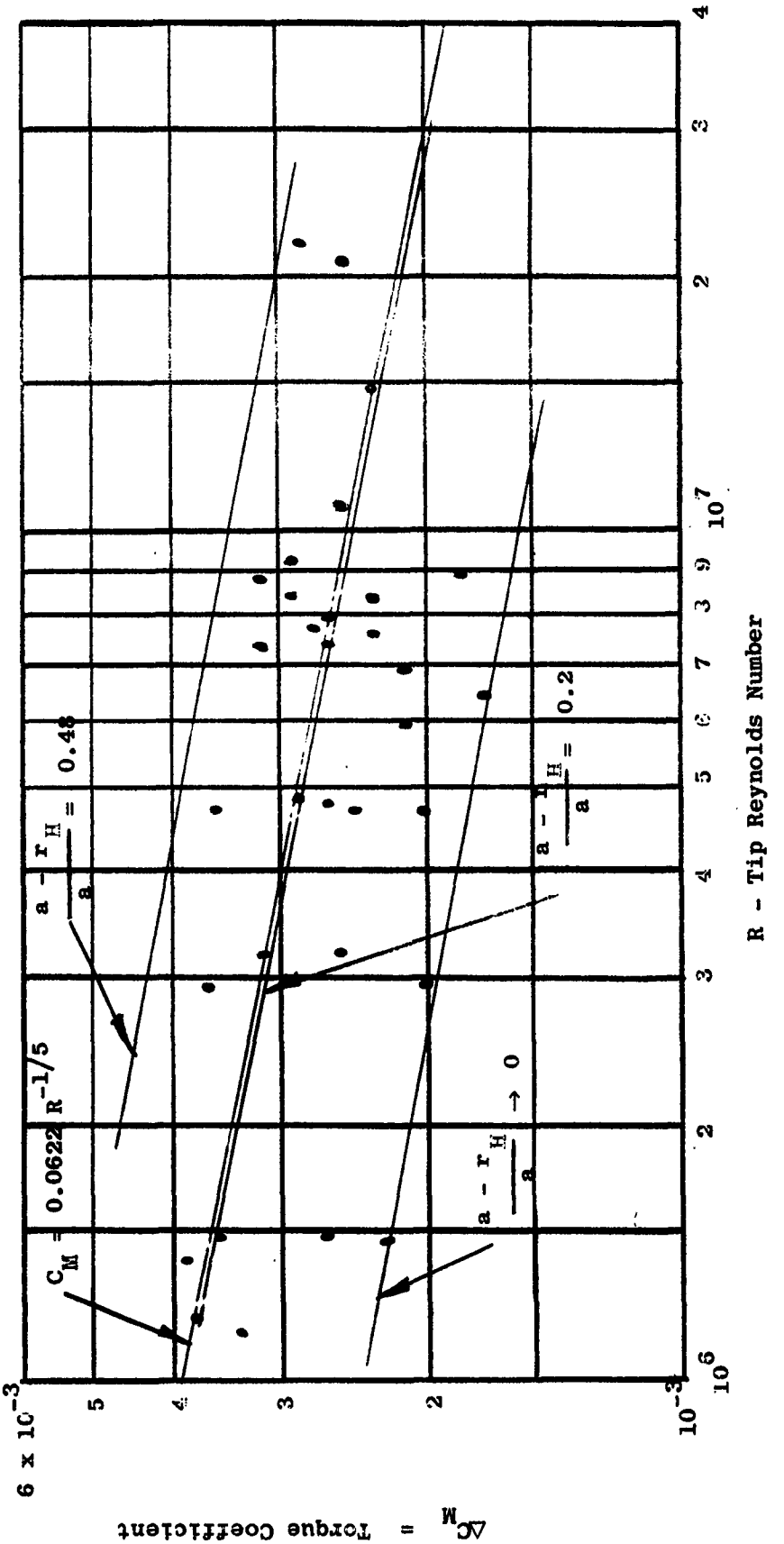

Figure 9i. Slinger Seal Torque Coefficient, $\frac{r_L}{a} = 0.52$, $\frac{S_L}{a} = 0.019$.

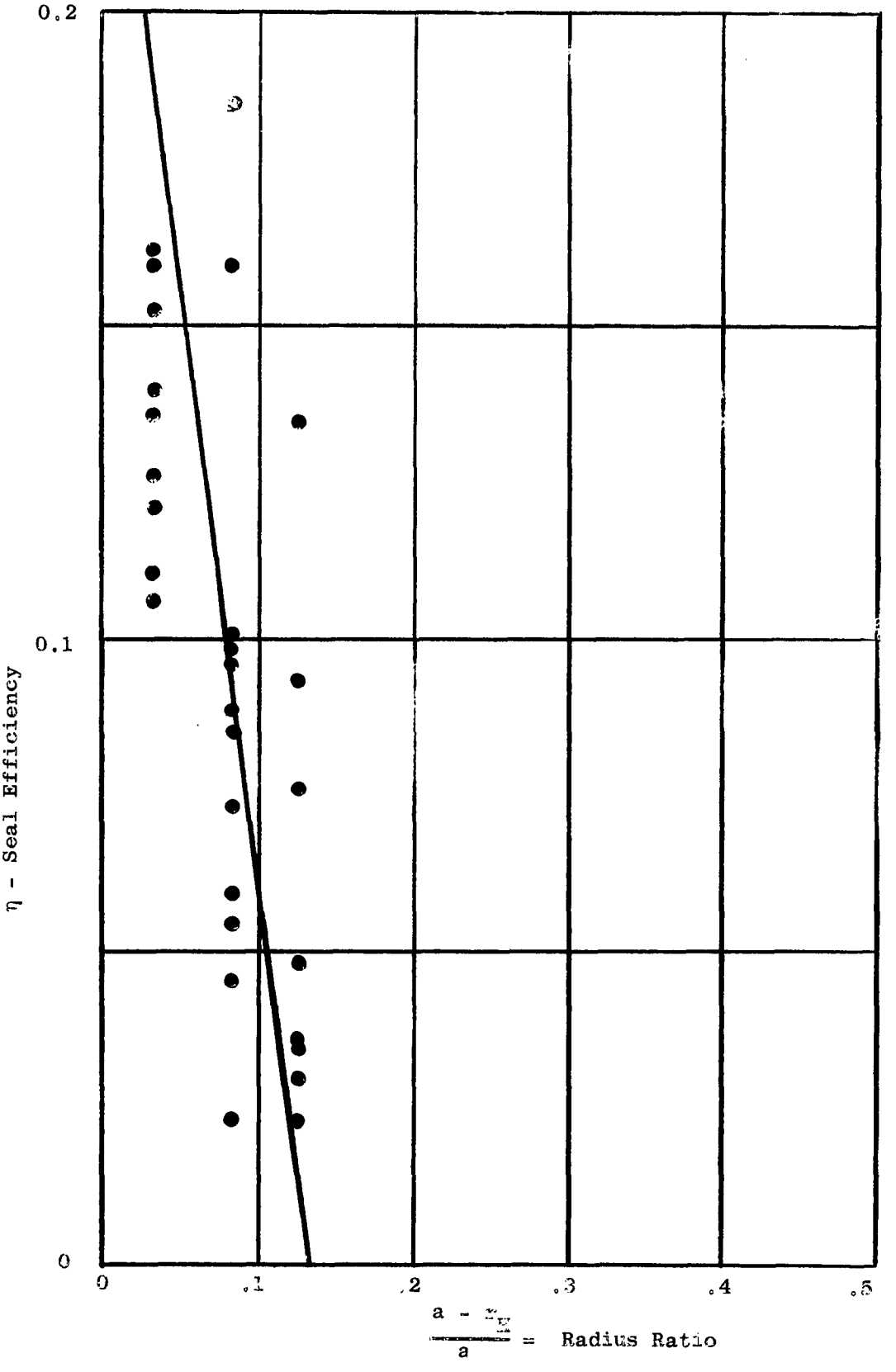

Figure 10a. Slinger Seal Efficiency, $\frac{r_L}{a} = 0.87$, $\frac{S_L}{a} = 0.167$.

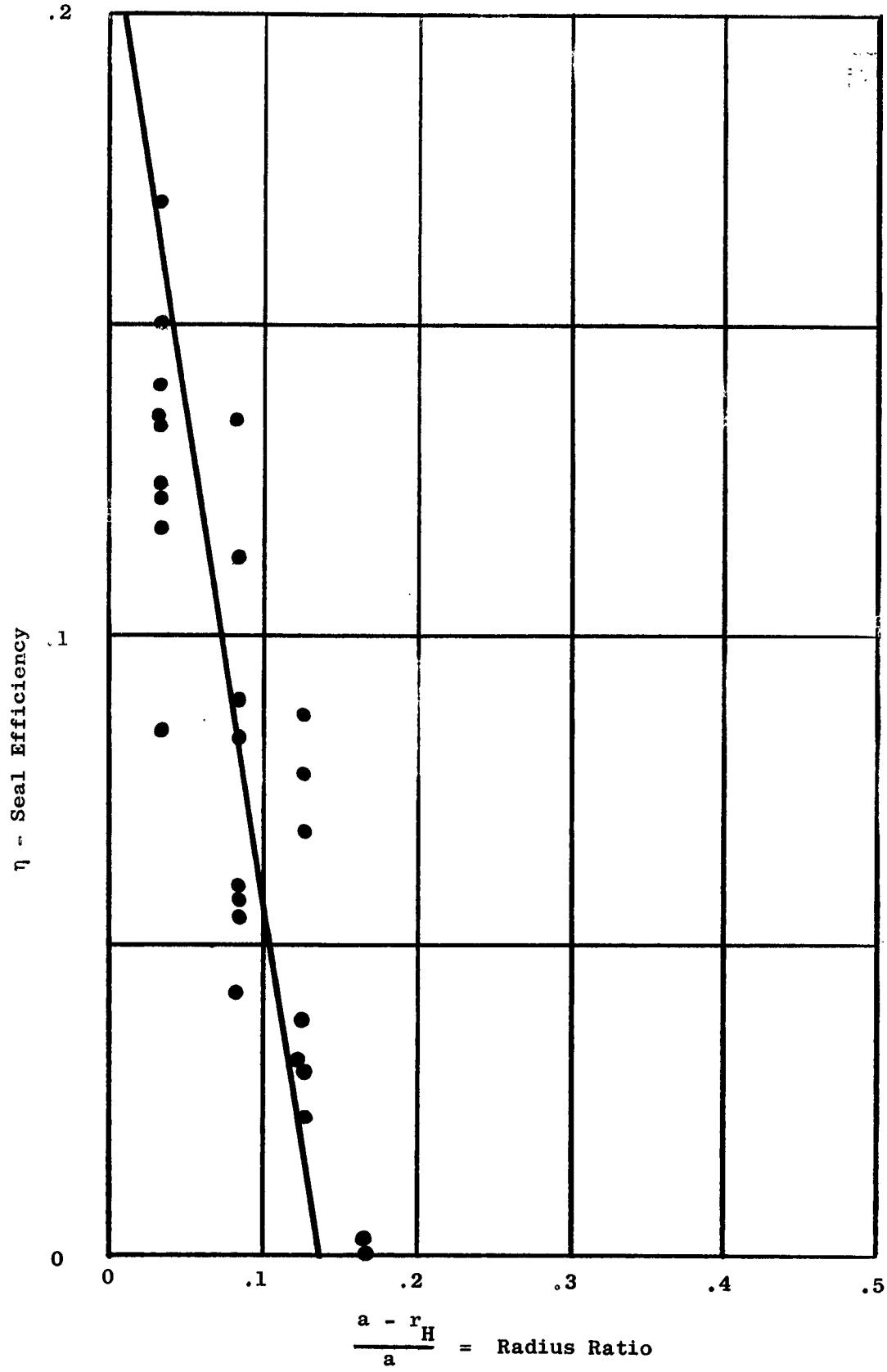

Figure 10b. Slinger Seal Efficiency, $\frac{r_L}{a} = 0.87$, $\frac{S_L}{a} = 0.092$.

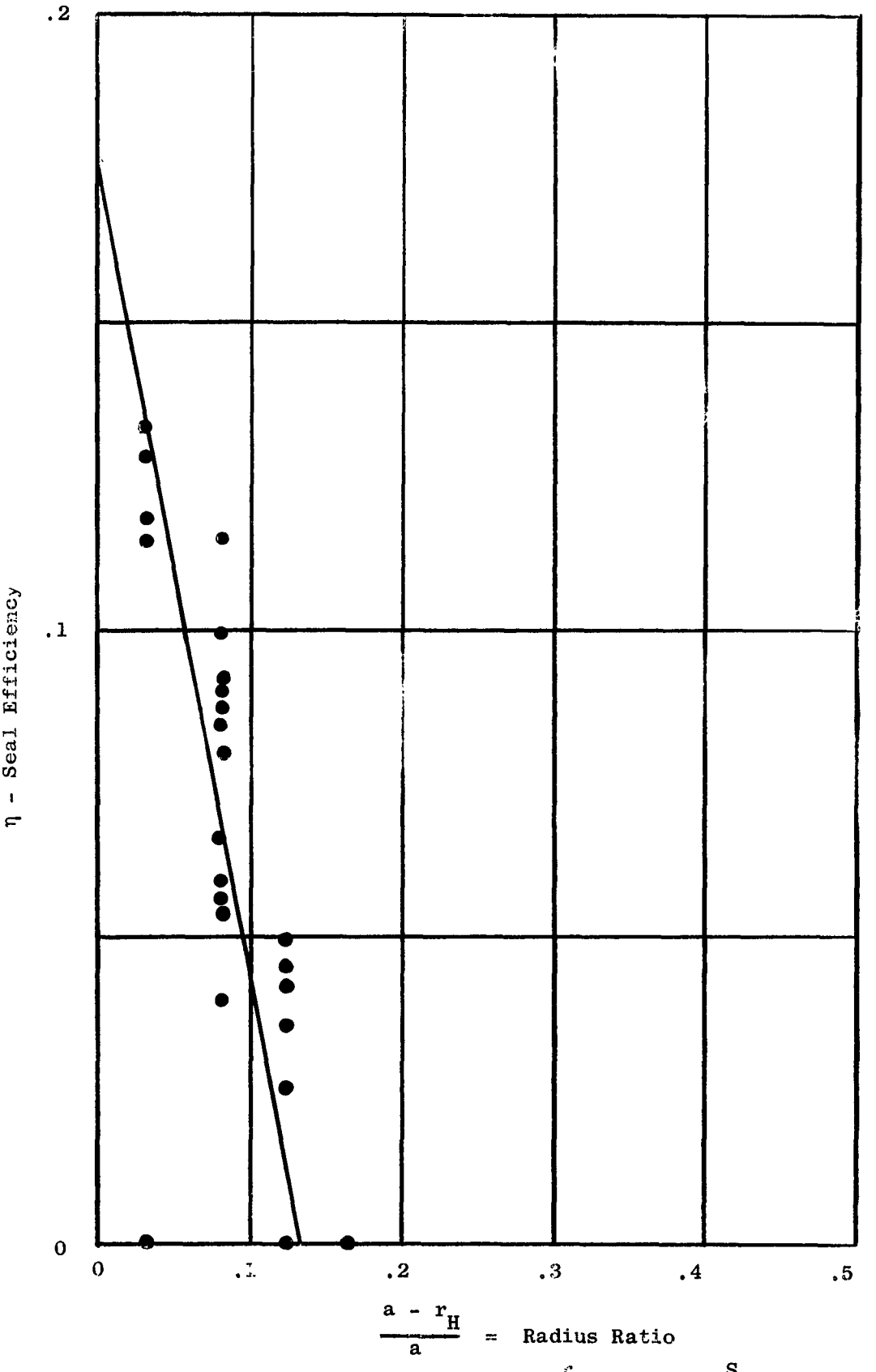

Figure 10c. Slinger Seal Efficiency, $\frac{r_L}{a} = 0.87$, $\frac{S_L}{a} = 0.019$.

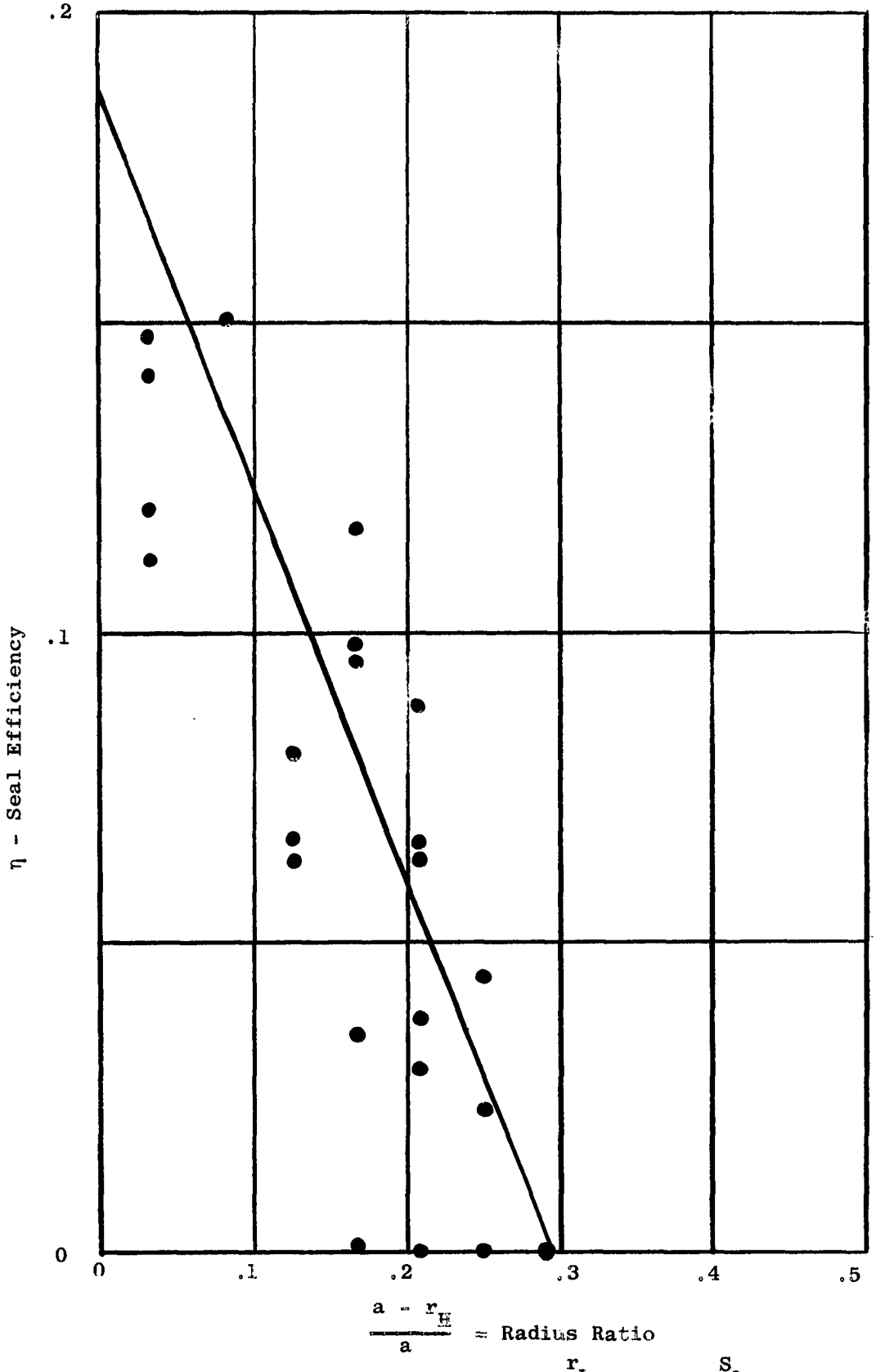

Figure 10d. Slinger Seal Efficiency, $\frac{r_I}{a} = 0.71$, $\frac{S_L}{a} = 0.167$.

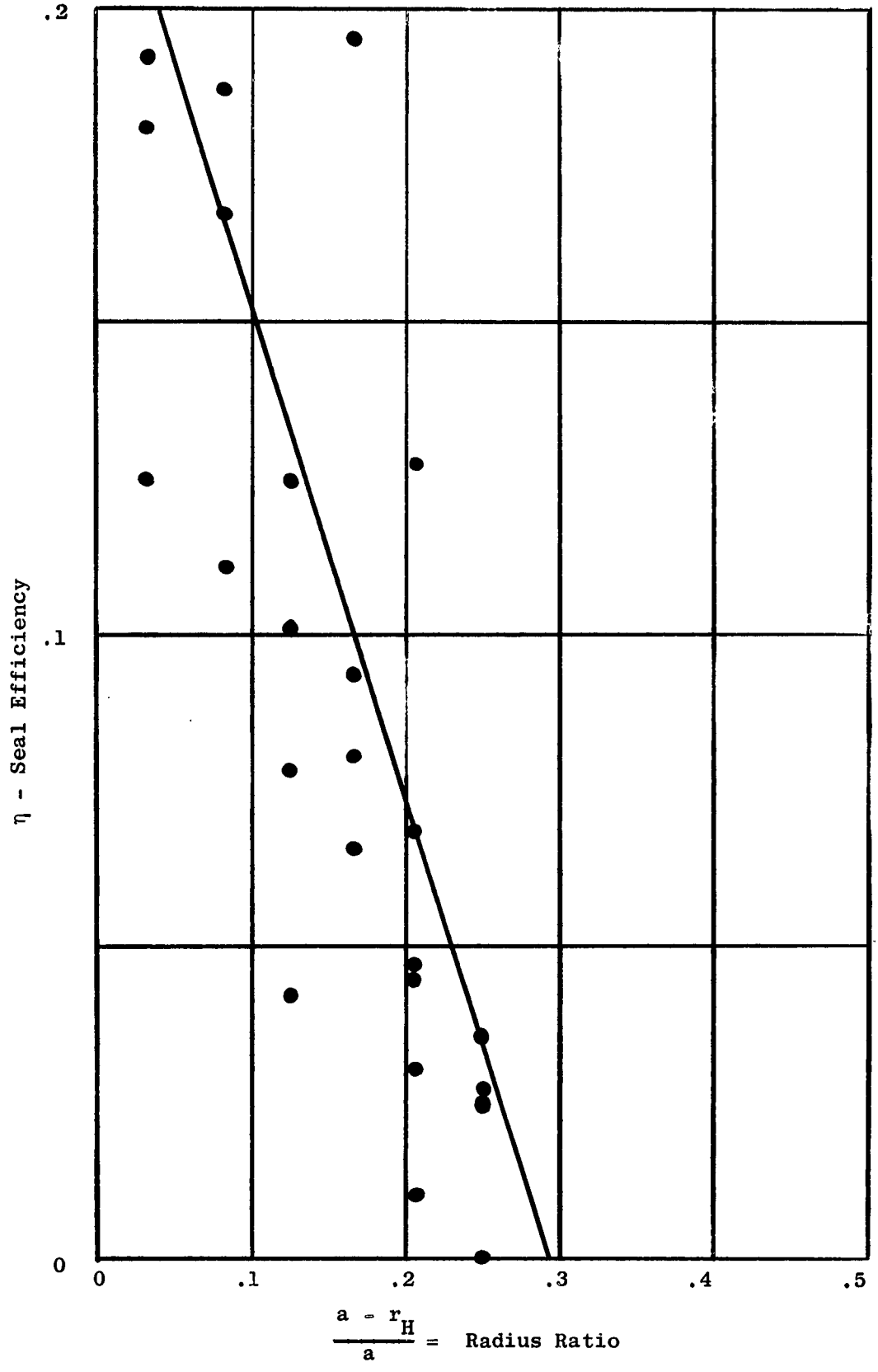

Figure 10e. Slinger Seal Efficiency, $\frac{r_L}{a} = 0.71$, $\frac{S_L}{a} = 0.092$.

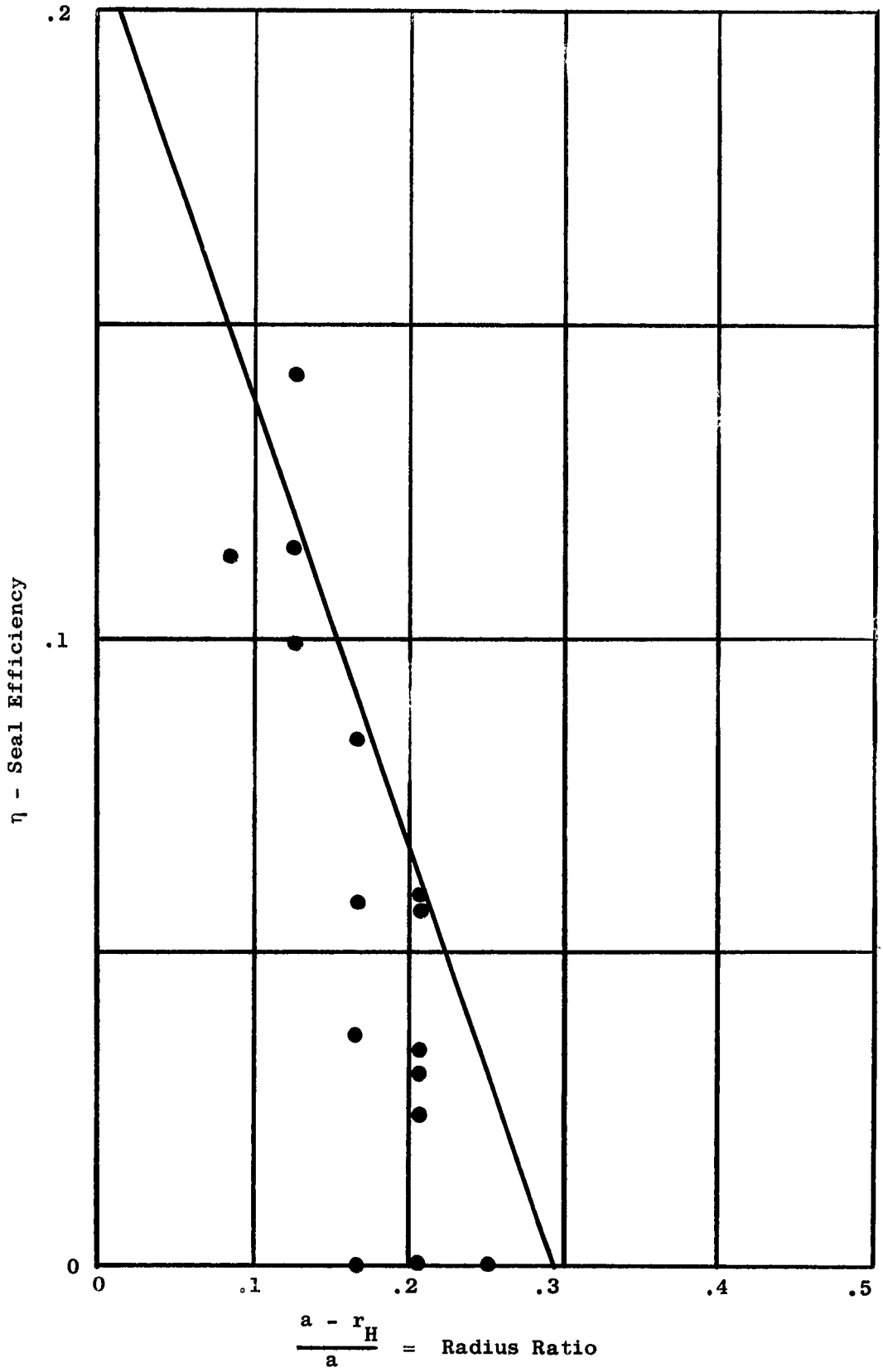

Figure 10f. Slinger Seal Efficiency, $\frac{r_L}{a} = 0.71$, $\frac{S_L}{a} = 0.019$.

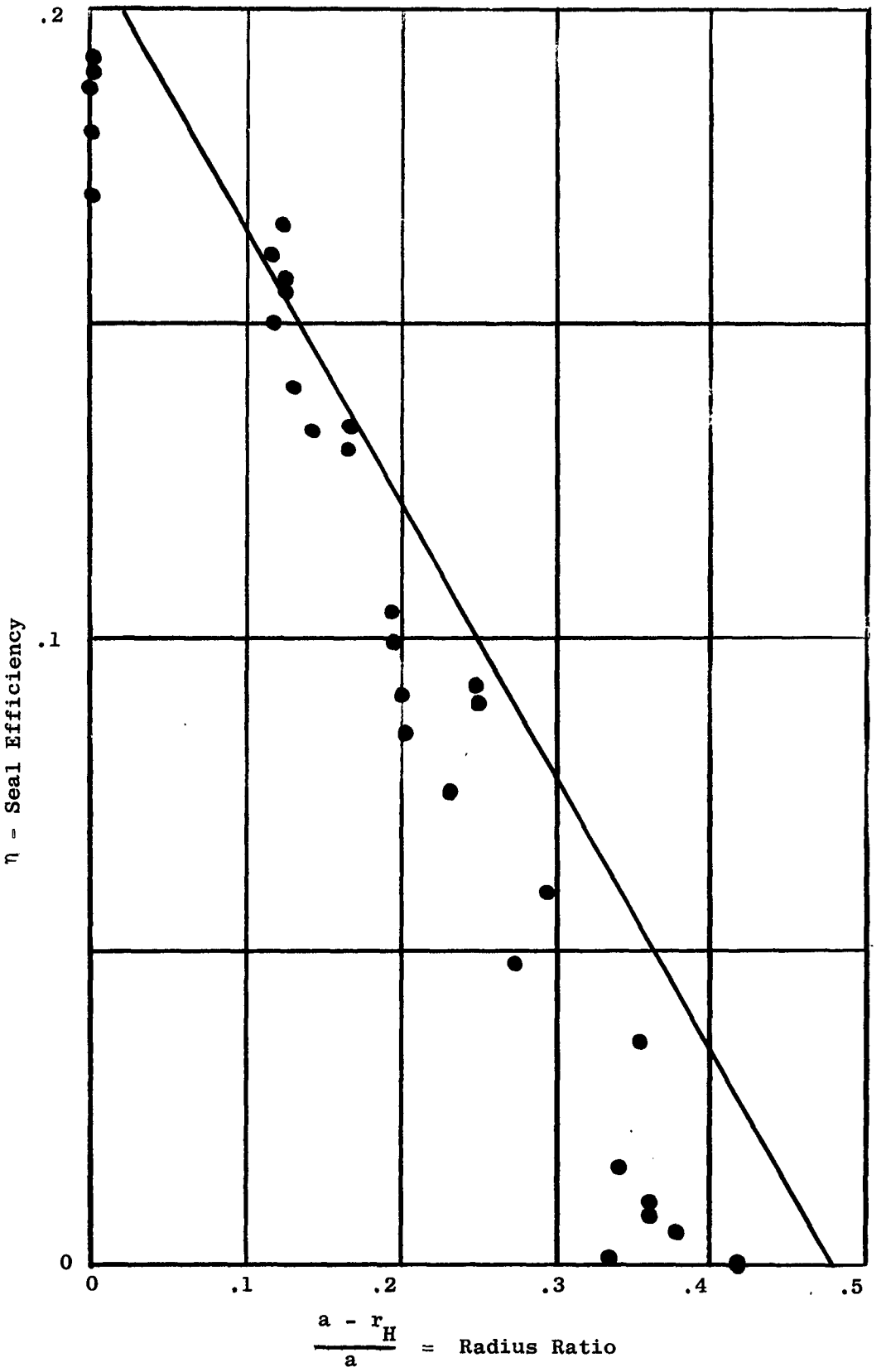

Figure 10g. Slinger Seal Efficiency, $\frac{r_L}{a} = 0.52$, $\frac{S_L}{a} = 0.167$.

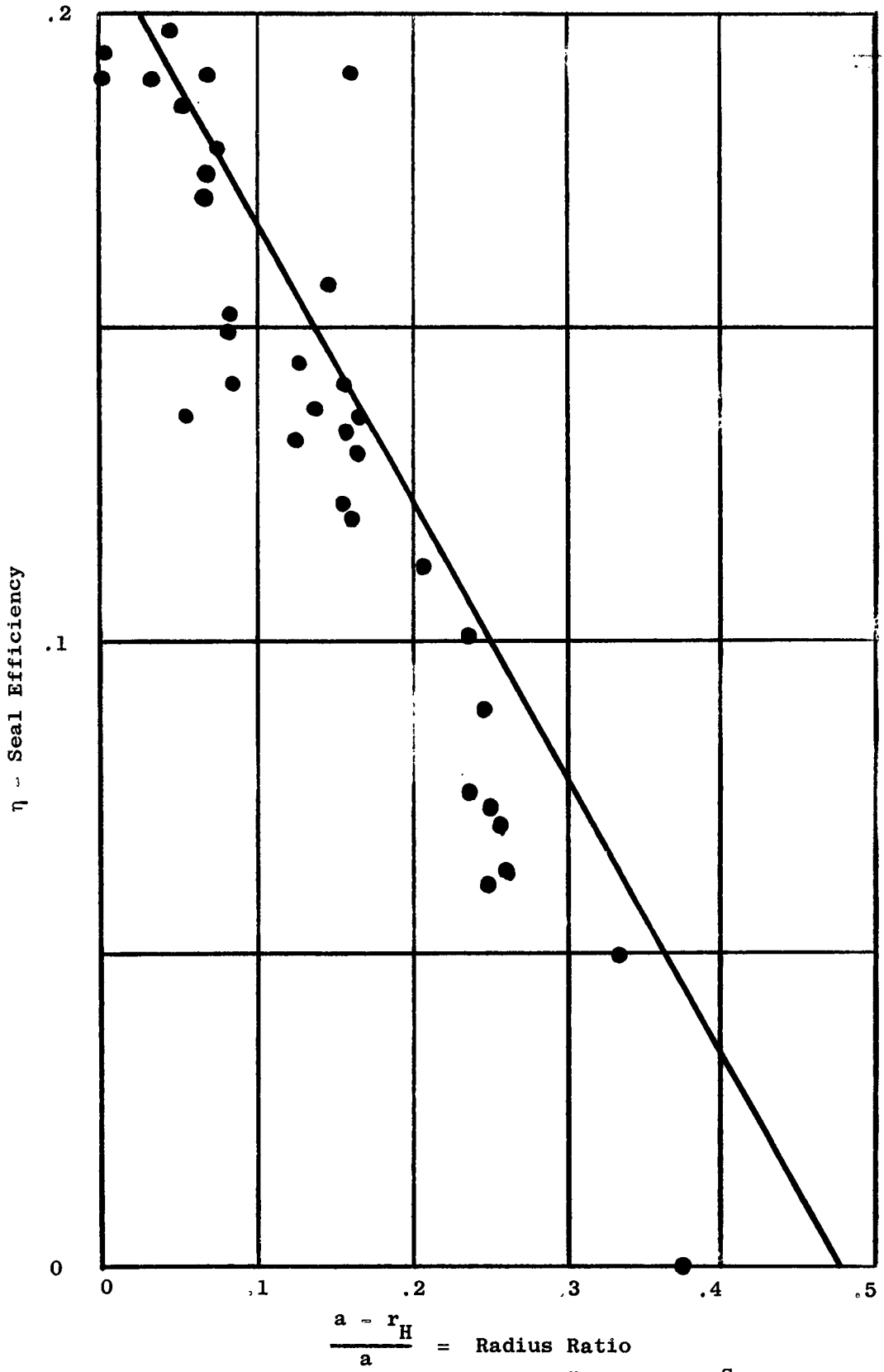

Figure 10h. Slinger Seal Efficiency, $\frac{r_L}{a} = 0.52$, $\frac{S_L}{a} = 0.092$.

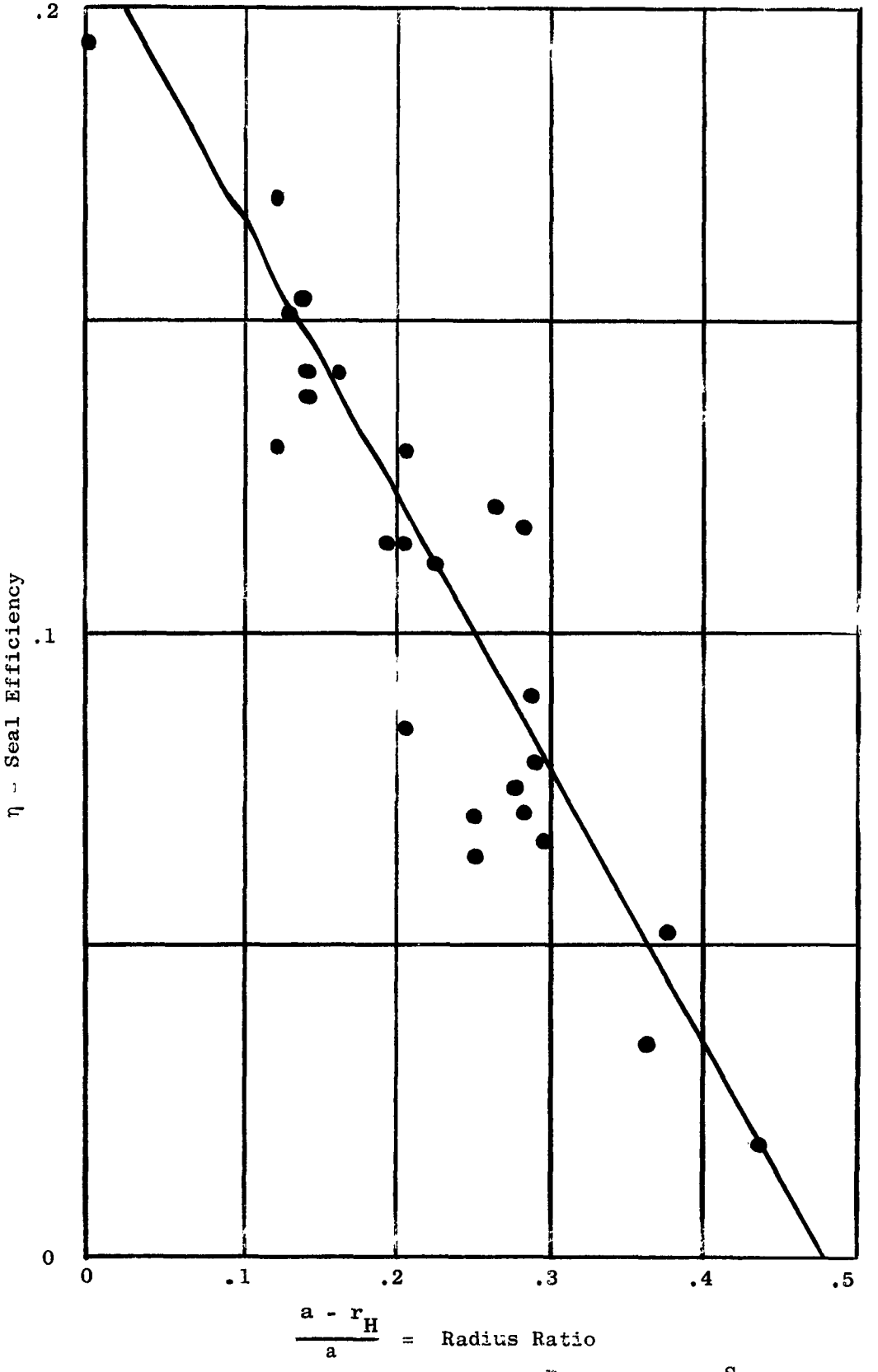

Figure 10i. Slinger Seal Efficiency, $\frac{r_L}{a} = 0.52$, $\frac{S_L}{a} = 0.019$.

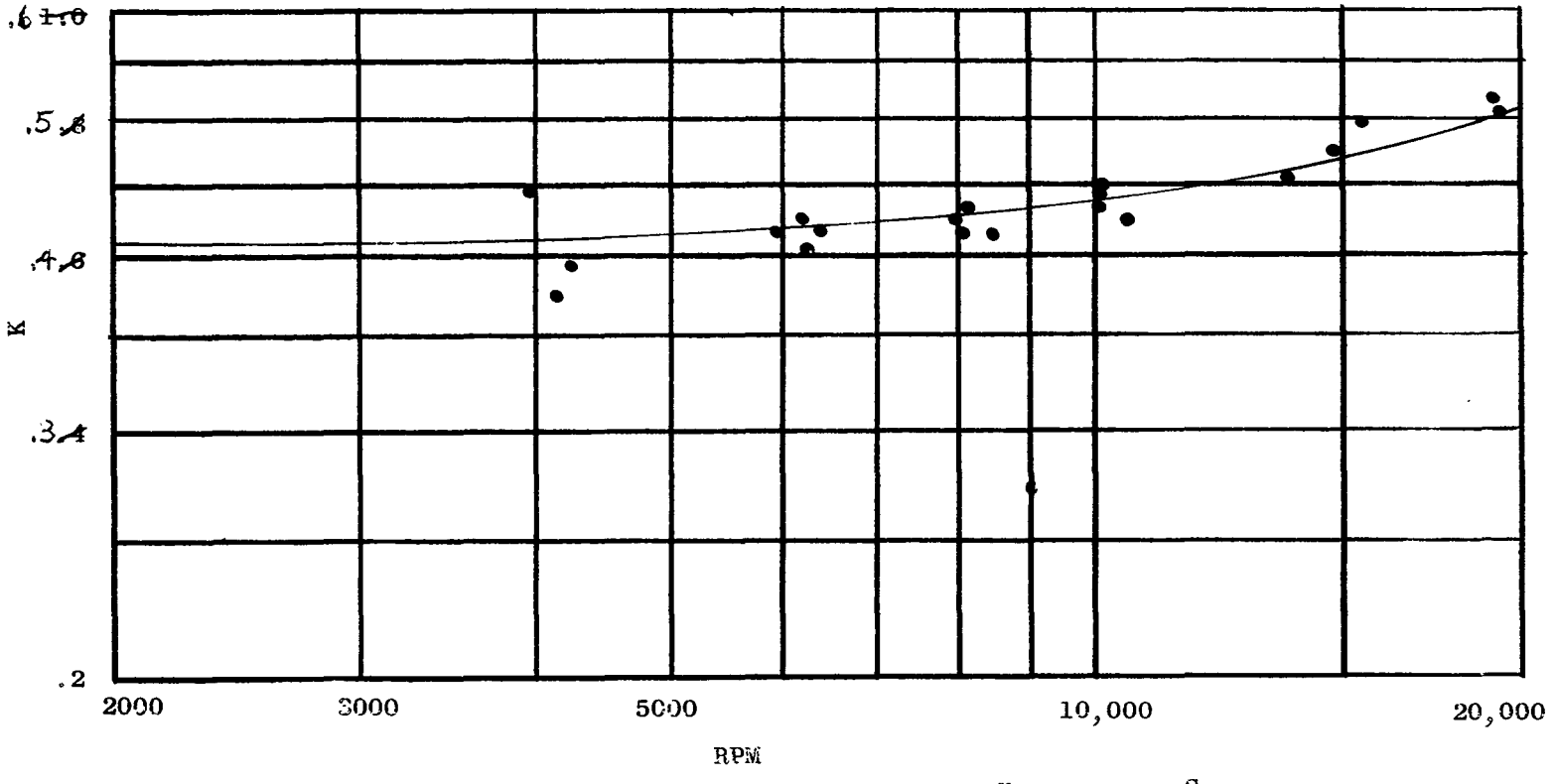

Figure 11a. Slinger Seal Water Ring Velocity Ratio, $\frac{r_L}{a} = 0.27$, $\frac{S_L}{a} = 0.167$.

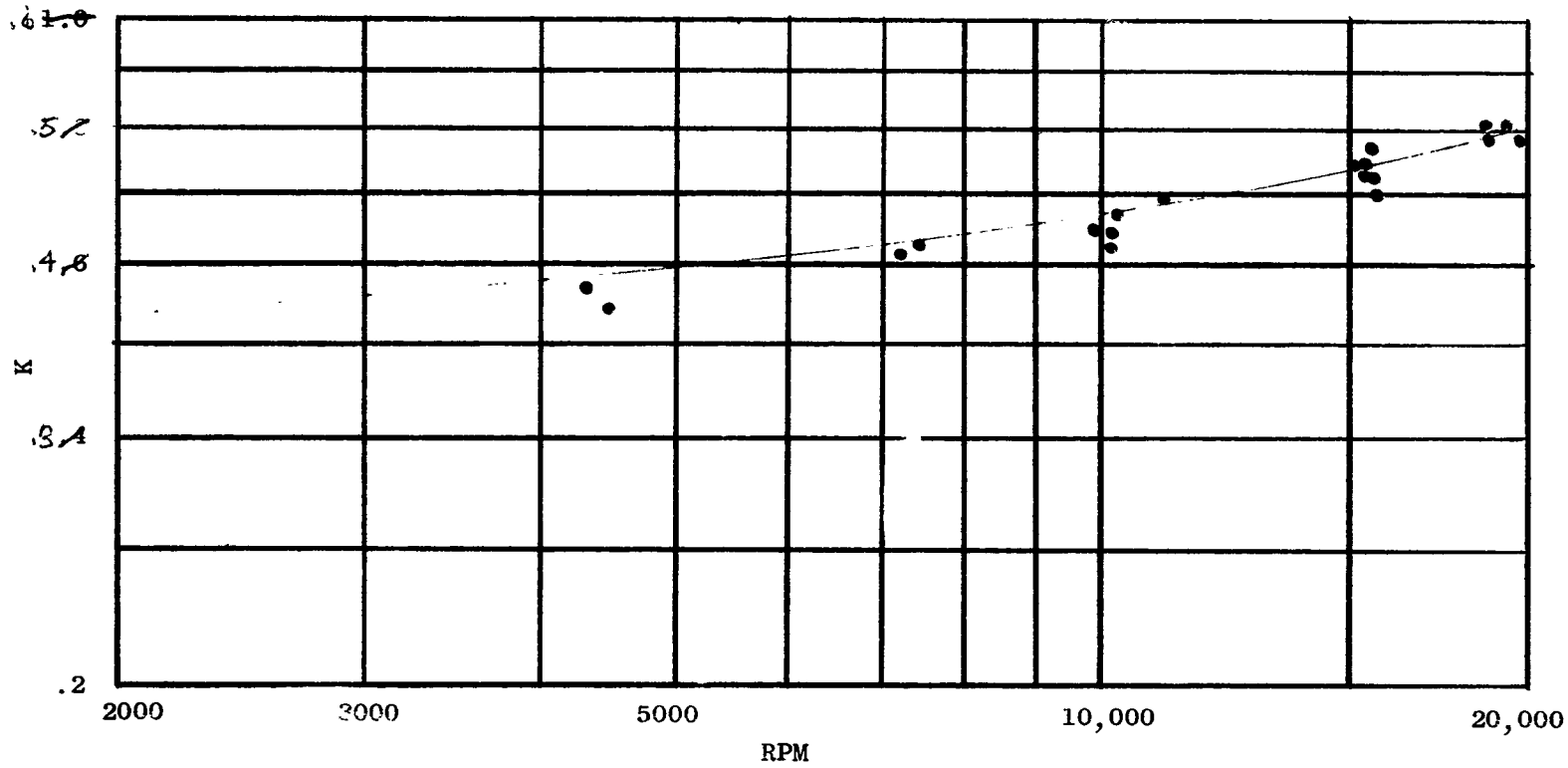

Figure 11b. Slinger Seal Water Ring Velocity Ratio, $\frac{r_L}{a} = 0.37$, $\frac{S_L}{a} = 0.092$.

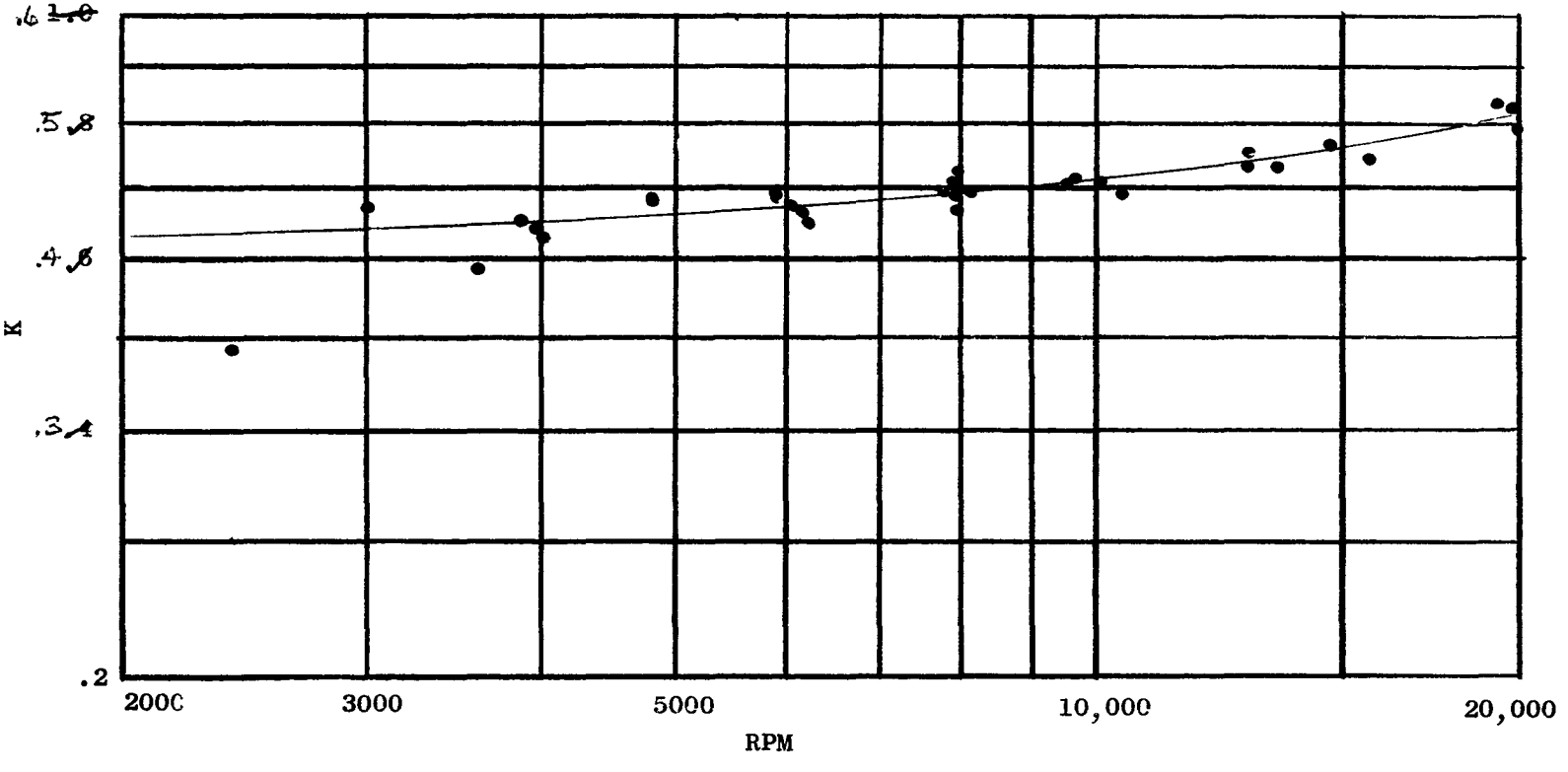

Figure 11c. Slinger Seal Water Ring Velocity Ratio, $\frac{r_L}{a} = 0.87$, $\frac{S_L}{a} = 0.019$.

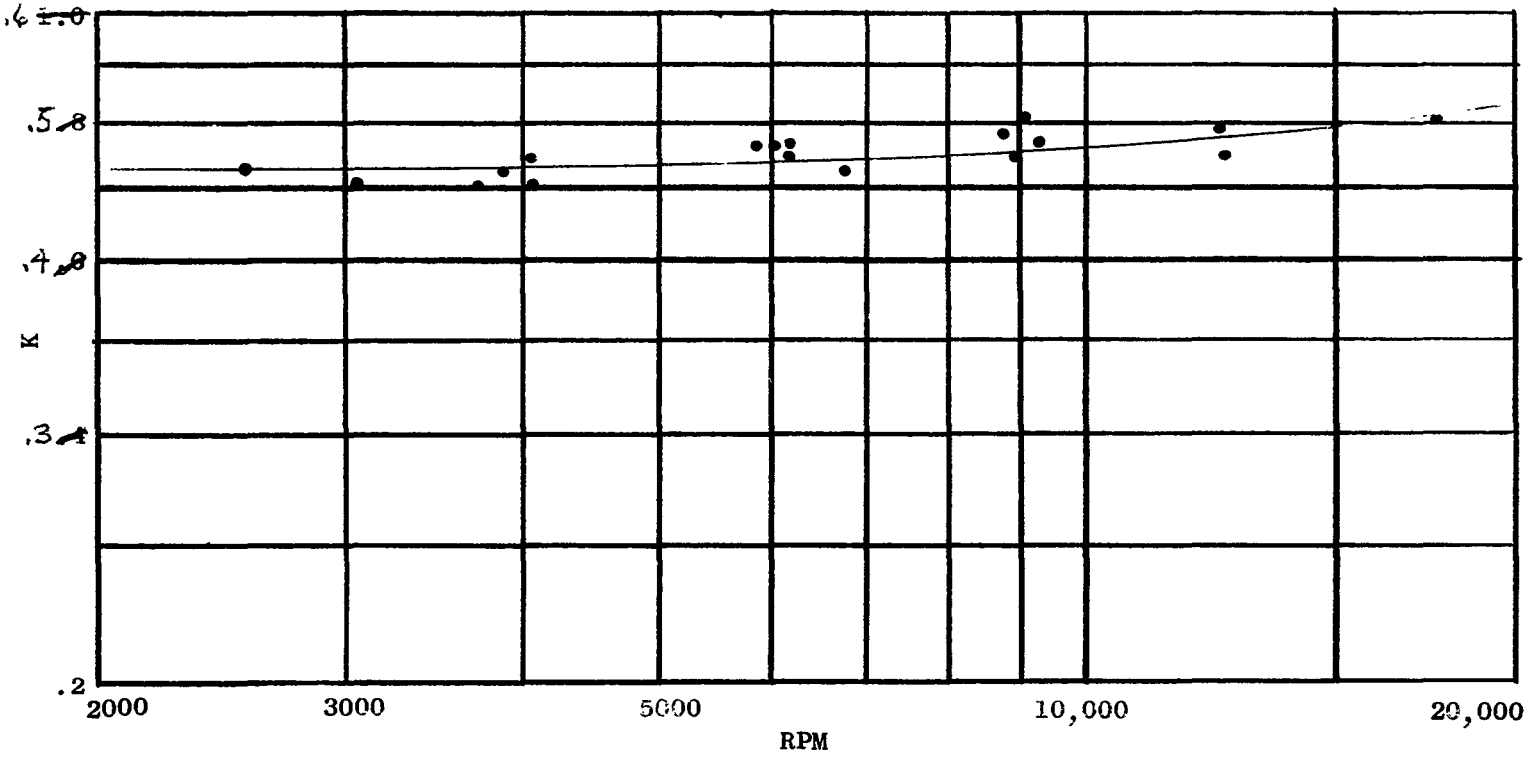

Figure 11d. Slinger Seal Water Ring Velocity Ratio, $\frac{r_L}{a} = 0.71$, $\frac{S_L}{a} = 0.167$.

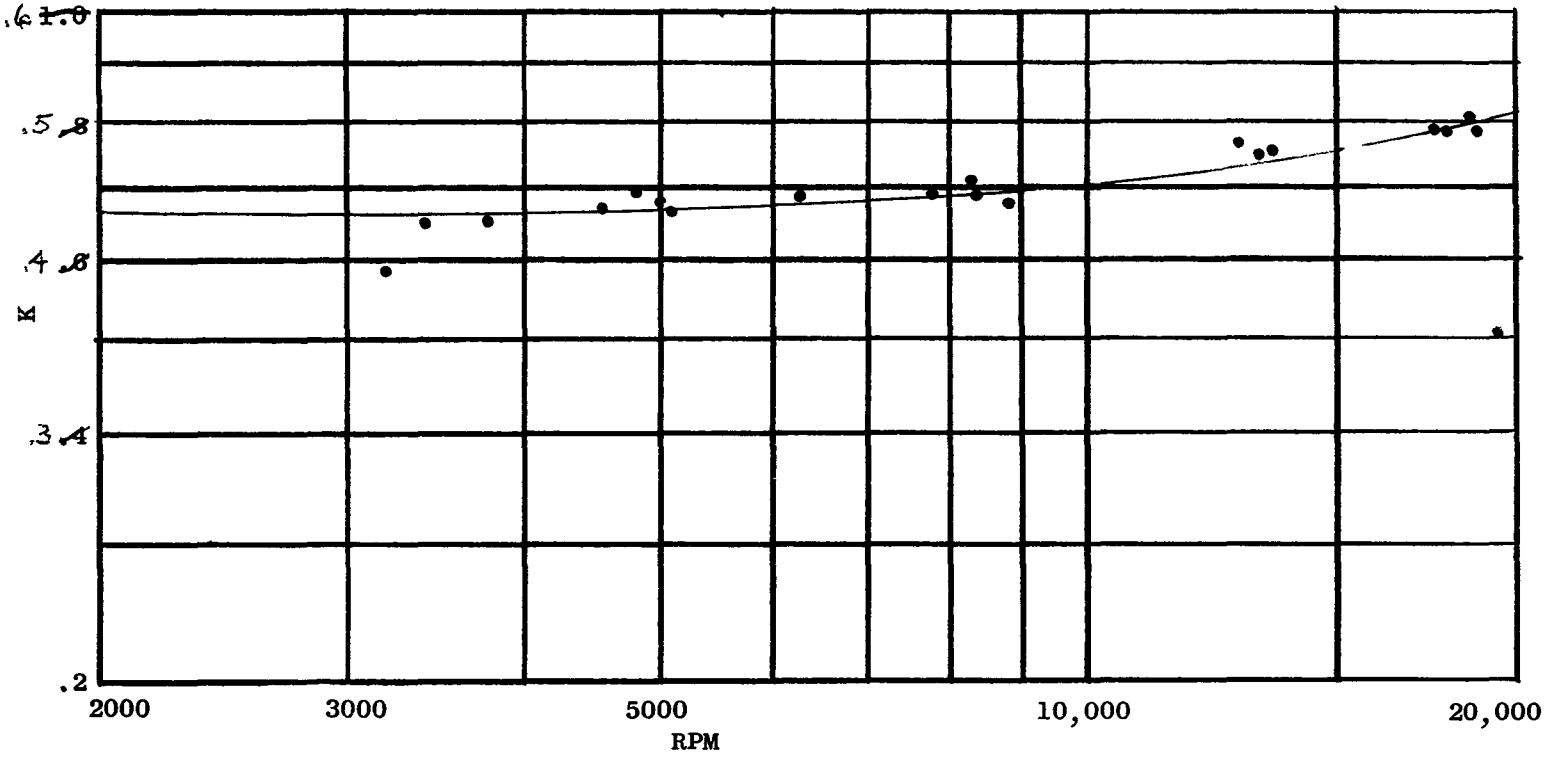

Figure 11e. Slinger Seal Water Ring Velocity Ratio, $\frac{r_L}{a} = 0.71$, $\frac{S_L}{a} = 0.092$.

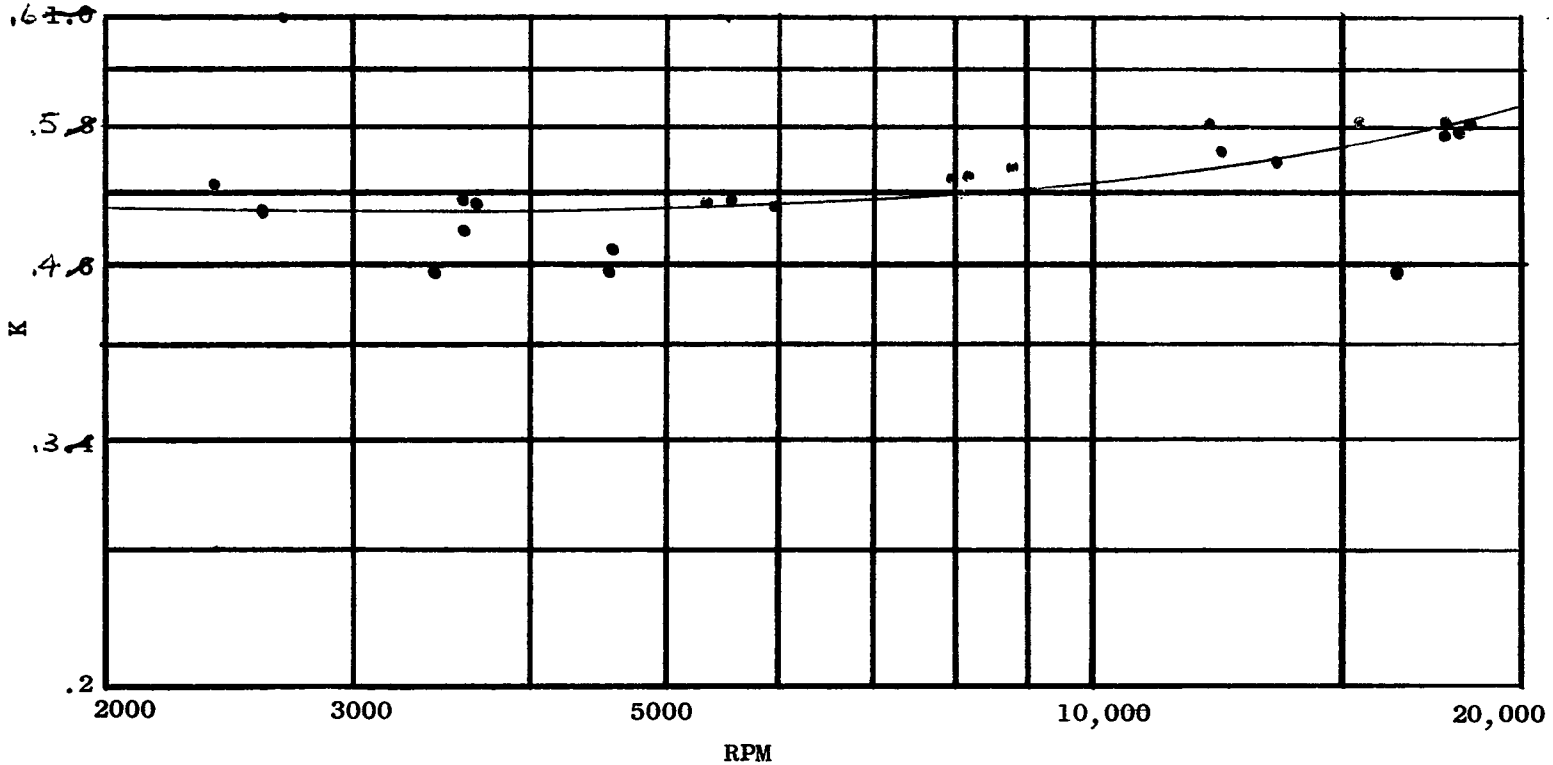

Figure 11f. Slinger Seal Water Ring Velocity Ratio, $\frac{r_L}{a} = 0.71$, $\frac{S_L}{a} = 0.019$.

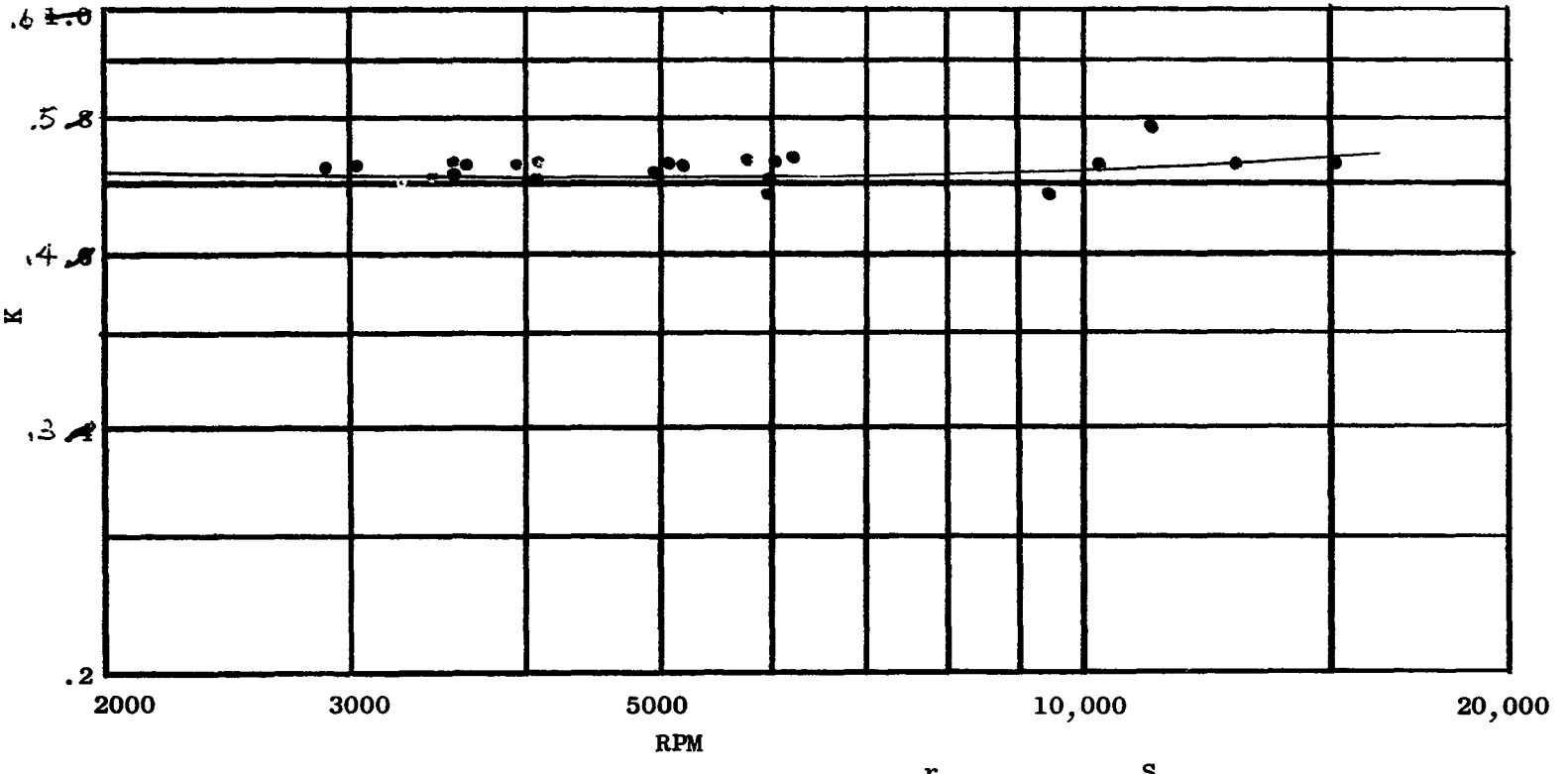

Figure 11g. Slinger Seal Water Ring Velocity Ratio, $\frac{r_L}{a} = 0.52$, $\frac{S_L}{a} = 0.167$.

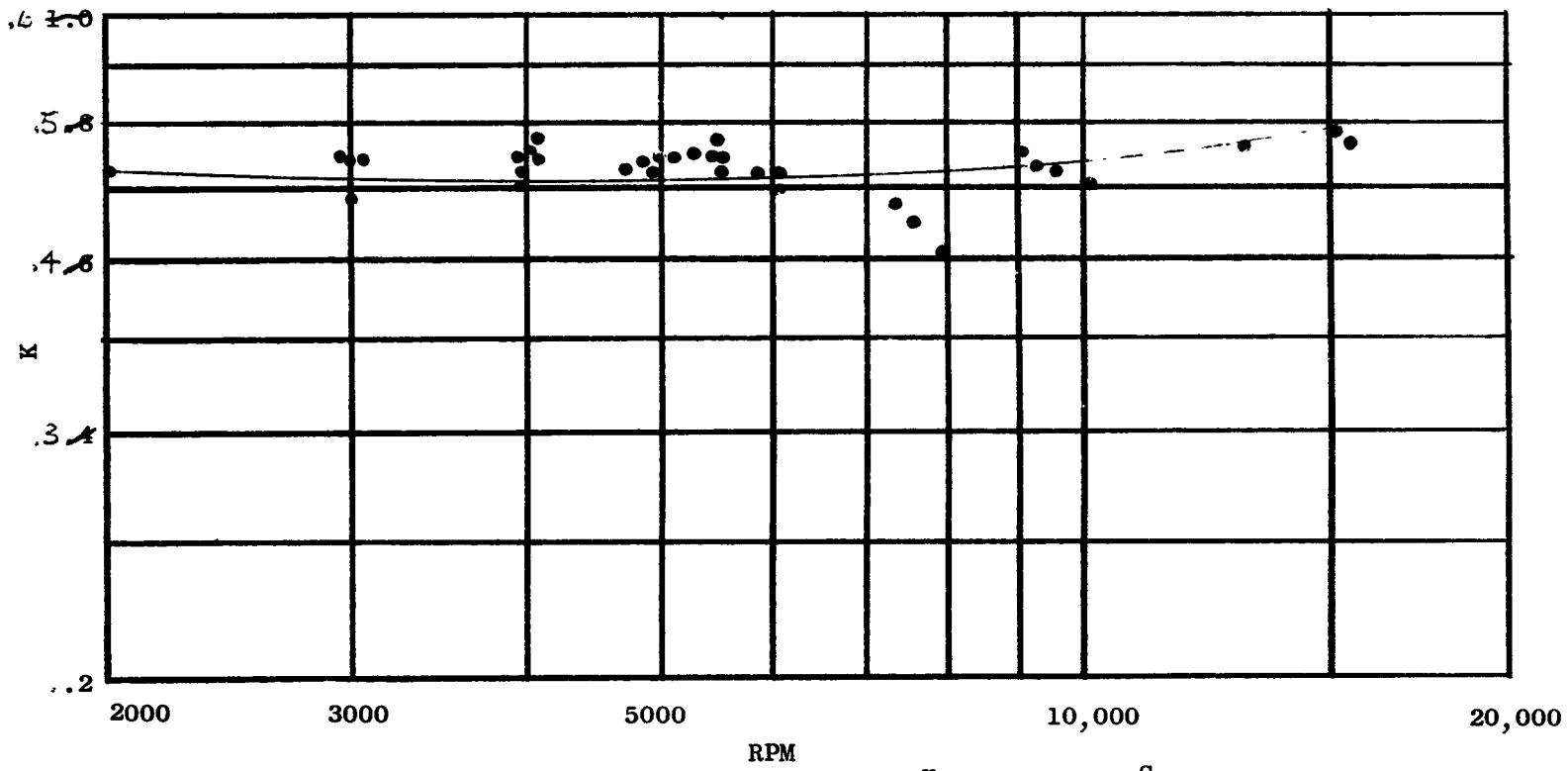

Figure 11h. Slinger Seal Water Ring Velocity Ratio, $\frac{r_L}{a} = 0.52$, $\frac{S_L}{a} = 0.092$.

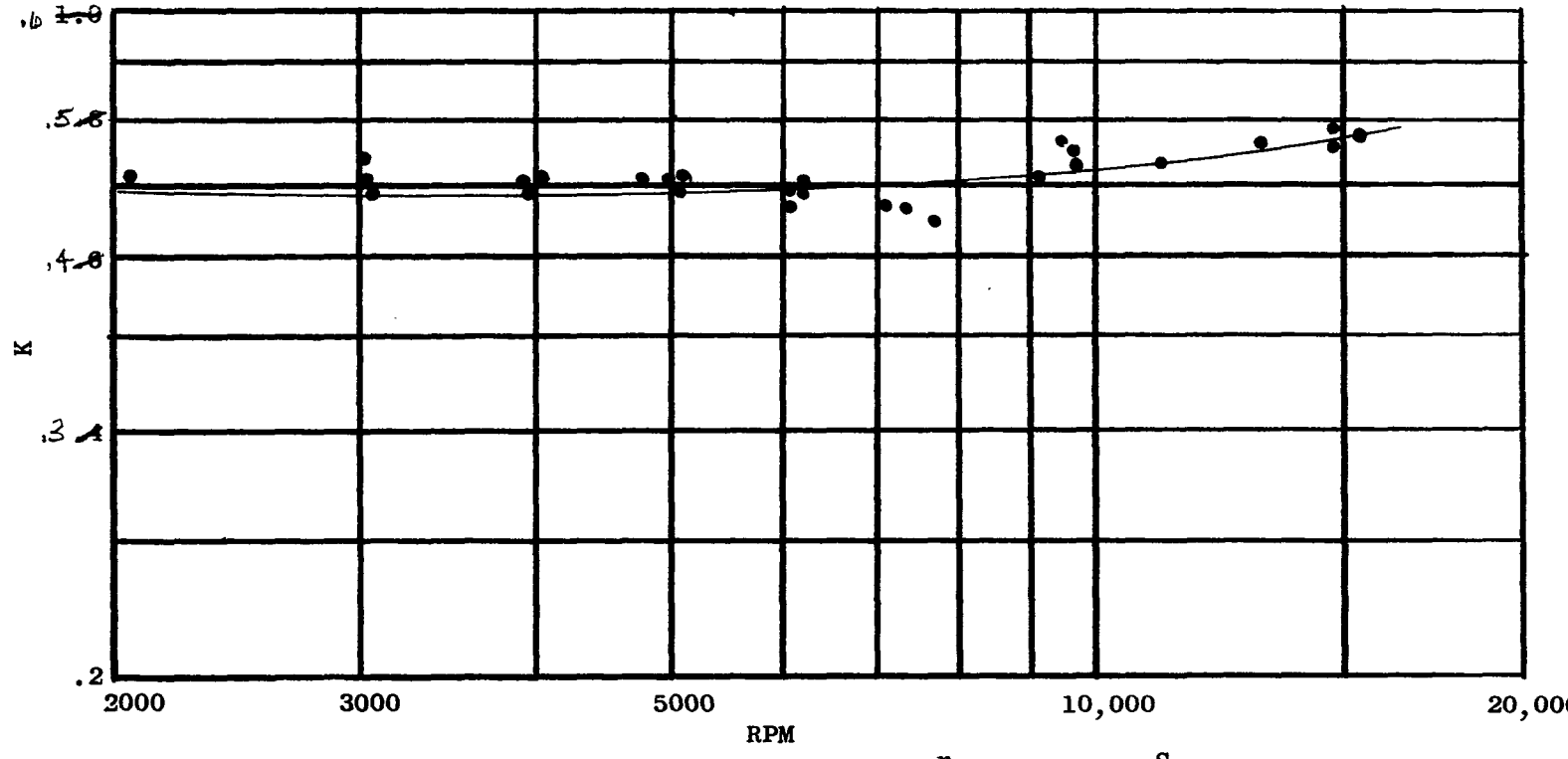

Figure 11i. Slinger Seal Water Ring Velocity Ratio, $\frac{r_L}{a} = 0.52$, $\frac{S_L}{a} = 0.019$.

Figure 12. Summary of Optimum Geometry for Screw Seals

	Optimization	S	φ	δ/h	t^*/w	h/w	Test Regimes
1.	Zotov - Reference 3	~.12	14.5	.32	1.635	.08	Lam. and Turb. Re_{cr} = 1300
2.	Asanuma - Reference 4	~.08	10°~11°	.2	2.04	.05 .2	Lam.
3.	Boon and Tal - Reference 2	~.09	15.8°	.422	2.08	---	Lam.
4.	" Frossel - Reference 5	~.02*	12°	.007*	---	---	Lam.
		~.03	15°~20°	.16*	---	---	Lam.
5.	Whipple et.al, Reference 7-11	~.09	13.8°	.38	2.06	---	Lam.

* Not Optimum Value

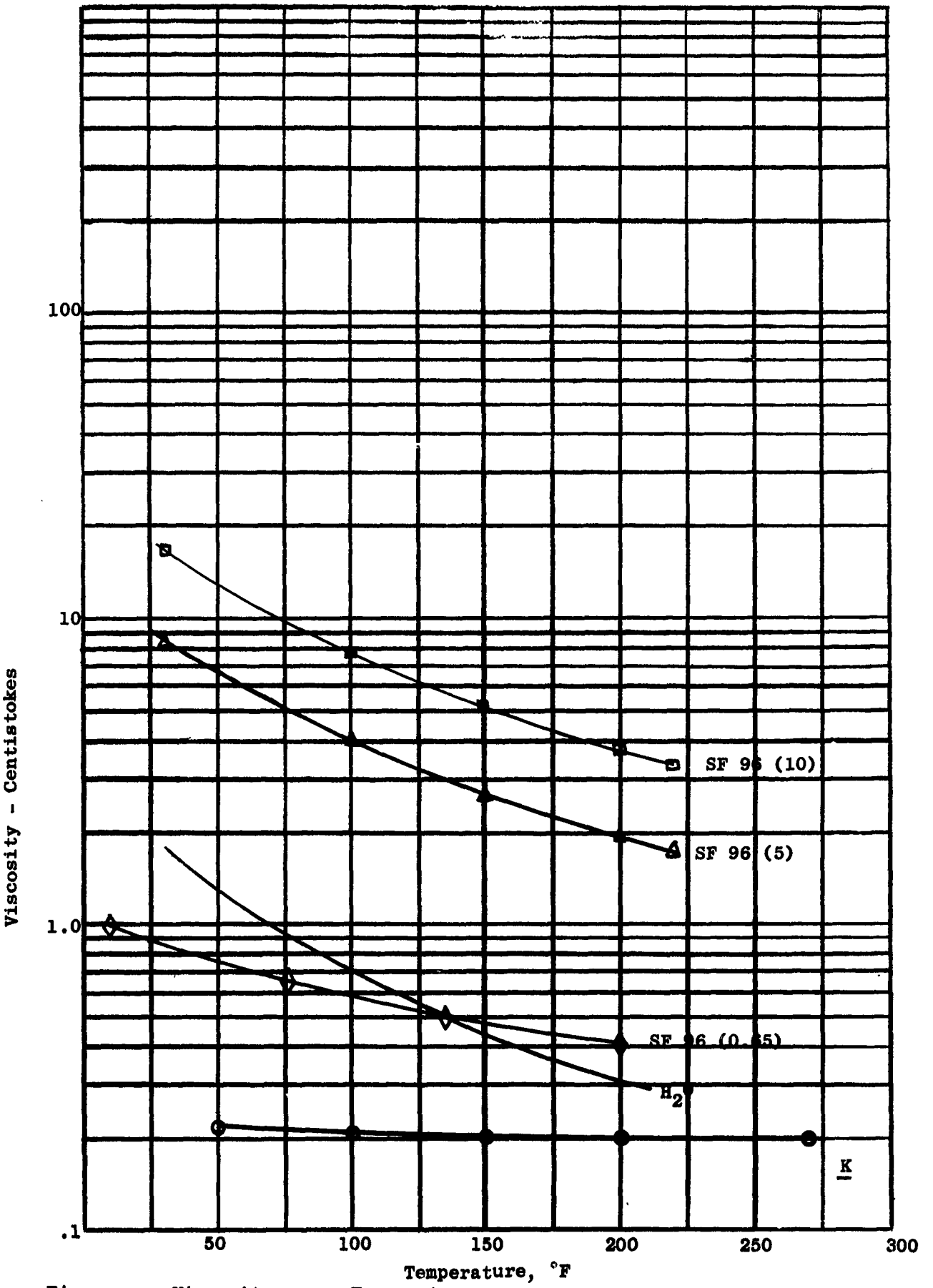

Figure 13. Viscosity vs. Temperature

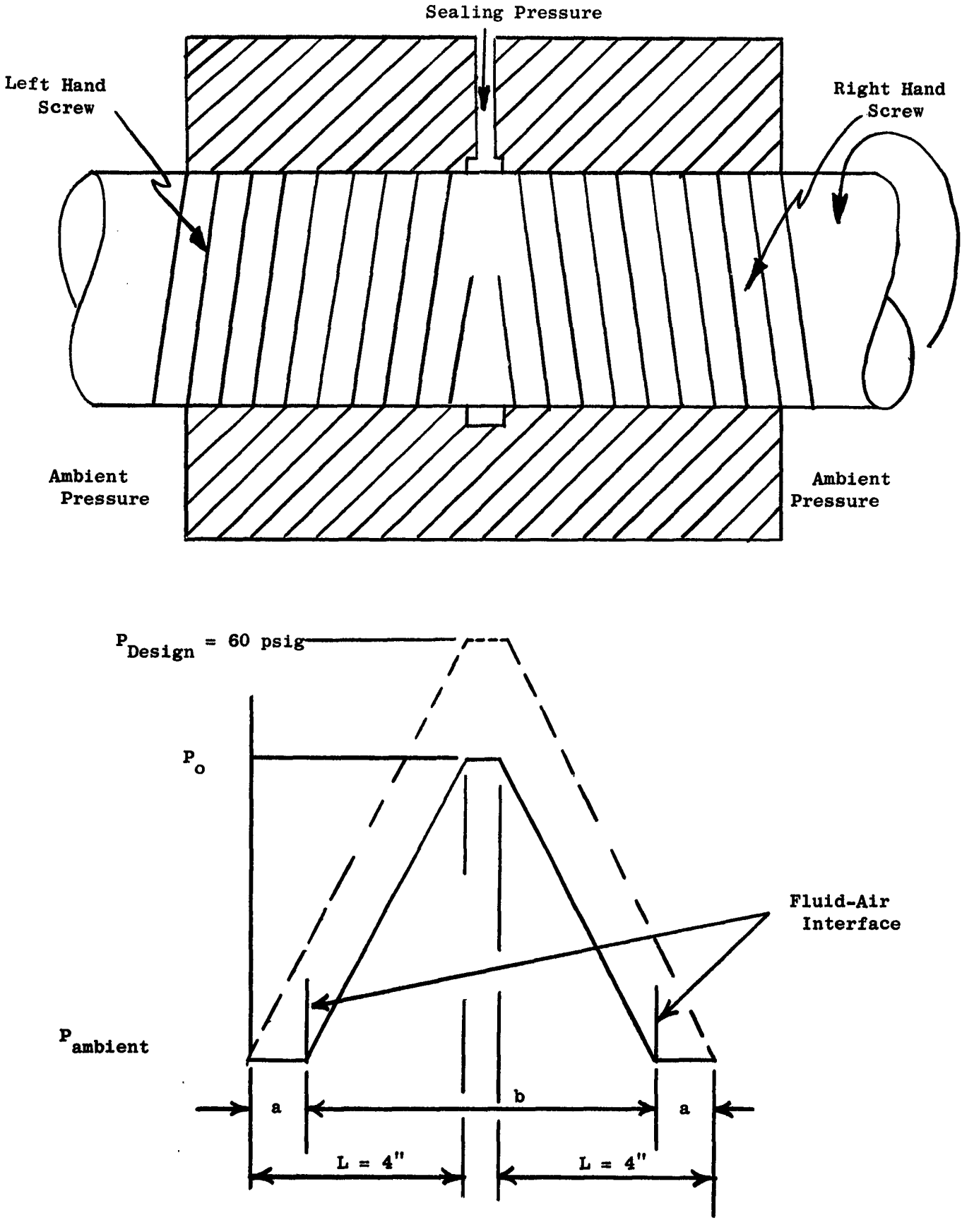

Figure 14. Use of Pressure Profile to Determine Location of Fluid-Air Interface.

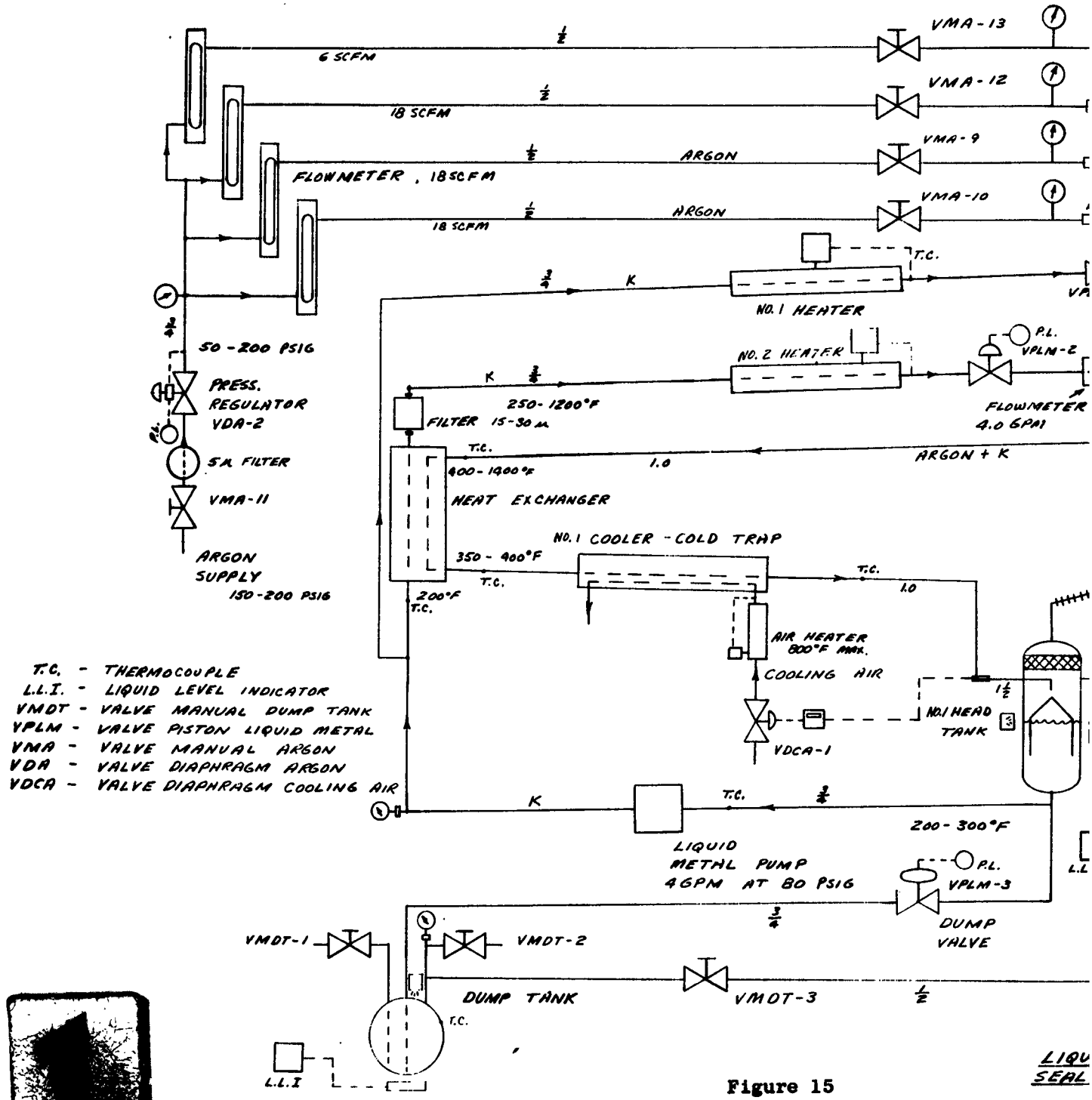
VMA-13
VMA-12
VMA-9
VMA-10
6 SCFM
18 SCFM
ARGON
FLOWMETER , 18SCFM
18 SCFM
ARGON
T.C.
NO. 1 HEATER
50 - 200 PSIG
PRESS. REGULATOR VDA-2
5M. FILTER
VMA-11
ARGON SUPPLY 150 - 200 PSIG
NO. 2 HEATER
P.L. VPLM-2
250 - 1200°F
FILTER 15-30 M
FLOWMETER 4.0 GPM
400 - 1400°F
HEAT EXCHANGER
1.0
ARGON + K
NO. 1 COOLER - COLD TRAP
350 - 400°F
200°F
AIR HEATER 800°F MAX.
COOLING AIR
VDCA-1
NO. 1 HEAD TANK
T.C. - THERMOCOUPLE
L.L.I. - LIQUID LEVEL INDICATOR
VMDT - VALVE MANUAL DUMP TANK
VPLM - VALVE PISTON LIQUID METAL
VMA - VALVE MANUAL ARGON
VDA - VALVE DIAPHRAGM ARGON
VDCA - VALVE DIAPHRAGM COOLING AIR
200 - 300°F
LIQUID METAL PUMP 4GPM AT 80 PSIG
P.L. VPLM-3
DUMP VALVE
VMDT-1
VMDT-2
DUMP TANK
VMDT-3
L.L.I

Figure 15

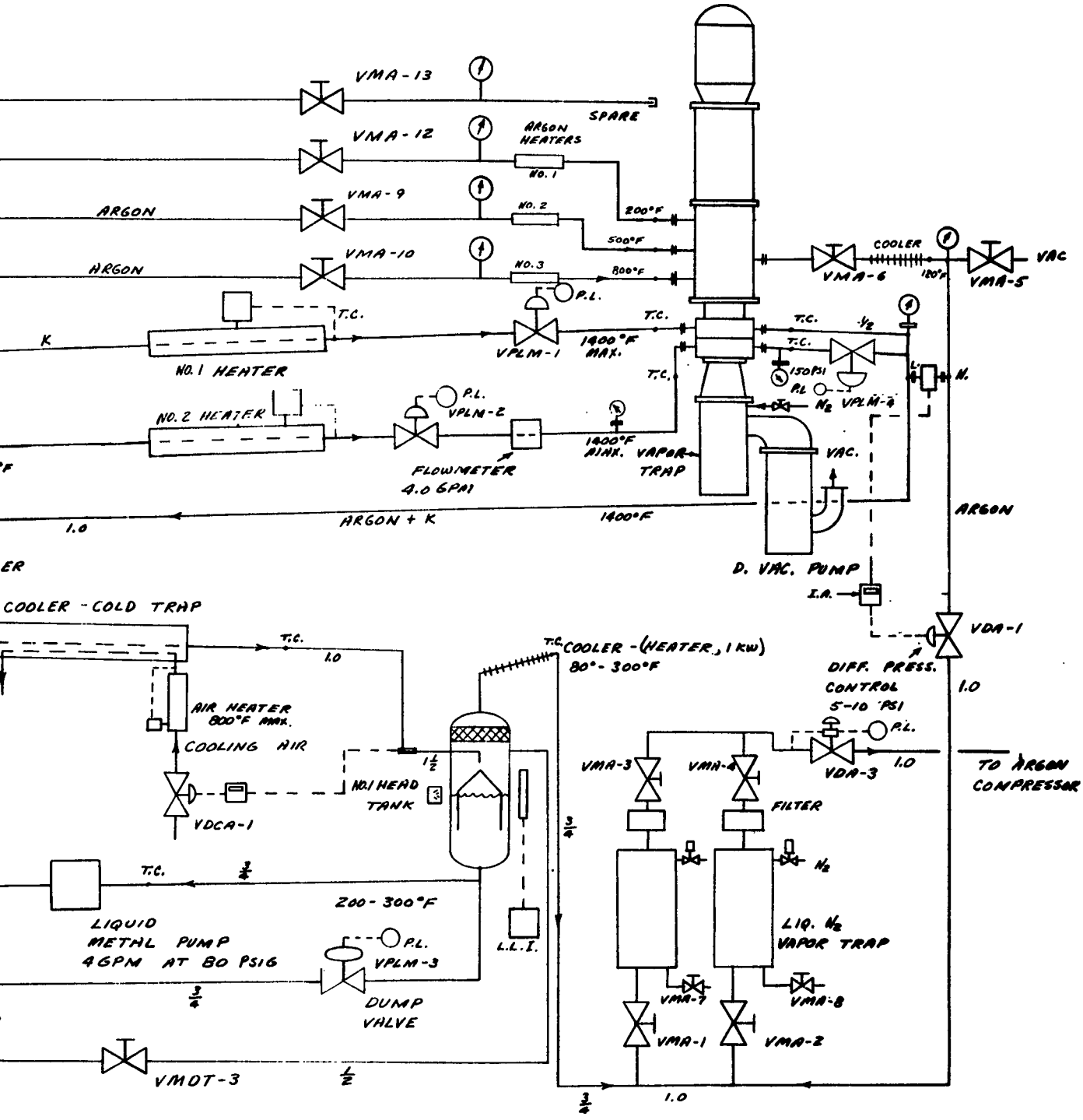

LIQUID METHL LOOP FOR SEAL AND BEARING TESTING

SCHEMATIC E 6-14

REV. 12-6-62
REV. 11-8-62
REV. 11-1-62
REV. 9-6-62

Figure 15

REFERENCES

1. Dynamic Shaft Seals in Space, First Quarterly Report, Period Ending July 15, 1962.

2. Dynamic Shaft Seals in Space, Monthly Report, Period Ending September 15, 1962.

3. Boon, E.F., Tal, S.E., "Hydrodynamische Dichtung für rotierende Wellen," (Hydrodynamic Seal For Rotating Shafts), Chemic-dug-Technik, Vol. 31, No. 3, January 31, 1959, pp 202-12.

4. Zotov, V.A., "Research on Helical Groove Seals," Machine Design and Calculation (Russia) Issue No. 10.

5. Asanuma, T., "Studies on the Sealing Action of Viscous Fluids," International Conference on Fluid Sealing, Paper A3, April 17-19, 1961, BHRA, Harlow Essex, England - 26 papers.

6. Frössel, W., "Hydrodynamisch Wirkende Wellendichtung," Kanstrucktron, Vol. 8, No. 11, November, 1956.

7. Stair, William K., "The Visco Seal -- A Survey" Engineering Experimental Station, The University of Tennessee, ME-5-62-2, March, 1962.

8. Whipple, R.T.P., "Herring-Bone Pattern Thrust Bearing," UKHEA, Atomic Energy Research Establishment, TIM-29, August 24, 1949.

9. Woodrow, J., "Viscosity-Plates Flow and Loading," UKHEA, Atomic Energy Research Establishment, E/M 31, December 22, 1949.

10. Whipple, R.T.P., "Theory of the Spiral Grooved Thrust Bearing with Liquid or Gas Lubricant," UKHEA, Atomic Energy Research Establishment, T/R 622, March 6, 1951.

11. Wordsworth, D.V., "The Viscosity Plate Thrust Bearing," UKHEA, Atomic Energy Research Establishment, E/R 2217, October, 1952.

REFERENCES (continued)

12. Snell, L.N., "Theory of Viscosity Plate Thrust Bearing Based on Circular Geometry," UKHEA, Ministry of Supply, Div. of Atomic Energy (Production) 5181 October 13, 1952.

13. Swisher, T.H., "Mercury Shaft Seal," General Electric Data Folder No. 61214.

14. "Investigations of Liquid Metal Lubricated Bearings," 50GL-231, November, 1950.

15. Smith, L.H., "Development of Seals for Fluid Powered Systems in Space Vehicles - Proposal," General Electric Company, September, 1960.

16. Ernst, H., "Liquid Metal Bearings and Seals, Volume II - Seals," General Electric Company Report DM59-372.

17. Dushmen, S., "Vacuum Technique," John Wiley, 1959.

DISTRIBUTION LIST

Copies	Organization
1	ASD (ASRCNL-2, Mr. John Morris) Wright Patterson AFB, Ohio
1	ASD (ASNPFS-3, Mr. R. Ling) Wright Patterson AFB, Ohio
1	ASD (ASRCNL, Mr. G. A. Beane) Wright Patterson AFB, Ohio
2	ASD (ASRMFP-3, Mr. R. J. Smith) Wright Patterson AFB, Ohio
1	U.S. Atomic Energy Commission Office of Technical Information P. O. Box 62 Oak Ridge, Tennessee
1	Thompson Ramo Wooldridge Attn: Mr. Carl Nau 23555 Euclid Avenue Cleveland 17, Ohio
1	Rocketdyne Division North American Aviation Attn: Mr. R. B. Dillaway Department 584 6633 Canoga Park Boulevard Canoga Park, California
1	Technical Information Center Aerospace Corporation P. O. Box 95085 Los Angeles 45, California
11	ASTIA Arlington Hall Station Arlington 12, Virginia
1	Cleveland Graphite Bronze Division of Clevite Corporation Attn: Mr. E. James Vargo 17000 St. Clair Avenue Cleveland 10, Ohio
1	Battelle Memorial Institute Attn: Mr. C. M. Allen Columbus 10, Ohio

1	SSD (SSTRE, Capt. W. W. Hoover) AF Unit Post Office Los Angeles 45, California
1	Power Information Center Moore School Building 200 South 33rd Street Philadelphia 4, Pennsylvania
1	National Aeronautics and Space Administration Lewis Research Center Attn: Mr. Joseph Joyce Space Electric Power Office 25000 Brookpark Road Cleveland 35, Ohio
1	AiResearch Manufacturing Company Attn: Mr. John Dennan 402 - 536th Street Phoenix 34, Arizona
1	Sundstrand Aviation Corporation Attn: Mr. K. Nichols 2480 West 70 Denver 21, Colorado
1	Aerojet-General Nucleonics Attn: Mr. Paul Wood Azusa, California
1	Pratt & Whitney Aircraft Division of United Aircraft Corp Attn: Mr. Frederick A. Corwin East Hartford, Connecticut
1	Mechanical Technology Inc. Attn: Mr. F. K. Orcutt Albany Shaker Road Latham, New York